# Investigating the Effects of the Insulin/PI3-Kinase/mTORC1 Signalling Pathway on Alzheimer's-Relevant Secretory Events Using the *Drosophila melanogaster* Secondary Cell Model


**Lingjin Kong (Eurus)**

St Anne's College

University of Oxford

Master of Science (by Research) in Physiology, Anatomy and Genetics

Supervisor: Professor Clive Wilson

Department of Physiology, Anatomy and Genetics

# i: Declaration

The thesis I am submitting is entirely my own work except where otherwise indicated in the text.

## ii: Acknowledgements

I would first like to express my sincere gratitude to my supervisor Professor Clive Wilson. He has been supportive, enthusiastic and incredibly professional throughout this entire journey. He always shared his time freely whenever I needed help and his encouragement never failed to lift me up. I am truly grateful to have been part of his lab. This year has been a great journey and the best beginning I could have hoped for as I start my academic life.

I also wish to thank all members of the Wilson lab, past and present. In particular, I am deeply grateful to Dr Bhavna Verma. I spent the most time with her and she has been one of the best mentors I have ever had. She was always patient and willing to answer my questions in detail, and she taught me everything about the experiments. She generously shared her past experience, which helped me become a better version of myself after this year. I would also like to thank Dr Mark Wainwright. His extensive knowledge of *Drosophila* and his willingness to offer help in the lab have been invaluable. His mental support during some of the most difficult periods of this year helped me keep going when I had to face many challenges on my own.

My sincere thanks also go to Dr Amy Cording and to our former research assistant Lewis Blincowe. Both have been exceptionally helpful and kind. They guided me when I first joined the lab, helped me get familiar with everything that was new and stayed positive for me whenever I felt uncertain or lacked confidence. I would not have completed this master project so successfully without each of them.

Meanwhile, many thanks go to our department graduate study administrator, Sarah Noujaim. Throughout the year she has encouraged me in my studies and worked very hard to organize every seminar and event. She always offered her help with genuine warmth and dedication, doing everything she could to help me overcome any difficulty, and I am truly thankful for that.

I would also like to thank my parents, who supported me financially so that I could complete this valuable degree and gain one of the most treasured experiences of my life. My friends have also been incredibly important, especially during moments when I felt lost. I am especially grateful to my closest friend Doris Li, who has been with me for more than ten years and has accompanied me through every major moment in my life. I also thank those long-time friends who encouraged me even though we were in different places during my master year, including Cathy, Sarah, Vanessa, Cece, Lilly, Jerry, Maggie, Julia, Isaac and Henry. I am equally grateful for the friends I met at St Anne's College, including Dongyi, Barbara, Marcello, Emma, Jocelyn and Cristie. We shared a wonderful year together and their presence made my time in Oxford warm and unforgettable.

Finally, I want to thank myself. Always pursue what I truly love and keep going until the very end.

# iii: Abstract

Alzheimer's disease (AD) is a progressive neurodegenerative disorder characterised by two hallmark pathologies, extracellular amyloid plaques and intracellular neurofibrillary tangles composed of hyperphosphorylated tau. In addition to these well-known pathologies, increasing evidence indicates that early defects in secretory and endolysosomal trafficking play a central role in disease progression. Insulin resistance and impaired insulin signalling are also frequently observed in brains with AD, leading to the proposal that metabolic dysregulation may contribute to neurodegeneration. However, the cellular mechanisms linking disrupted insulin signalling to pathological protein trafficking remain poorly understood.

This study investigated how modulation of the insulin/PI3K/mTORC1 signalling pathway regulates dense core granule (DCG) biogenesis and endolysosomal trafficking using *Drosophila melanogaster* male accessory gland secondary cells (SCs) as a specialised secretory model. Insulin/PI3K/mTORC1 signalling activity was altered through targeted genetic manipulation of key components, including InR, PI3K, PTEN, Akt, Tsc1/2, Rheb and mTOR. In parallel, human Tau 2N4R wild type was overexpressed in SCs to model tauopathy observed in AD. DCGs were visualised via GFP-tagged MFAS, while lysosomes and acidified compartments were labelled with LysoTracker and analysed by live cell imaging.

Modulation of insulin/PI3K/mTORC1 signalling in healthy SCs revealed that both pathway upregulation and downregulation disrupted normal DCG biogenesis. Reduced signalling, particularly following *PI3K* knockdown, produced pronounced mini-core phenotypes and increased DCG acidification and lysosomal area, consistent with enhanced endolysosomal trafficking. In contrast, increased signalling

promoted DCG compartments formation but also led to structural abnormalities. hTau2N4R overexpression induced DCG compartments with cylindrical cores, increased compartment numbers and expanded lysosomal area, indicating substantial trafficking defects. Notably, both up- and down- regulation of insulin/PI3K/mTORC1 signalling partially rescued tau-induced DCG abnormalities, although normal endolysosomal trafficking was not fully restored.

Together, these findings demonstrate that insulin/PI3K/mTORC1 signalling showed bidirectional control over secretory and endolysosomal pathways and must be tightly balanced to maintain cellular homeostasis. Disruption of this equilibrium may predispose cells to early pathological changes associated with AD, supporting a mechanistic link between metabolic dysregulation and neurodegenerative progression.

# iv: List of abbreviations

AD: Alzheimer's disease
Akt: Protein kinase B (PKB)
APP: Amyloid precursor protein
APPL: Amyloid precursor protein-like
Aβ: Amyloid beta
BACE1: Beta-site amyloid precursor protein cleaving enzyme 1 / beta-secretase 1
BF: Bright field
BMP: Bone morphogenetic protein
Cdc42: Cell division cycle 42 / cell division control protein 42
DCGs: Dense core granules
DILPs: Drosophila insulin-like peptides
dsx: double-sex
Ecad: E-cadherin
EcR: Ecdysone receptor
ELMs: E-cadherin-enriched lipid microdomains
ESCRT: Endosomal sorting complex required for transport
FOXO: Forkhead box O (class O) family
GFP: Green fluorescent protein
GLP-1: Glucagon-like peptide-1
GSK3β: Glycogen synthase kinase 3 beta
GTPase: Guanosine triphosphatase
IGF-1: Insulin-like growth factor 1
IIS: Insulin/IGF signalling
ILVs: Intraluminal vesicles
InR: Insulin receptor
IRS: Insulin receptor substrate
MAG: Male accessory gland
MAPK: Mitogen-activated protein kinase
MAPT: Microtubule-associated protein tau
MCs: Main cells
MFAS: Midline fasciclin
mTOR: Mechanistic target of rapamycin

MVBs: Multivesicular bodies

NFkB: Nuclear factor kappa B

NFTs: Neurofibrillary tangles

PBS: Phosphate-buffered saline

PI3K: Phosphoinositide 3-kinase

PIP2: Phosphatidylinositol 4,5-bisphosphate

PIP3: Phosphatidylinositol 3,4,5-trisphosphate

PTEN: Phosphatase and tensin homolog

Rab: Ras-associated binding

Rac1: Ras-related C3 botulinum toxin substrate 1

Ras: Rat sarcoma viral oncogene homolog

RFP: Red fluorescent protein

Rheb: Ras homolog enriched in brain

ROS: Reactive oxygen species

SCs: Secondary cells

siRNA: small interfering RNA

T2DM: Type 2 diabetes mellitus

TFEB: Transcription factor EB

TGFBI: Transforming growth factor beta induced

Tsc: Tuberous sclerosis complex

# v. Table of Contents

# Introduction

## Alzheimer's disease and its complexity

Alzheimer's disease (AD) is a progressive neurodegenerative disorder characterized by memory loss and cognitive decline, which is the most common cause of dementia among global aging populations (DeTure & Dickson, 2019). AD is a mixed proteinopathy with the presence of two hallmark pathologies (Zheng & Wang, 2025). Extracellular amyloid plaques in AD are primarily composed of aggregated amyloid beta (Aβ) peptides derived from aberrant cleavage of transmembrane amyloid precursor protein (APP) by β- and γ-secretase (Thal et al., 2002; Gouras et al., 2014). Meanwhile, the intracellular neurofibrillary tangles in AD are composed of hyperphosphorylated tau (Congdon et al., 2023), a microtubule-associated protein that normally stabilizes the cytoskeleton and regulates intracellular transport (Hervy & Bicout, 2019). In AD, tau undergoes abnormal post-translational modifications, leading to filamentous aggregations, neuronal dysfunction and a pattern of progression that correlates strongly with cognitive decline (Alquezar et al., 2021; Boccalini et al., 2023).

Amyloid and tau pathologies remain central to AD research, and there are already treatments targeting abnormal Aβ protein aggregations in the brain using monoclonal antibody-based approaches (Holmes et al., 2008; Kim et al., 2025). However, it has so far only slowed the disease progression without halting or reversing the cognitive decline (Travis, 2018). This therapeutic gap suggests that as well as amyloid and tau histopathology, there must be other mechanisms involved in initiating or exacerbating pathological events in AD. In recent years, increasing attentions have

turned towards changes in cellular mechanisms controlling secretory and endolysosomal trafficking, which are considered as important contributors to metabolic dysregulation and early AD-associated defects in intra- and inter- cellular transport (Acker et al., 2019; Lee et al., 2022).

## Aβ generation and endolysosomal trafficking in AD

Disruptions in intracellular trafficking directly contribute to Aβ pathology in AD, while accumulating Aβ in turn exacerbates those trafficking defects, creating a vicious cycle. On the secretory pathway side, proteins that control vesicle sorting are crucial for controlling where APP is processed. APP is a transmembrane protein that traffics through the secretory and endocytic pathway, and the location of its cleavage by secretases determines whether harmless or toxic fragments are produced (Choy et al., 2012). For example, the clathrin AP-1 at the trans-Golgi network normally helps to assign APP into the proper post-Golgi compartments, and loss of AP-1 shifts APP processing toward the amyloidogenic route, leading to excessive production of neurotoxic Aβ fragments (Januário et al., 2022). On the endocytic pathway side, the endosomal network is a major site of Aβ production and also the process to trigger Aβ toxicity. β-secretase (BACE1) colocalises with APP in both early and recycling endosomal compartments (Das et al., 2015). If the recycling or retargeting of APP and BACE1 is disrupted, APP can stay in these endosomes longer than it should, resulting in excessive cleavage, promoting Aβ production. This is also seen in the case of certain AD risk genes like *BIN1* and *CD2AP,* which are regulators of endocytic trafficking, by keeping APP and BACE1 apart in early endosomes. When either regulator is reduced, there is an increased rate of convergence between

APP and BACE1 in early endosomes, thus accelerating Aβ generation (Ubelmann et al., 2016).

Recent studies demonstrated that extracellular release of Aβ oligomers can bind to APP at other neurons across synapses and trigger additional APP endocytosis and cleavage, effectively promoting further production (Rolland et al., 2020). Meanwhile, Aβ oligomers and fibrils enhance the colocalization between APP and BACE1 inside recycling endosomes, accelerating amyloidogenic processing of APP and intracellular accumulation of Aβ42 in a positive feedback loop (Antonino et al., 2022). Additionally, the insoluble Aβ42 accumulates in synaptic endosomal vesicles that have characteristics of multivesicular bodies (MVBs) (Eckman et al., 2023). These Aβ-rich MVBs can fuse with the plasma membrane to release their internal vesicles as exosomes, spreading toxic Aβ species between neurons.

## Intracellular trafficking events are regulated by APP in AD

A challenge in forming a unified model of intracellular trafficking in AD is that pathological APP processing, Aβ and Tau aggregation occur in multiple cellular compartments. A recent *Drosophila* study revealed that APP resides on the limiting membrane of regulated secretory compartments, where its extracellular domain normally promotes the membrane-dependent aggregation of luminal proteins to form a dense-core granule (DCG; Singh et al., 2025). APP is then cleaved to release the aggregated proteins so that they form a central DCG in the compartment. When human Aβ peptides are expressed, the formation of these secretory compartments is severely perturbed and specifically the Rab11-positive secretory compartments are

abnormally rerouted to lysosomes. As part of this AD-mimicking pathology, recycling endosomes, also known as secretory compartments in this case, containing BACE1 and APP fuse more frequently to late endosomes/lysosomes, which contain gamma secretase (Pasternak et al., 2003). Since gamma secretase is critical for the generation of Aβ peptides, this altered trafficking pattern further promotes the amyloidogenic cleavage (Hur, 2022). Thus, APP normally facilitates controlled membrane-dependent protein aggregation and subsequent dissociation from membranes in the secretory pathway, whereas Aβ pathologically disrupts this mechanism.

Consistent with these findings, mammalian models show that intraluminal vesicles (ILVs) and exosomes are integral to APP/Aβ trafficking. Neurons release exosomes containing full-length APP and Aβ, and exosomes isolated from mouse brains indeed carry these APP metabolites and processing enzymes (Perez-Gonzalez et al., 2012). Dysregulation of endosomal recycling causes APP fragments to accumulate in endosomes and be secreted in Rab11-dependent exosomes, increasing extracellular Aβ oligomers (Walsh et al., 2021; Daly et al., 2023). Worth noting, neuronal exosomes are enriched in raft-like lipid microdomains (e.g. GM1 ganglioside-rich domains) that can nucleate Aβ aggregation, implicating that certain exosome subtypes may also play a role for Aβ oligomerization and amyloid seeding (Ariga et al., 2001; Hayashi et al., 2004; Liang et al., 2023).

The biogenesis and maturation of secretory compartments are closely linked to cytoskeletal and membrane dynamics. For example, E-cadherins and small GTPase Rap1 likely help to recycle and stabilize endosomes during cell-cell adhesion (Balzac

et al., 2005), while actin-binding proteins and microtubule regulators (e.g. cofilin and Tau) facilitate the sorting of secretory cargos into transport vesicles and control dynamic trafficking (Ohashi et al., 2000; Curwin et al., 2012). In AD, Aβ oligomers induce an aberrant phosphorylation of cofilin that locks actin in a stable state (Cichon et al., 2012; Rush et al., 2018), and expression of pathological Tau is known to disrupt microtubule stability and secretory trafficking events, thereby preventing vesicles with pathological aggregates degrading.

In summary, APP's physiological role in coordinating the regulated secretory pathway becomes dysregulated in AD, involving not only abnormal cleavage that generates toxic Aβ species but also the induction of secretory and cytoskeletal dysfunction. However, the exact mechanism of how these cytoskeletal proteins function in intracellular trafficking and how they become dysregulated in AD is still poorly defined and requires further study.

## Tau–Aβ crosstalk and vesicle trafficking defects

Tau pathology is also tightly linked to secretory trafficking and endolysosomal dysfunction in AD. The hyperphosphorylation of tau and its aggregation into neurofibrillary tangles (NFTs) destabilize microtubules, impairing the axonal transport of vesicles and organelles (Reddy, 2011). The over-abundance of tau, as well as NFTs, can fragment the Golgi apparatus, undermining its role in protein processing and sorting (Liazoghli et al., 2005; Jiang et al., 2014; Joshi et al., 2015). Tangled tau itself can also promote new intracellular aggregates by damaging the

endomembrane and helping luminal content escape into the cytosol (Calafate et al., 2016).

Adding to this complexity, Aβ and tau appear to potentiate each other's toxicity through feedback loops in trafficking pathways. Aβ42 can be endocytosed by neurons and induce endolysosomal protofibrils to form, causing endolysosomal leakage that releases proteases (e.g. asparagine endopeptidase) and in turn triggers tau hyperphosphorylation (Gao et al., 2025). Conversely, tau-induced endosomal traffic jams favour the accumulation of toxic Aβ species by dampening the ability of cells to degrade them (Small et al., 2017). There is also evidence that Aβ and tau both bind to the luminal proton pump (V-ATPase), and this inhibition reduces proton pumping and impairs acidification of endolysosomes (Kim et al., 2023). These defects in endolysosomal functional integrity are not only consequences of Aβ and tau pathologies, but also the response to induced neurotoxicity. However, it still remains unclear which pathology initiates the vicious cycle. Regardless of that, most studies now view AD progression as the result of pathogenic crosstalk between Aβ, tau, and endolysosomal dysfunction, rather than a linear cascade (Villegas et al., 2022). Intervening in this complicated network has become a key therapeutic target for delaying AD onset and slowing down the disease progression.

## Linking AD and insulin signalling: Type 3 Diabetes Hypothesis

In recent years, many studies have noticed parallels between AD and Type 2 Diabetes Mellitus (T2DM), leading to a statement that AD may be considered as "Type 3 diabetes". Epidemiologically, individuals with T2DM have ~1.5 times higher

chance of being diagnosed with cognitive impairment (Xue et al., 2019) and a ~60% increased risk of getting dementia compared to non-diabetics (Cao et al., 2024; Mateusz Kciuk et al., 2024). AD brains gradually develop insulin resistance and impaired glucose metabolism reminiscent of T2DM (Steen et al., 2005). Postmortem and clinical studies show that insulin signalling in AD brains is dysregulated with insensitive insulin receptors and disrupted downstream signalling components, even in patients without peripheral diabetes (Rivera et al., 2005; Suzanne & Wands, 2008).

In peripheral tissues, insulin binding to its receptor activates two major cascades: the PI3K-Akt pathway and the Ras-MAPK pathway (Boucher et al., 2014). Both are also present in neurons and play vital roles in cell survival, metabolism and plasticity (Scherer et al., 2021). Under normal conditions, insulin or IGF-1 binding to receptors initiates a cascade of phosphorylation events, which recruits and activates the Class I phosphatidylinositol 3-kinase (PI3K). PI3K generates PIP3 lipid messengers, which dock Akt kinase to the membrane where it is phosphorylated and activated. Active Akt promotes anabolic and pro-survival processes, leading to the enhancement of glucose uptake and utilization, and supporting synaptic protein synthesis. Insulin signalling also activates the mechanistic Target of Rapamycin Complex 1 (mTORC1) pathway via Akt. It mainly modulates protein synthesis and autophagy. High mTORC1 activity tends to promote protein synthesis and suppress autophagy, whereas reduced mTORC1 activity has the opposite effect, leading to enhanced autophagic degradation. The Ras-MAPK signalling pathway functions in parallel with the PI3K-Akt pathway, and is crucial to regulate the transcriptional programs for synaptic plasticity, memory formation and emotional behavior (C. Mazzucchelli &

Brambilla, 2000; Héctor Albert-Gascó et al., 2020). Dysregulation of this pathway has been implicated in several neurodegenerative conditions (Gravandi et al., 2023), but compared with PI3K-Akt, its role in AD pathology seems less direct and more poorly defined.

## Dysregulation of insulin signalling pathways in AD

Insulin signalling in the brain is closely correlated to pathological mechanisms of AD, although whether it is a primary cause or a secondary consequence remains unresolved. Current evidence shows that insulin and IGF-1 signalling normally regulate the balance between amyloidogenic and non-amyloidogenic processing of APP through the PI3K-Akt pathway (Elham Razani et al., 2021; Kumar & Bansal, 2021; Miao et al., 2024). When insulin resistance develops due to T2DM, this signalling cascade is impaired, resulting in overactive GSK3β due to insufficient inhibition of Akt and downregulated mTORC1 signalling, along with reduced levels of insulin and IGF-1 receptors in some regions (Berlanga-Acosta et al., 2020). Under these conditions, APP is preferentially processed by β-secretase, promoting amyloidogenic cleavage and Aβ accumulation (Zhang et al., 2018; Sędzikowska & Szablewski, 2021).

Meanwhile, decreased Akt activity promotes tau phosphorylation and aggregation into neurofibrillary tangles, and may also affect axonal transport by phosphorylating kinesin motor proteins, leading to abnormal vesicle movement and synaptic dysfunction when insulin signalling fails (Hong et al., 1997; Morfini et al., 2002). Loss of PI3K-Akt signalling overactivates the GSK3β activity, which targets multiple

proline-directed sites on tau, resulting in tau detachment from microtubules and destabilisation of the cytoskeletal network (Kumar & Bansal, 2021). Hyperphosphorylated tau not only disrupts microtubule assembly but also tends to self-aggregate into paired helical filaments and NFTs, driving cytoskeletal collapse, impaired intracellular trafficking, and eventually leading to neuronal death (Kitagishi et al., 2014; Yang et al., 2020). In general, insulin resistance as a key hallmark of pre-diabetes, creates an environment in which both Aβ and tau pathologies are more likely to emerge and propagate.

Additionally, in healthy neurons, constitutive autophagy and lysosomal biogenesis are highly efficient and play an important role in clearing harmful protein aggregates, in which they are highly regulated by the transcription factor EB (TFEB). Activation of the TFEB-dependent autophagy-lysosomal pathway protects neurons (Franco-Juárez et al., 2022; Song et al., 2025). However, this process appears to be inefficient in both AD and T2DM with insulin resistance. Neurons accumulate large numbers of autophagosomal vesicles, though it remains unclear whether this results from continued activation and formation of autophagosomes, or instead a failure in their clearance through lysosomal degradation and cargo trafficking (Boland et al., 2008; Nixon, 2017). Dysregulated insulin/PI3K/mTORC1 signalling further exacerbates these abnormalities by altering APP processing and disturbing TFEB-dependent autophagy. This amplifies Aβ production while increasing lysosomal activity, but also blocks effective trafficking to these lysosomes in pathology, which ultimately reduces degradative capacity (Son et al., 2012; Cheng et al., 2023).

In Parkinson's disease models, boosting insulin signalling, such as with GLP-1 receptor agonists, primarily used as diabetic treatments, displayed improvements on energy metabolism and neuroprotection. These drugs activate the PI3K-Akt signalling pathway and promote dopaminergic neuron survival by reducing apoptosis, improving cognitive and motor dysfunction (Dongliang et al., 2024). However, in some experiments on neurodegenerative diseases, interventions suppressing the insulin/PI3K/mTORC1 pathway have shown significant neuroprotective effects. Using transgenic mice with AD, long-term inhibition of mTOR with rapamycin prevented the development of AD-like cognitive impairments and significantly lowered the toxic Aβ42 levels (Spilman et al., 2010). Rapamycin treatment also reduced tauopathy via enhanced autophagic clearance, effectively delaying the AD disease progression (Zeba Mueed et al., 2019).

In Huntington's disease (HD) mouse models, both IGF-1 supplementation and the diabetic drug metformin alleviate motor and neuropsychiatric symptoms by modulating the pathway (Sanchis et al., 2019; Niels Henning Skotte et al., 2020). IGF-1 activates Akt-mediated pro-survival signalling and has shown therapeutic benefits in HD mice, while metformin's activation of AMP-activated protein kinase (upstream antagonist of mTORC1) suppresses mTORC1 signalling and enhances lysosomal function to clear mutant huntingtin aggregates and improve behavioural outcomes.

Evidence shows that people with T2DM are more likely to develop not only AD but also other neurodegenerative diseases (Santiago et al., 2023). Also, there is an even larger chance for patients who already have neurodegenerative diseases and pre-

diabetes to experience faster progression compared to those without metabolic disorders. T2DM and dysregulated insulin signalling are strongly linked to neurodegenerative diseases, even though the exact mechanisms remain unclear and increasing or decreasing insulin/PI3K/mTORC1 signalling activity can have both positive and negative effects in AD models (Figure 1). Despite these complexities, these observations have suggested that normalizing insulin signalling pathway in neurodegenerative patients with concurrent T2DM might help to delay the onset or slow the progression of the disease. Furthermore, they indicate that precise modulations of insulin/PI3K/mTORC1 signalling may be required for a positive therapeutic effect and may therefore require assessment at a personalised, patient-by-patient level.

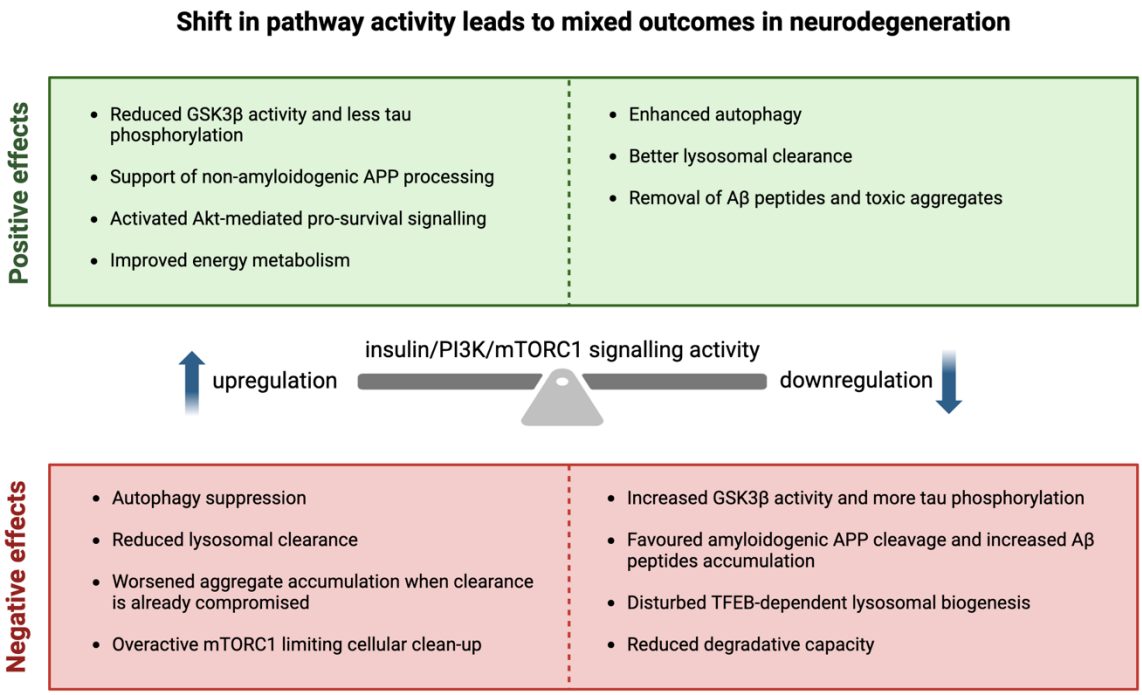


**Figure 1. Effects of bidirectional insulin/PI3K/mTORC1 signalling modulation on neurodegeneration.**

This diagram illustrates how both increased and reduced insulin/PI3K/mTORC1 signalling can lead to a mix of beneficial and harmful outcomes under neurodegeneration, which highlights that a balanced pathway is likely required for optimal neuronal health.

## Using *Drosophila melanogaster* as a model organism to study AD cell biology

In this study, I used *Drosophila melanogaster* as a model organism. The fruit fly offers unique advantages as an experimental system. It has many signalling pathways that are highly conserved when compared to human pathways and low genetic redundancy. Also, flies have a very short generation time and are easily maintained and manipulated genetically (Yadav et al., 2016; Verheyen, 2022). These features make *Drosophila* cost-effective for many experiments, enabling large-scale screening of different genes and rapid identification of gene and protein functions in disease-related pathways.

*Drosophila* has been widely used in AD research so far because flies have homologs of key AD-related proteins. For instance, the γ-secretase complex and its substrates, such as the fly APP-like protein APPL, are conserved between flies and humans (Ye & Fortini, 1999; Jeon et al., 2020). Similarly, *Drosophila* expresses a tau homolog that binds microtubules and also has disease-related phosphorylation sites conserved with human tau (Heidary & Fortini, 2001). Transgenic flies expressing human Aβ, APP/BACE or tau develop age-dependent neurodegeneration, neuronal loss and cognitive defects that parallel with human AD symptoms (Wittmann et al., 2001; Sowade & Jahn, 2017). Building on those findings, recent studies have successfully established *Drosophila* as a powerful model for studying neurodegenerative diseases, particularly AD in the context of the insulin signalling pathway and its potential neuroprotective effects (Chen et al., 2016; Wei et al., 2025).

## Conservation of the insulin signalling pathway

The insulin/IGF signalling (IIS) pathway is highly evolutionarily conserved between *Drosophila* and humans (Krishnan et al., 2024). In both species, IIS is a key regulator of growth, metabolism, stress resistance, reproduction and lifespan (Giannakou & Patridge, 2007; Templeman & Murphy, 2018). *Drosophila* has a single insulin/IGF receptor (InR) that is highly homologous to the human insulin receptor. In both flies and mammals, binding of insulin (or *Drosophila* insulin-like peptides, DILPs) causes the InR to autophosphorylate and recruit adapter proteins, insulin receptor substrate (IRS) in humans and Chico in flies, as shown in Table 1 and Figure 2 (Brogiolo et al., 2001; Grönke et al., 2010). Additionally, downstream core steps are shared in flies and humans. The *Drosophila* gene *dp60* encodes the homolog of the mammalian PI3K regulatory subunit p85, which couples InR to the catalytic phosphoinositide-3-kinase (PI3K), subunit *dp110*. This activates PI3K, which converts $PIP_2$ to $PIP_3$, then recruiting Akt to be phosphorylated and activated. PTEN acts as the main negative regulator of the PI3K-Akt pathway, forming a key inhibitory node that opposes PI3K activity and decreases the availability of PIP3 (Georgescu, 2010). Active Akt phosphorylates multiple downstream targets, including the Tsc complex, the transcription factor FOXO and GSK3β (*Drosophila shaggy*), thereby integrating nutrient and growth signals into cell growth and metabolic homeostasis (Sadagurski & White, 2012). The Tsc/Rheb axis in turn activates mTOR or TOR, driving a series of anabolic reactions, including protein and lipid synthesis in cells. Overall, this strong extent of conservation (see Table 1 for component comparison and Figure 2 for the IIS pathway comparison) makes *Drosophila* a suitable and powerful model to explore the insulin signalling pathway.

| **Compounds** | **Human** | ***Drosophila melanogaster*** |
|---|---|---|
| Ligand | Insulin, IGF | *Drosophila* insulin-like peptides 1-8 (DILPs 1-8) |
| Receptor | Insulin receptor, InR | dInR |
| Insulin receptor substrate | IRS 1-6 | Chico |
| Regulatory subunit | p85 | dp60 |
| Catalytic subunit | p110 | dp110 |
| Phosphatidylinositol 3-kinase | PI3K | PI3K |
| PTEN phosphatase | PTEN | dPTEN |
| Protein kinase B | Akt | dAkt |
| Tuberous sclerosis complex | Tsc1, Tsc2 | Tsc1, Tsc2 |
| Rheb (Ras homolog enriched in brain) | Rheb | dRheb |
| mTOR complex 1 | mTOR, Raptor, Rictor | dTOR, Raptor, Rictor |
| FOXO transcriptional factor | FOXO | dFOXO |
| Glycogen synthase kinase 3 | GSK3β | Shaggy (sgg) |
| Ras | Ras | Ras85D |
| Raf | Raf | dRaf |
| MEK1/2 | MEK1, MEK2 | Dsor1 (Downstream of raf 1) |
| MAPK (ERK) | ERK1 (MAPK3) ERK2 (MAPK1) | Rolled (rl) |

**Table 1. Comparison of insulin signalling pathway components in human and *Drosophila melanogaster.***

The table lists key components of the two major insulin signalling pathway branches, both of which are illustrated in Figure 2 below. Mammalian counterparts are shown

alongside their *Drosophila* orthologs to highlight pathway conservation. Information was adapted from Semaniuk et al., (2021) and supplemented with information from FlyBase (https://flybase.org/).

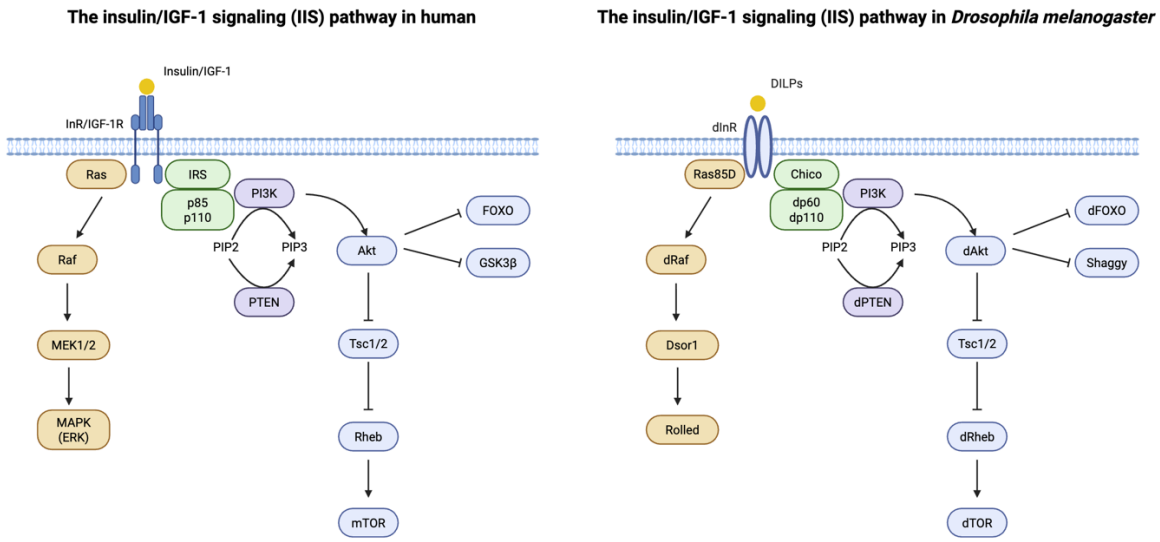


**Figure 2.** Overview of the insulin/IGF-1 signalling (IIS) pathway in human and in *Drosophila*.

## The *Drosophila* male accessory gland and secondary cells as the model for regulated secretion and physiological APP function

Most models used for neuroscience research offer limited access to intracellular secretory dynamics because neuronal secretory vesicles are too small to be visualized internally by conventional light microscopy. In contrast, prostate-like secondary cells of the adult *Drosophila* male accessory gland (MAG), a reproductive secretory organ, have been developed as an *in vivo* model for regulated secretion (Wells et al., 2023). The MAG consists of abundant main cells (MCs) and a small proportion of specialized secondary cells (SCs). The latter have giant Rab11-positive regulated secretory compartments, which are many thousand-fold larger than typical neuronal granules (Redhai et al., 2016). They produce large DCGs and, at the same time, generate small intraluminal vesicles (ILVs) that can be released from the cell as exosomes when the cells are stimulated, processes that might be considered analogous to neuropeptide secretion in humans. The large size of these compartments makes it possible to visualize and quantify the dynamic secretory and trafficking events taking place in real time. This has allowed the cellular processes that underpin maturation of regulated secretory compartments to be assessed for the first time (Fan et al., 2020; Wells et al., 2023; Marie et al., 2023; Singh et al., 2025). Meanwhile, a recent study has successfully used the *Drosophila* MAG to study the insulin signalling pathway in main cells, further demonstrating this novel model is reliable for investigating conserved secretory mechanisms *in vivo* (Rambur et al., 2020).

Immature SC regulated secretory compartments originate from the Golgi apparatus (marked by Rab6) but then acquire recycling endosomal Rab11-positive inputs and identity as they mature, as shown in Figure 3. This Rab6-to-Rab11 transition is essential for DCG formation and ILVs biogenesis in *Drosophila*, and current evidence from human cells indicates that this maturation step is evolutionarily conserved (Wells et al., 2023; Stockhammer et al., 2024).

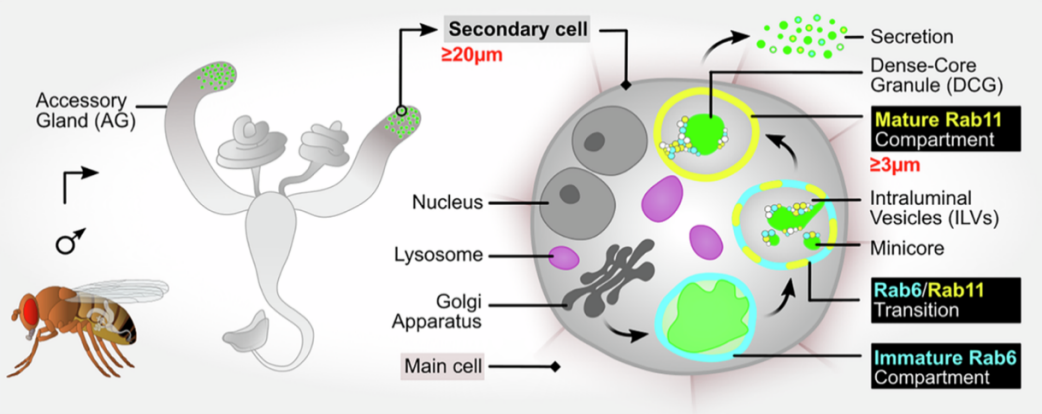


**Figure 3.** Schematic of the *Drosophila* male accessory gland (MAG), highlighting secondary cells (SCs) at the distal tip, their main intracellular compartments with dense core granule (DCG), and the Rab6-to-Rab11 transition (Adapted from Singh et al., 2025).

Our lab developed a unique GFP-MFAS line, expressed from the endogenous *mfas* gene locus, as a marker for DCG protein aggregation. This GFP-MFAS line fluorescently labels Midline Fasciclin (MFAS), which is the *Drosophila* orthologue of human extracellular matrix protein, TGFβ-induced (TGFBI), and is very highly expressed in DCGs (Hu et al., 1998; Singh et al. 2025). According to findings from our lab, numerous small GFP-MFAS aggregates first emerge along the limiting membrane of immature regulated secretory compartments. These transient mini-cores are mobile within the lumen and quickly merge through coalescence, resulting in a single and circular, centrally located DCG (Singh et al., 2025), as shown in Figure 4A. In addition, SCs with *mfas* knockdown form large Rab11-positive compartments devoid of any visible DCG, indicating that MFAS is required for protein aggregation in the regulated secretory pathway of SCs.

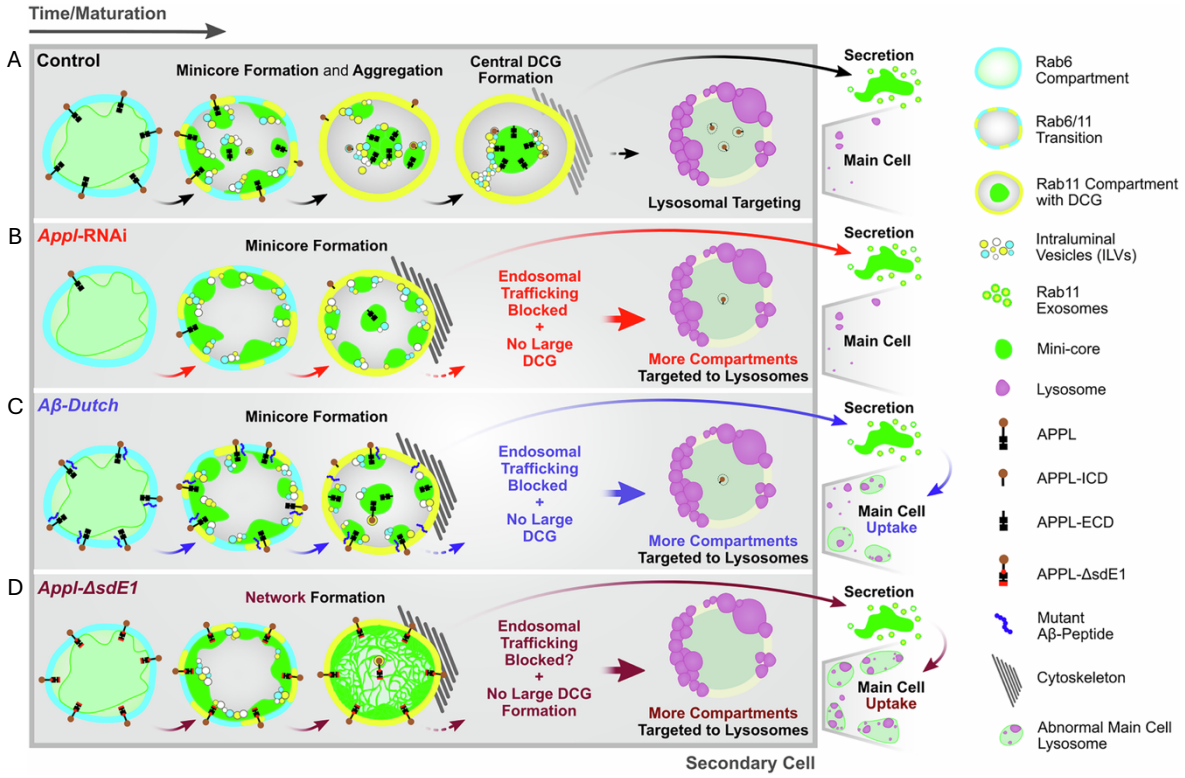


**Figure 4.** Diagrams illustrating DCG biogenesis and lysosomal acidification within SCs, together with the phenotypic propagation observed in main cells, under the following conditions: (A) control (B) *Appl* knockdown (C) pathological Aβ42-Dutch mutant expression and (D) non-cleavable form of APPL (APPL-ΔsdE1 mutant) expression (Adapted from Singh et al., 2025).

Surprisingly, APPL (the fly APP homologue) also regulates MFAS aggregation, DCG biogenesis and regulated secretory compartments, and its proteolytic cleavage is critical for DCG maturation (Figure 4B). This process may parallel the mechanism for amyloidogenic APP processing in humans, which occurs in recycling endosomes. APPL contains conserved α-, β-, and γ-secretase cleavage sites that release fragments similar to human Aβ peptides (Fossgreen et al., 1998). Under normal conditions, membrane-associated APPL appears to prime DCG protein aggregation and then its cleavage releases its extracellular domain associated with these aggregates, allowing them to dissociate from the compartmental limiting membrane and fuse into a single mature DCG (Singh et al., 2025). When APPL is non-cleavable or absent, aggregates stay attached to the membrane, often as mini-cores, and impair DCG maturation (Figure 4B and 4D). This abnormal biogenesis process also promotes the lysosomal targeting of these compartments, which are acidified, but fail to be degraded by lysosomes, which parallels the early endolysosomal dysfunctions observed in AD.

Human APP expression can partially rescue DCG biogenesis in SCs, as well as behavioural defects induced by *Appl* loss of function in flies (Luo et al., 1992; Singh et al., 2025), suggesting both functions are conserved. Pathogenic human Aβ expression disrupts APP-regulated protein aggregation; compartments mature to Rab11 identity but mini-core aggregates remain immobile at the compartmental limiting membrane and fail to coalesce (Singh et al., 2025). These compartments are targeted for lysosomal degradation, but they do not traffic normally and their contents appear to be secreted (Figure 4C). Moreover, these SC-derived secretions are endocytosed by main cells and induce endolysosomal defects. Both non-cleavable

APPL and Aβ expression induce abnormal accumulation of GFP-MFAS in lysosomal compartments in main cells, propagating the endolysosomal phenotype. This phenomenon will be referred to as the main cell phenotype, also known as phenotypic propagation.

Therefore, using the SC model, it has been shown that *Appl* loss or Aβ expression alters DCG dynamics, leading to endolysosomal trafficking defects that propagate between cells, phenotypes that are highly relevant to AD pathology.

## Tau and the cytoskeleton also regulate DCG biogenesis

The *Drosophila* SC system has been successfully employed to study subcellular and sub-compartmental dynamic phenotypes induced by AD-relevant genetic manipulations (e.g. APPL variants and loss-of-function, Aβ wild type and mutants), providing mechanistic insight into how secretory and endolysosomal trafficking might become compromised in early disease stages. Notably, our lab also observed that loss of cofilin produces cylindrical cores in SC compartments that remain in contact with the limiting membrane, indicating a requirement for actin turnover to ensure normal aggregates release and granule morphology during DCG maturation (B. Verma, unpublished data).

Recent unpublished work (B. Verma) shows that overexpression of human Tau 2N4R in SCs reproduces the *cofilin*-knockdown phenotype (see Figure 11). Tau 2N4R refers to a specific isoform of the human microtubule-associated protein Tau, which plays a central role in microtubule stabilization and axonal transport in neurons

(Cario & Berger, 2023; Buchholz & Zempel, 2024). Tau protein is encoded by the *MAPT* gene, which undergoes alternative splicing to generate six major isoforms in the adult human brain. These isoforms differ by the inclusion or exclusion of two N-terminal inserts (0N, 1N, or 2N) and by having either three or four microtubule-binding repeat domains (3R or 4R) (Bachmann et al., 2021; Shahpasand-Kroner et al., 2022). Tau 2N4R represents the longest human isoform, containing two N-terminal inserts and four microtubule-binding repeats, giving it a total length of 441 amino acids (Iqbal et al., 2010). This isoform is widely used in experimental AD and tauopathy models because it is the most toxic among all tau species and relatively abundant in adult cortical neurons (Pampuscenko et al., 2021). Tau 2N4R can induce neuronal loss even under a low molecular concentration and is prone to undergo hyperphosphorylation, driving neurofibrillary tangle formation.

Live cell imaging shows that overexpression of human Tau 2N4R in SCs stabilises GFP-MFAS aggregates at the compartmental limiting membrane, forming elongated cylindrical cores touching the compartmental limiting membrane instead of central and spherical morphology. In this way, disruptions of two different cytoskeletal regulators (cofilin and Tau) converge on a common abnormal DCG morphology, suggesting that defective maturation of DCG compartments can be tightly linked to abnormal functioning of the cytoskeletal network (Cichon et al., 2012).

## Study Rationale and Objectives

The findings described above motivate the focus of my present project. SCs in the *Drosophila* male accessory gland allow direct and real-time visualisation of DCG biogenesis, which makes it possible to test how different regulators modulate secretory outcomes. Experiments to date implicate defective cytoskeletal assembly and endolysosomal trafficking in response to AD-related genetic manipulations. As discussed above, the insulin/PI3K/mTORC1 signalling controls cytoskeletal and endolysosomal dynamics, and this can positively or negatively impact on AD-associated neurodegeneration via multiple mechanisms. I therefore aimed to:

1. Examine how modulating insulin/PI3K/mTORC1 signalling affects secretory and endolysosomal trafficking events in SCs.

2. Determine whether upregulation or downregulation of the insulin/PI3K/mTORC1 signalling pathway can suppress the defects induced by overexpressing cytoskeletal tau, including restoring DCG biogenesis, compartment maturation and normal routing of secretory and endolysosomal trafficking.

My overall objective was to clarify how metabolic signalling, also implicated in T2DM, interplays with early secretory and endolysosomal trafficking pathology in AD to shed light on why modulating insulin/PI3K/mTORC1 signalling can have variable effects on pathological outcomes.

# Materials and Methods

## Fly stocks

| **Experimental models: Organisms/Strains** | | | |
|---|---|---|---|
| ***Drosophila* Genotypes** | **Name in text** | **Source** | **Stock Number** |
| **Transgenic/Reporter lines** | | | |
| *$w^{1118}$; GFP-mfas$^{MI11275\text{-}GFSTF.2}$* | N/A | BDSC | # 63204 |
| *$w^{1118}$; if/CyO; dsx-GAL4/TM6B* | N/A | Goodwin Lab, Oxford (Rideout et al, 2010) | N/A |
| *$w^{1118}$; tub-GAL80$^{ts}$; TM2/TM6B,Tb* | N/A | BDSC | # 7108 |
| *$w^{1118}$; tub-GAL80$^{ts}$/CyO; dsx-GAL4/TM6B* | N/A | Wilson Lab (Corrigan et al, 2014) | N/A |
| *$w^{1118}$; tub-GAL80$^{ts}$/CyO; dsx-GAL4,GFP-mfas/TM6B* | td-GFP-MFAS | Wilson Lab | N/A |
| *$w^{1118}$; P{UAS-hTau.2N4R.wt}attP40; +* | N/A | BDSC | # 90949 |
| *$w^{1118}$; hTau-2N4R-WT, tub-GAL80$^{ts}$/CyO; dsx-GAL4, GFP-mfas/TM6B* | td-GFP-MFAS-Tau2N4R | Wilson lab | N/A |
| **UAS-transgenes** | | | |
| *$y^1$ sc* $v^1$ sev$^{21}$; P{ry$^{TRiP.HMS02827}$};+* | *rosy*-RNAi | BDSC | # 44106 |
| *$w^{1118}$* | *$w^{1118}$* | Partridge Lab, UCL | N/A |
| *$y^1$ $v^1$; +; P{Pi3K92E$^{TRiP.JF02770}$}* | *PI3K*-RNAi #1 | BDSC | # 27690 |
| *$w^{1118}$; +; P{Dp110$^{GD11228}$}* | *PI3K*-RNAi #2 | VDRC | # 38985 |
| *$y^1$ $v^1$; +; P{Akt1$^{TRiP.HM04007}$}* | *Akt1*-RNAi #1 | BDSC | # 31701 |
| *$y^1$ $v^1$; +; P{Akt1$^{TRiP.HMS00007}$}* | *Akt1*-RNAi #2 | BDSC | # 33615 |
| *$y^1$ sc* $v^1$ sev$^{21}$; +; P{tor$^{TRiP.GL00156}$}* | *tor*-RNAi | BDSC | # 35578 |
| *$w^{1118}$; +; P{PTEN$^{GD13500}$}* | *PTEN*-RNAi | VDRC | # 35731 |
| *$w^{1118}$; P{$w^+$; UAS-DPTEN FF20.2}/CyO; +* | UAS-*PTEN* | Goberdhan Lab (Goberdhan et al., 1999) | N/A |

| | | | |
|---|---|---|---|
| *$w^{1118}$; +; UAS-Tsc1 UAS-Tsc2/TM6* | UAS-*Tsc1/2* | Wilson Lab | N/A |
| *$w^{1118}$; +; P[$w^{+}$;UAS-$InR^{wt}$]/TM3 Sb* | UAS-*InR* | Hafen Lab (Brogiolo et al., 2001) | N/A |
| *$y^{1}$ $w^{1118}$; +; dRheb$^{AV4}$/TM3* | UAS-*Rheb$^{AV4}$* | Lengyel Lab (Patel et al., 2003) | N/A |

**Table 2.** All *Drosophila* stocks used in this thesis are detailed in the table above. Genotypes, name in text, source and stock number (if applicable) are shown. Stocks were sourced from collaborating labs, and two public stock centres, Bloomington *Drosophila* Stock Centre (BDSC) (Ni et al., 2009) and Vienna *Drosophila* Resource Centre (VDRC) (Dietzl et al., 2007).

## Fly husbandry

All *Drosophila* lines were maintained in either plastic vials or bottles with a standard cornmeal agar diet [12.5 g agar (F.Gutlind & Co.Ltd), 75 g cornmeal (B. T. P. Drewitt), 93 g glucose (Sigma-Aldrich, #G7021), 31.5 g inactivated yeast (Fermipan Red, Lallemand Baking), 8.6 g potassium sodium tartrate tetrahydrate (Sigma-Aldrich, #S2377), 0.7 g calcium chloride dihyrdrate (Sigma-Aldrich, #21907), and 2.5 g nipagin (Sigma-Aldrich, #H5501) dissolved in 12 ml ethanol, per litre]. Stocks were generally kept at 25°C and transferred into fresh vials or bottles every 2-4 weeks. Bottles from two GFP-MFAS knock-in reporter lines td-GFP-MFAS and td-GFP-MFAS-Tau2N4R were used for virgin female flies collection daily in the morning, isolated in small groups (8-10 flies) and kept for several days at 19°C to confirm they were unmated before use. For experimental crosses, those virgin female flies were

crossed with healthy male flies (usually 4-5 male flies) with UAS-transgenes of interest to permit induction of SC-specific expression.

Crosses were maintained at 25°C to increase the rate of development, with adults transferred into new vials with fresh food medium every 4–6 days to avoid overcrowding and mating between the parental flies and their offspring. Virgin male progenies from experimental crosses were collected on eclosion and typically shifted to the 29°C incubator for 6 days to activate post-developmental SC-specific transgene expression. Subsequent dissections and imaging were carried out at the end of this induction period.

## Dissection and mounting accessory glands for imaging

Accessory glands were dissected from six-day-old adult virgin male flies under $CO_2$ anaesthesia. Dissections were carried out in ice-cold 1x PBS (Thermo Fisher Scientific), with the male reproductive tract gently removed by pulling the terminal abdominal segment using fine forceps. Non-gland tissues (the testes, seminal vesicles, ejaculatory bulb, fat tissues, and the gut) were carefully detached to minimise folding or interference during imaging. Then glands were incubated with 500nM Lysotracker Red DN-99 (Invitrogen) for 5 minutes on ice, aiming to mark lysosomes and acidified compartments, followed by a gentle wash in chilled 1x PBS. Following dissection, glands were transferred into microtubes containing ice-cold 1x PBS and stored in a polystyrene box on ice to preserve tissue viability throughout the imaging session.

Prepared glands were mounted in a small drop of PBS between a rectangular coverslip (No. 1, 22 × 50 mm, Fisher Scientific, #1237-3128) and a round coverslip (No. 1, 13 mm, #49492, VWR), which were held in place using a custom-built metal mount. Excess PBS was gently removed with filter paper until the glands were slightly flattened against the glass. To minimise variability, glands were imaged in the order they were dissected, ensuring that each sample experienced a comparable interval between dissection and imaging (Marie et al., 2023; Singh et al., 2025).

## Live-cell imaging and deconvolution

All imaging was performed on a Leica Thunder inverted wide-field microscope (Leica Microsystems) equipped with a 100x oil-immersion objective (Leica HCX PL FLUOTAR, NA 1.3) and a K8 sCMOS camera. For each accessory gland, four SCs were imaged from at least ten individual virgin male flies. Image acquisition was carried out in HDR combined gain mode (16-bit digitization). Z-stacks were collected at 0.2 µm intervals, typically spanning 10–16 µm depending on the size of the SCs. SC morphology was visualised in Bright Field (BF) mode with an exposure time of 38ms, intensity set to 108, and an aperture of 24. For fluorescence imaging, LED illumination was used with the following settings: GFP channel, 475 nm excitation at 10% laser intensity with 280ms exposure; and RFP channel (Lysotracker), 550 nm excitation at 55% laser intensity with 40ms exposure. Thunder small volume computational clearing (SVCC) was applied to enhance image contrast, remove background noise and suppress out-of-focus signal. Deconvolution was not applied to the BF channel. For GFP and RFP channels, deconvolution was performed under widefield parameters using a refractive index of 1.33000 and water as the mounting

medium. The deconvolution settings were strength 60%, sensitivity 1, regularisation 0.05 and high smoothing.

## Analysis on ImageJ/Fiji

### (a) SC size and nucleus size

All images were analysed in ImageJ/Fiji. The area of secondary cells (SCs) and their nuclei was measured. In the brightfield (BF) channel, planes in which the boundaries of SCs and both nuclei were most clearly visible were identified and selected. These were not necessarily from the same Z-stack plane. The freehand selection tool was then used to carefully trace the outline of each SC and its nucleus. Once the regions of interest were defined, their areas were measured using the “Measure” function in Fiji. All measurements were recorded with the scale calibrated so that the output values were expressed in $\mu m^2$.

### (b) DCG phenotypes and number of mature compartments

DCGs labelled with GFP-MFAS, together with their associated compartments, were scored manually in experiments using the td-GFP-MFAS reporter line. DCGs were considered abnormal if they showed one of three features: a GFP-negative centre, mini-/deformed structure, or direct contact with the limiting membrane. For defining these features, DCGs were classified as containing GFP-negative centre when they contained a central non-fluorescent region with a diameter ≥1 μm. The mini-/deformed phenotype was assigned when multiple small cores with a diameter ≥0.5

μm were present within a single compartment and/or when the DCG was misshapen, with the ratio of its longest to shortest axis exceeding 1.4. DCGs in contact with the limiting membrane including both intact and misshapen DCGs, were scored if they maintained membrane contact throughout the entire Z-stack or if they shifted between staying at the central axis and contacting with the limiting membrane across several planes. All abnormal phenotypes were scored manually by examining the full Z-stack in both the BF and GFP/Lys merged channels. The percentage of abnormal DCG compartments was then calculated relative to the total number of DCG compartments per SC.

**(c) Number of DCG compartments with cylindrical cores in hTau2N4R overexpression experiments**

The number of DCG compartments in Tau overexpression experiments using the td-GFP-MFAS-Tau2N4R line was scored using ImageJ/Fiji. For each SC, a single plane was selected from the GFP channel Z-stack, corresponding to the plane containing the greatest number of visible DCGs. The BF channel was then used to identify the SC boundary with the freehand tool, following by a full outside-region-clearance. To reduce background fluorescence, a subtraction value of 10 pixels was applied across all genotypes, with the exception of *PTEN*-RNAi, where a value of 15 pixels was consistently used to account for the larger and brighter DCGs. Images were further processed using the “threshold” function, and the “Analyse Particles” function was applied with particle size 0.1-15. To distinguish between DCG phenotypes, two circularity ranges were used, which were 0.0-0.6 to capture elongated or irregular shaped (classified as cylindrical cores), and 0.0-1.0 to capture

the total number of DCGs. The number of DCG compartments with cylindrical cores was recorded per SC, and the percentage was calculated as a proportion of the total number of DCG compartments within the selected plane.

**(d) Acidification of secretory compartments**

The DCG acidification phenotype occurs when mature DCG compartments are first targeted for lysosomal clearance (Singh et al., 2025), and these were categorized as acidified compartments.

There are four different stages during lysosomal targeting and clearance, which were all scored as acidified compartments:

1. Compartments with a slightly diffused DCG but the shape is relatively intact, and typically a single peripheral acidic vesicle associates with the limiting membrane
2. Compartments with diffuse GFP-MFAS and associated with one or more acidic domains inside or at the limiting membrane
3. Compartments with completely diffuse GFP-MFAS
4. >80% of compartment area covered by acidified domains, but the compartment still retains its circular boundary

For experiments using the td-GFP-MFAS reporter line, the number of acidified compartments per SC was scored in the merged GFP/Lys channel across the entire Z-stack. For experiments using the td-GFP-MFAS-Tau2N4R line, scoring was

performed in the merged GFP/Lys channel using the same single plane that had been selected previously for quantifying the number of DCG compartments with cylindrical cores. To ensure accurate representation of each acidified compartment, movement by up to two planes above or below the selected plane was permitted when necessary to capture all relevant signals.

The total number of acidified compartments per SC was then recorded and shown as the percentage of all compartments (DCG + acidified compartments), allowing comparisons of acidification phenotypes between diverse genotypes with different numbers of DCG compartments.

**(e) Lysosomal area**

Lysosomal area within SCs was measured using ImageJ/Fiji. For experiments using the td-GFP-MFAS reporter line, a complete Z-stack maximum intensity projection of the Lysotracker (Lys) channel was generated to capture the full extent of the SC. In contrast, for experiments using the td-GFP-MFAS-Tau2N4R line, a single plane from the Lys channel Z-stack was analysed instead of the complete projection. This plane was the same one used for quantifying the number of DCG compartments with cylindrical cores in the hTau2N4R overexpression experiments.

The BF channel was used to outline individual SCs with the freehand tool. The corresponding regions were then applied to the Lys channel full projection or the single plane, and areas outside the SC were cleared. After this, images were automatically thresholded by the Fiji software to include the total acidic/red pixels.

Manual adjustment of the threshold was then performed to exclude compartments where more than 80% of the area was covered by acidified domains but the circular boundary remained intact, as these were already categorized as DCG acidified compartments. Following this adjustment, the threshold was fine-tuned to ensure maximal inclusion of the remaining regions corresponding to misshapen lysosomal structures. The “Analyse Particles” function was used to measure the lysosomal area. Finally, the percentage of lysosomal area was calculated as the ratio of the total lysosomal area to the total SC area.

**(f) GFP-MFAS containing main cells (main cell/propagation phenotype)**

GFP-MFAS distribution in main cells was assessed using ImageJ/Fiji. For each image, a fixed square region was defined using the rectangle tool. The size of this field of view was kept constant across genotypes (600 × 600 pixels) and was increased to 800 × 800 pixels for samples from *PTEN*-RNAi crossed with td-GFP-MFAS, to make sure that the significantly larger secondary cells (SCs) and surrounding main cells could still be included.

For the series of td-GFP-MFAS experiments, the average SC size across most genotypes was approximately 600 µm², whereas SCs in the *PTEN*-RNAi background reached close to 1000 µm². This indicates roughly a 1.7-fold increase in size. Scaling the square region from 600x600 pixels (area = 360,000 pixels$^2$) to 800x800 pixels (area = 640,000 pixels$^2$) provides a proportional increase in field size around 1.8 times.

For all experiments using the td-GFP-MFAS-Tau2N4R line, a constant field size of 800 × 800 pixels was applied across genotypes. SCs in these backgrounds were consistently larger, so adopting a larger square region avoided partial exclusion of SCs boundaries and limited inclusion of GFP-MFAS-positive areas in main cells.

To measure the main cell phenotype, the GFP channel was merged with the brightfield (BF) channel to identify SCs. Using the freehand selection tool, the boundary of each SC was outlined, making sure not to include any main cell GFP-MFAS that was extremely close to SCs. A square region was then positioned with the SC in the centre and adjusted so that no other SCs were included in the field of view. The SC area and area of the square were both measured.

Within the complete Z-stack maximum intensity projection, the SC area was cleared and the remaining field was cropped to the area of the square. Threshold values were adjusted manually until the GFP-MFAS in the main cells was fully captured. The “Analyse Particles” function in Fiji (size: 0–∞; circularity: 0–1) was applied to calculate the total GFP-positive area. Finally, the percentage of main cell area containing GFP-MFAS was calculated as: total GFP-MFAS containing area / (square area – SC area)

## Statistical analysis

All statistical analysis was carried out using GraphPad Prism. When comparing multiple experimental genotypes with the control, the normal distribution of data sets was first assessed using the normality and lognormality test. If the data were

normally distributed, they were analysed using the ordinary one-way ANOVA, and post hoc multiple comparisons were performed using the Dunnett's multiple comparisons test to identify differences between each experimental genotype and the control. Statistical significance was set at $p < 0.05$. For comparisons between two groups (one control and one experimental group), an unpaired parametric t-test was used. All graphical data are presented as genotype mean values with error bars indicating the standard error of the mean (SEM). For each analysis, n=10 refers to the number of *Drosophila* accessory glands assessed per genotype, where the value for a single gland was obtained by calculating the average measurements from four SCs. Similar results were observed across three independent replicate experiments.

# Results

## Control of transgene expression in SCs

All the major *Drosophila melanogaster* lines utilized in this thesis were previously validated in the literature. The GFP-MFAS protein trap line (*w*$^{1118}$*; GFP-mfas*$^{MI11275\text{-}GFSTF.2}$, BDSC #63204) originates from a genome-wide collection of GFP-tagged gene traps (Nagarkar-Jaiswal et al., 2015). This line inserts a GFP tag into the endogenous *mfas* locus, resulting in a N-terminally tagged fluorescent MFAS protein. The genotype *w*$^{1118}$*; tub-GAL80*$^{ts}$*/CyO; dsx-GAL4/TM6B,* incorporates a ubiquitous temperature-sensitive GAL80, and has been used effectively to express UAS-constructs in SCs, specifically in the adult male accessory gland (Corrigan et al., 2014). Our lab combined these features by using a recombinant td-GFP-MFAS knock-in reporter line (*w*$^{1118}$*; tub-GAL80*$^{ts}$*/CyO; dsx-GAL4,GFP-mfas/TM6B)* as the principal genetic background in a recent study (Singh *et al*., 2025), which explored how amyloid-β and APP affect protein aggregation and membrane recycling in SCs. These lines have been successfully validated in previous studies, demonstrating reliable and consistent expression patterns in the targeted tissues.

To drive gene expression specifically in the SCs of the male adult *Drosophila* accessory glands, the UAS/GAL4/GAL80$^{ts}$ regulatory system was applied (Figure 5). In this system, GAL4 acts as a transcriptional activator that binds UAS sequences upstream of the gene of interest, whereas GAL80$^{ts}$ is a temperature-sensitive repressor of GAL4 activity. At temperatures below 29°C, GAL80$^{ts}$ effectively inhibits GAL4, thereby preventing transgene expression. When flies are shifted to the restrictive temperature (29°C), GAL80$^{ts}$ becomes non-functional, allowing GAL4 to

activate transcription of the UAS-linked transgene at high levels (McGuire et al., 2004; McClure et al., 2022).

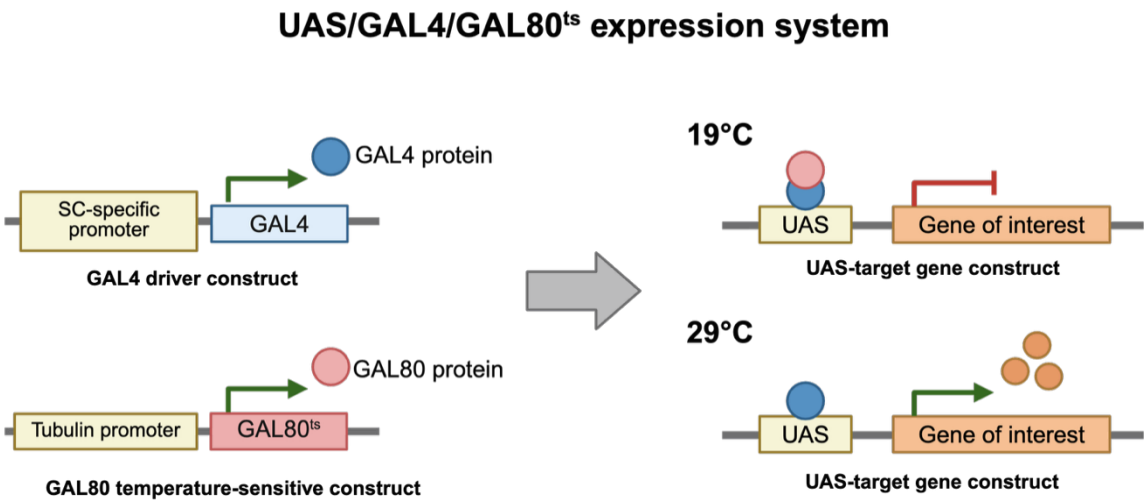


**Figure 5. Schematic of UAS/GAL4/GAL80$^{ts}$ regulatory/expression system.** For SC-specific targeting, GAL4 was placed under the control of the *doublesex* (*dsx*) regulatory sequence, which is strongly expressed exclusively by SCs within the adult accessory gland. In combination with the ubiquitously expressed GAL80$^{ts}$, the whole setup enables precise temporal control of UAS-transgene expression specifically in adult SCs. In practice, male offsprings were collected at eclosion and transferred to 29°C for six days, ensuring post-developmental induction of SC-specific transgenes, before dissection and imaging.

## Insulin/PI3K/mTORC1 signalling regulated cellular and nuclear growth in SCs

The first part of this study aimed to test whether components of the insulin/PI3K/mTORC1 signalling pathway regulate DCG biogenesis and secretory/endolysosomal trafficking in SCs. To address this, I manipulated genes encoding key proteins from the pathway using *tub-GAL80$^{ts}$; dsx-GAL4,GFP-mfas* as the background line (Singh et al., 2025). Building on a previous DPhil work from our lab (Wells, 2024), I employed several same genetic UAS-transgenes targeting key components of the insulin/PI3K/mTORC1 signalling pathway in this project.

Controls included crosses to a UAS-*rosy*-RNAi line, since this gene is not thought to affect DCG biogenesis in SCs and to a *w$^{1118}$* line containing no transgenes. RNAi-mediated knockdown was performed for the Class I PI3-kinase catalytic subunit Dp110 (UAS-*PI3K*-RNAi #1; UAS-*PI3K*-RNAi #2), Akt (UAS-*Akt1*-RNAi #1; UAS-*Akt1*-RNAi #2), and mTOR (UAS-*tor*-RNAi). In addition, the overexpression of Insulin-like Receptor (UAS-*InR*) was used in this study (first used by Brogiolo *et al*., 2001 to demonstrate InR's cell autonomous control of organ size), and PTEN levels were also modulated both by RNAi (UAS-*PTEN*-RNAi) and by overexpression (UAS-*PTEN*, originally shown by Goberdhan *et al*., 1999 to antagonize Dp110/PI3K and reduce cell growth). To further probe downstream pathway activity, I examined flies co-expressing UAS-*Tsc1* and UAS-*Tsc2*, and UAS-*Rheb$^{AV4}$*. Most of the lines used in this thesis have been previously reported and validated in published work. A full stock list is provided in Table 2.

Representative images of single SCs for each genotype are shown in Figures 6 and 7. While bright-field imaging revealed the boundaries of the SC and large intracellular compartments, GFP marked the DCGs inside secretory compartments and secreted material that had been endocytosed by neighbouring main cells (Singh et al., 2025). Glands were also stained with LysoTracker Red to mark acidified secretory compartments and lysosomes, which are also highly enlarged in these cells.

*tub-GAL80$^{ts}$; dsx-GAL4,GFP-mfas*

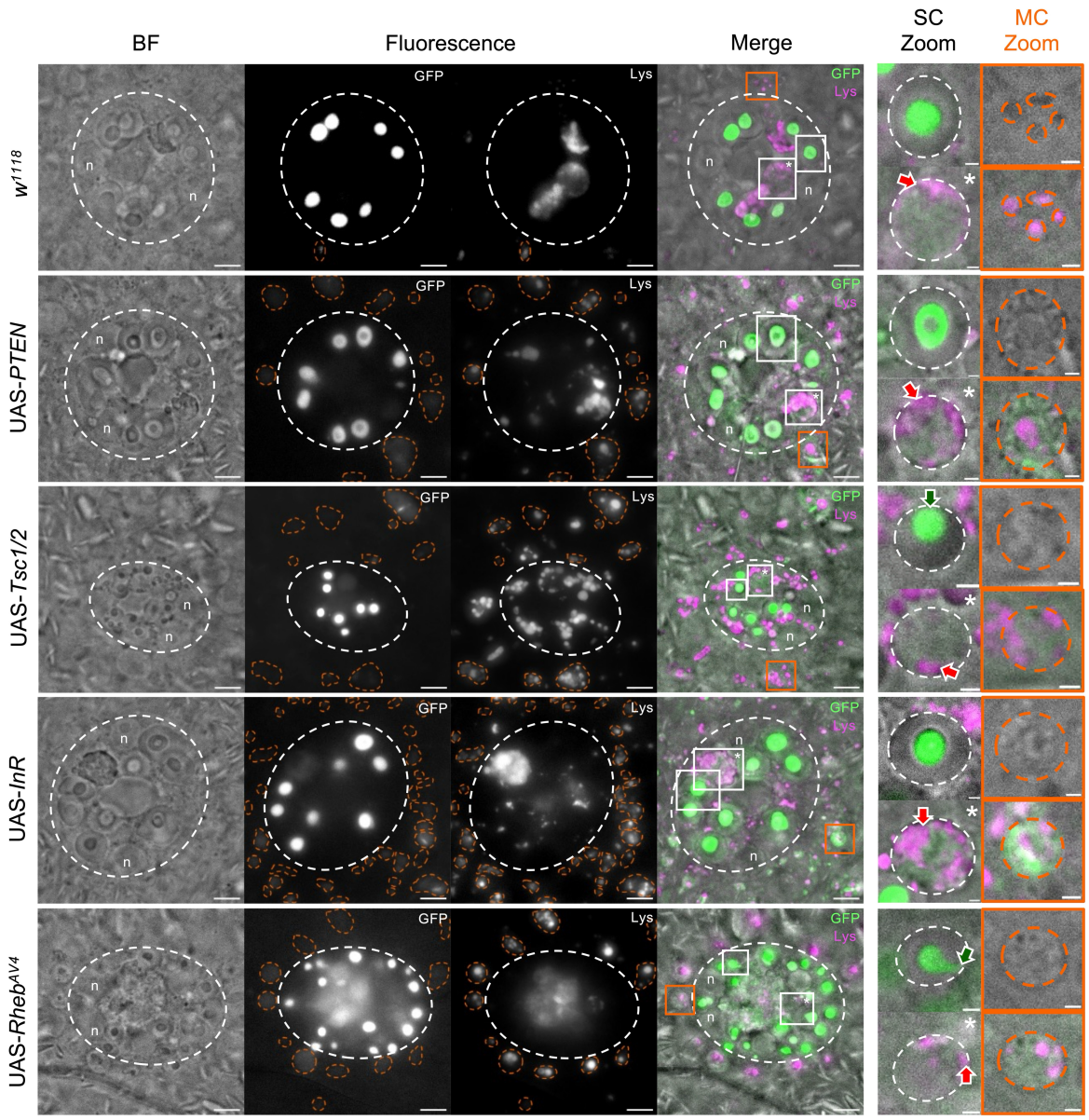


**Figure 6. Modulating the insulin/PI3K/mTORC1 signalling pathway affects DCG biogenesis in SCs.**

Representative images of SCs expressing td-GFP-MFAS and no other transgene (*w$^{1118}$*) or overexpressing SC-specific UAS-*PTEN*, UAS-*Tsc1/2*, UAS-*InR* and UAS-*Rheb$^{AV4}$*. In bright-field (BF), Fluorescence and Merge columns, the SC boundary is outlined by white dashed lines. Abnormal accumulation of GFP-MFAS and associated increased areas of acidification in main cell (MC) endolysosomes, which

are normally small (see control), is highlighted by orange dashed outlines in the fluorescence images. In the Merge column, white boxes mark regions magnified in the SC zoom panels. The upper SC zoom panels show representative DCG phenotypes. Green arrowheads indicate DCGs contacting the limiting membrane (UAS-*Tsc1/2* and UAS-*Rheb*$^{AV4}$). White boxes marked with asterisks indicate DCG acidification phenotype, shown in the lower SC Zoom panels, where red arrowheads point out selected acidic microdomains. Orange boxes in the Merge column illustrate regions magnified in the MC Zoom panels. The upper MC Zoom panels show the BF channel, while the lower panels display the corresponding merged image (BF, GFP and Lys). In all images, n marks nuclei and LysoTracker Red (magenta) labels the acidic domains/compartments. Scale bars: 5 μm (BF, fluorescence, Merge) and 1 μm (SC Zoom and MC Zoom).

*tub-GAL80$^{ts}$; dsx-GAL4,GFP-mfas*

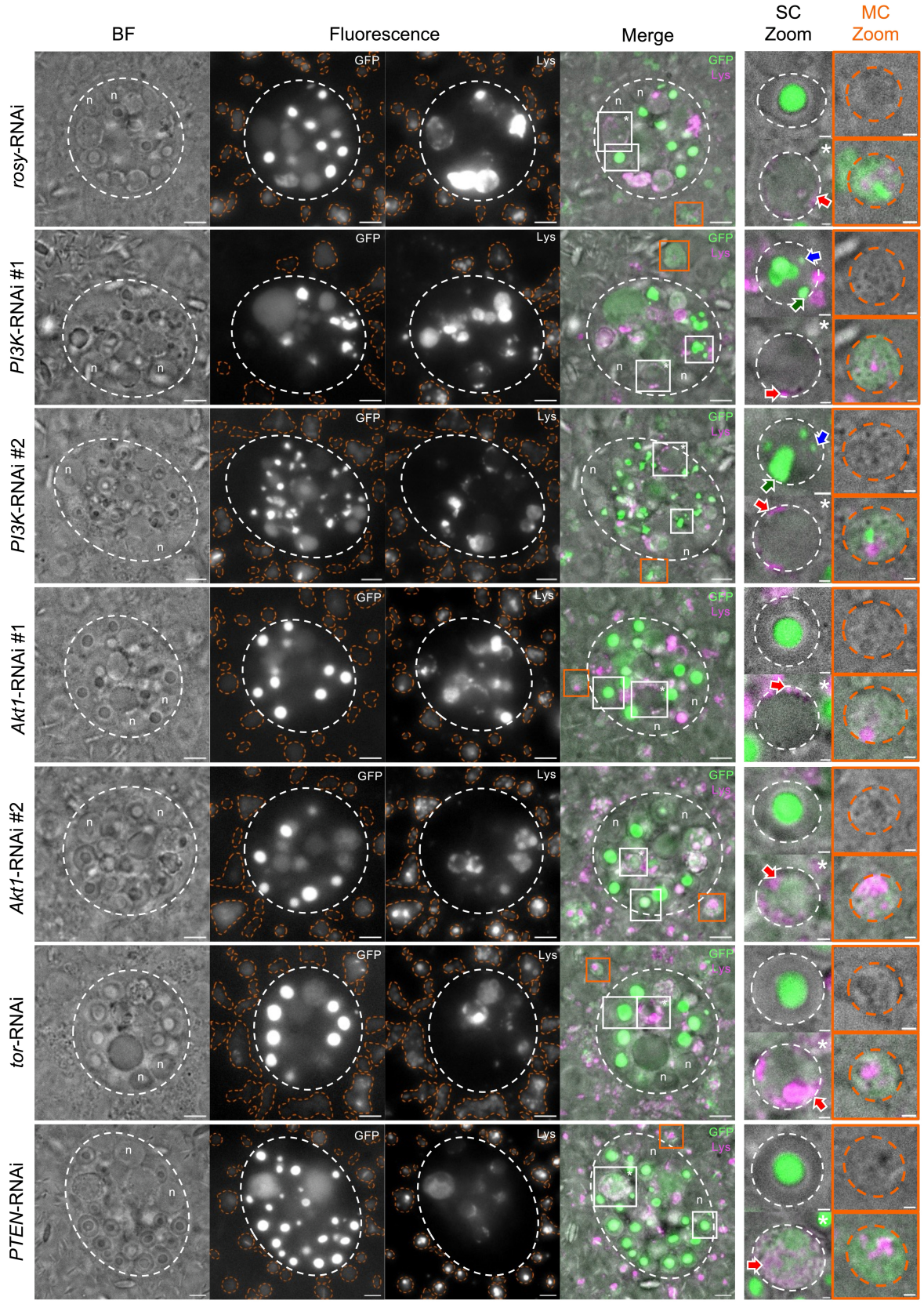

**Figure 7. Modulating the insulin/PI3K/mTORC1 signalling pathway affects DCG biogenesis in SCs.**

Representative images of SCs expressing td-GFP-MFAS in combination with SC-specific control RNAi (*rosy*-RNAi) or RNAi knockdown of *PI3K* (*PI3K*-RNAi #1 and #2), *Akt1* (*Akt1*-RNAi #1 and #2), *tor*-RNAi and *PTEN*-RNAi. In the BF, Fluorescence and Merge columns, the SC boundary is outlined by white dashed lines. Abnormal accumulation of GFP-MFAS in acidic MC compartments is highlighted by orange dashed outlines in the Fluorescence columns. In the Merge column, white boxes mark regions magnified in the SC zoom panels. The upper SC zoom panels show representative DCG phenotypes. Green arrowheads indicate DCGs contacting the limiting membrane and blue arrowheads mark the multiple mini-cores in *PI3K*-RNAi #1 and #2 genotypes. White boxes marked with asterisks indicate DCG acidification phenotype, shown in the lower SC Zoom panels, where red arrowheads point out selected acidic microdomains. Orange boxes in the Merge column illustrate regions magnified in the MC Zoom panels. The upper MC Zoom panels show the BF channel, while the lower panels display the corresponding merged image (BF, GFP and Lys). In all images, n marks nuclei and LysoTracker Red (magenta) labels the acidic endosomal domains/compartments and lysosomes. Scale bars: 5 μm (BF, fluorescence, Merge) and 1 μm (SC Zoom and MC Zoom).

The insulin/PI3K/mTORC1 pathway affects both cellular and nuclear growth in post-mitotic cells (Goberdhan et al., 1999; Brogiolo et al., 2001), so I first assessed whether there were any obvious effects on SC size and nuclear size (Figure 8). The cytoplasmic volume of SCs is strongly dependent on the size and number of secretory compartments (Leiblich et al., 2012). For most genotypes, SC size did not differ significantly from the *rosy*-RNAi or $w^{1118}$ controls, indicating that modulation of the insulin/PI3K/mTORC1 signalling pathway generally does not affect overall SC size. However, *PTEN*-RNAi resulted in a highly significant enlargement of SCs, while co-expression of *Tsc1* and *Tsc2* caused a strong and opposite reduction in SC size. SC nuclear size is also affected by growth-regulatory stimuli (Leiblich et al., 2012; Sekar et al., 2023). I found that although most manipulations of the insulin/PI3K/mTORC1 signalling pathway had no significant effect on nuclear size, *PTEN*-RNAi resulted in a marked enlargement of nuclei, following the same trend as overall SC size, while the UAS-$Rheb^{AV4}$ induced a weaker but still significant increase.

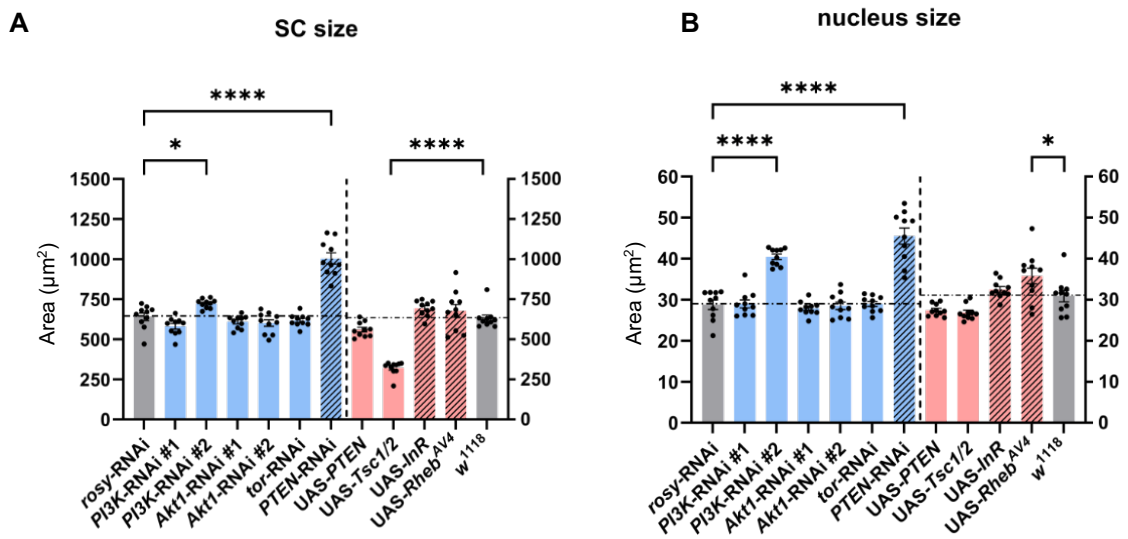


**Figure 8. Bar charts showing the effects of insulin/PI3K/mTORC1 signalling pathway manipulations on SC size and nuclear size.**

The x-axis indicates the different genotypes, and the y-axis shows the measured area (µm²) of cells (A) and nuclei (B). Blue bars represent UAS-RNAi transgenes, which were compared with the *rosy*-RNAi control (left y-axis), and red bars represent UAS-transgenes, which were compared with the $w^{1118}$ control (right y-axis). Non-shaded bars correspond to genotypes that downregulate the insulin/PI3K/mTORC1 signalling pathway, whereas shaded bars indicate genotypes that upregulate pathway activity. Data are shown as mean ± SEM, with each dot representing the average measurement from four SCs of an individual fly (n = 10). Data were normally distributed and statistical analysis was therefore performed using the ordinary one-way ANOVA followed by post hoc multiple comparisons, specifically the Dunnett's multiple comparison test with automatic correction of p-values. Significance levels are indicated as *p < 0.05, **p < 0.01, ***p < 0.001, ****p < 0.0001, bars without asterisks are not significantly different from controls.

The growth-promoting effects of *PTEN*-RNAi and *Rheb* overexpression, together with the growth inhibitory effects of *Tsc1/Tsc2* co-overexpression are consistent with previously reported roles for these genes and the insulin/PI3K/mTORC1 pathway in post-mitotic cell growth regulation and control of endoreplication (Goberdhan et al., 1999; Potter et al., 2001; Patel et al., 2003), which affects nuclear growth in SCs (Sekar et al., 2023)

The *PI3K*-RNAi #2 has been successfully used in previous studies, although not in the adult *Drosophila* accessory glands. For example, Ferreira and Milán (2015) used this line in developing wing imaginal discs to perturb the insulin/PI3K/mTORC1 signalling, and reported that *PI3K* knockdown caused a non-autonomous reduction in the growth of adjacent cell populations (Ferreira & Milán, 2015). This outcome is consistent with PI3K's established role as a positive regulator of cellular growth in the insulin/PI3K/mTORC1 signalling pathway (Frappaolo & Giansanti, 2023). However, the phenotypes induced by *PI3K*-RNAi #2 in this thesis were unexpected and inconsistent with PI3K's known functions. This genotype produced a large and significant increase in nucleus size and a weak but still significant increase in SC size (shown in Figure 8). Particularly since *PI3K*-RNAi #1 did not induce these phenotypes, the most likely explanation is that they are attributable to off-target effects. *PI3K*-RNAi #2 was therefore excluded from the subsequent analysis.

## Insulin/PI3K/mTORC1 signalling regulated DCG biogenesis in SCs

I analysed the number and morphology of DCG compartments following the different genetic manipulations affecting insulin/PI3K/mTORC1 signalling. Quantification of the number of DCG compartments revealed strong effects of pathway modulation (Figure 9A). Among genotypes that increased signalling activity, *PTEN*-RNAi had the most pronounced effect compared with the *rosy*-RNAi control, elevating the number of DCG compartments by more than two-fold. Similarly, UAS-*Rheb*$^{AV4}$ displayed such an increase as well. In contrast, UAS-*Tsc1/Tsc2* showed a small, but still significant reduction in the number of DCG compartments; the other genotypes did not differ significantly from controls, though in all cases where signalling was reduced, there was a trend toward reduced numbers of DCG compartments.

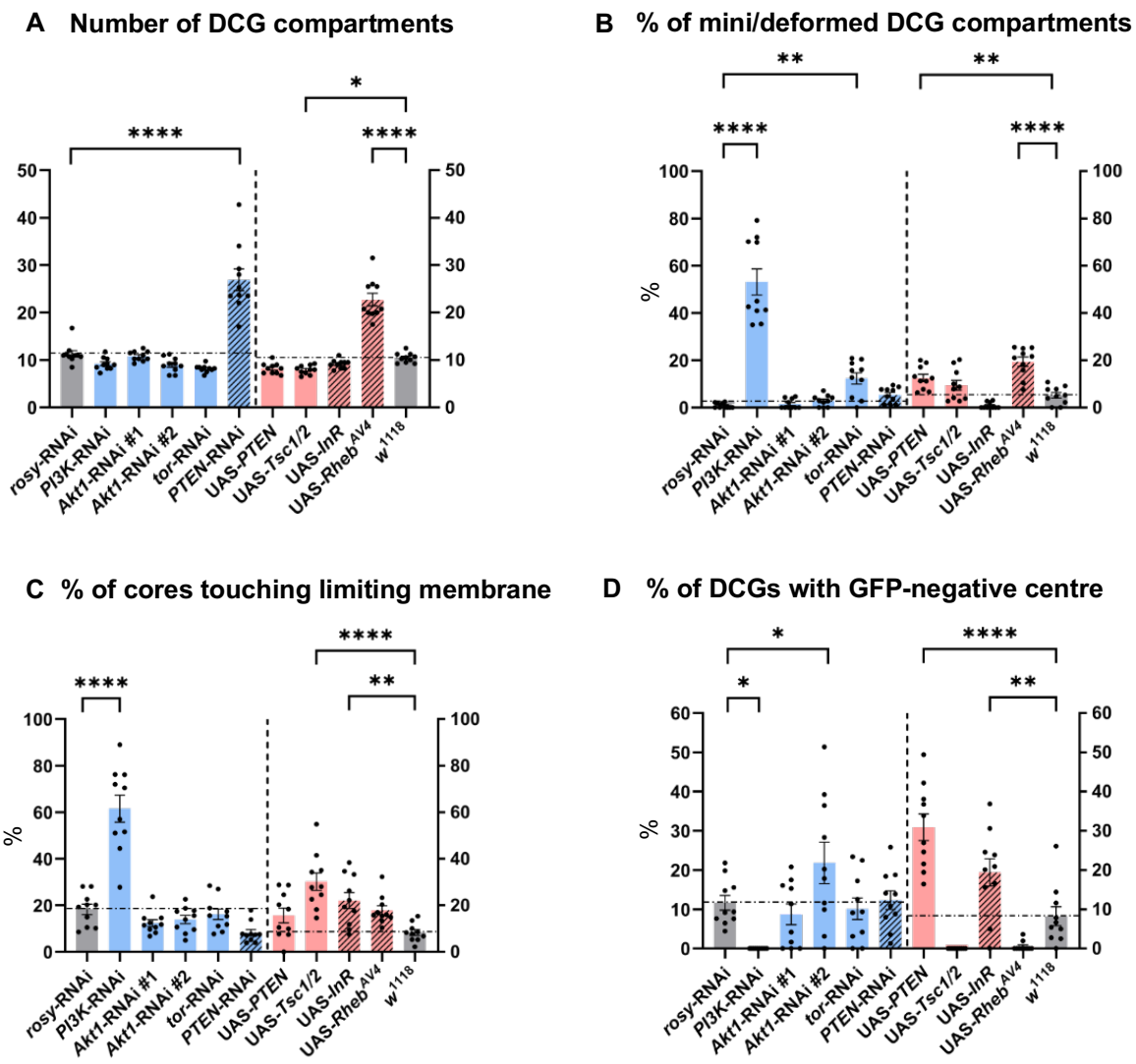


**Figure 9. Bar charts showing the effects of insulin/PI3K/mTORC1 signalling pathway manipulations on DCG biogenesis and morphology.**

(A) The number of DCG compartments, (B) % of mini/deformed DCG compartments, (C) % of cores touching limiting membrane, and (D) % of DCGs with a large GFP-negative centre were determined for different genotypes. The x-axis indicates the different genotypes. Blue bars represent UAS-RNAi transgenes, which were compared with the *rosy*-RNAi control (left y-axis), and red bars represent UAS-transgenes, which were compared with the $w^{1118}$ control (right y-axis). Non-shaded bars correspond to genotypes that downregulate the insulin/PI3K/mTORC1

signalling pathway, whereas shaded bars indicate genotypes that upregulate pathway activity. Data are shown as mean ± SEM, with each dot representing the average measurement from an individual fly (n = 10). Data were normally distributed and statistical analysis was therefore performed using the ordinary one-way ANOVA followed by post hoc multiple comparisons (the Dunnett's multiple comparison test with automatic correction of p-values). Significance levels are indicated as *$p < 0.05$, **$p < 0.01$, ***$p < 0.001$, ****$p < 0.0001$, bars without asterisks are not significantly different from controls.

Emerging evidence suggests that the insulin/PI3K/mTORC1 signalling regulates endosomal organization and Rab11-dependent exosome biogenesis in SCs, which are considered as essential steps in DCG biogenesis, potentially through effects on E-cadherin microdomains and the cytoskeletal architecture of DCG compartments (Adam, PhD thesis; Marie et al., 2023; Singh et al., 2025; see Introduction). These previous studies also indicate that PI3K signalling may directly influence E-cadherin microdomains, providing the rationale for the experiments undertaken next. I therefore examined whether altering this pathway influenced DCG morphology, as defects in the cytoskeleton, intraluminal vesicles (ILVs) formation, and membrane–aggregate interactions are known to disrupt DCG biogenesis.

Surprisingly, genotypes in which insulin/PI3K/mTORC1 signalling was either increased or decreased could affect the percentage of intact or deformed DCGs. Three genotypes in which signalling is reduced increased the proportion of defective DCGs. Most notably, *PI3K*-RNAi induced a strong increase in compartments with abnormal DCGs (Figure 9B). In addition, more modest but still significant increases were observed with *tor*-RNAi and UAS-*PTEN*, when compared to *rosy*-RNAi and $w^{1118}$, respectively, while *Tsc1/Tsc2* co-overexpression also showed a trend toward increased levels. Unexpectedly, UAS-$Rheb^{AV4}$ displayed a robust increase in deformed DCG compartments, even though *PTEN*-RNAi, which produces strong growth phenotypes, had no obvious effect. These results suggest that suppression the insulin/PI3K/mTORC1 signalling pathway can interfere with normal DCG biogenesis, while the effect of increased signalling is less clear-cut.

Regarding specific defects in the positioning of DCGs, it also appeared that reduced insulin/PI3K/mTORC1 signalling can disrupt normal detachment of DCGs from the compartmental limiting membrane. Most notably, about 60% of compartments in *PI3K*-RNAi-expressing SCs contained limiting membrane-associated DCGs, which were often mini-cores (Figure 7 and Figure 9C), present due to their failure to fuse with each other, the phenotype also produced by knockdown of *Drosophila App* (*Appl*; Singh et al., 2025). Moreover, UAS-*Tsc1/Tsc2* and UAS-*InR*, manipulations that respectively decrease and increase signalling, also induced an increase in DCGs contacting the limiting membrane, although in these cases, the DCGs were large and spherical (Figure 6). Therefore, most genetic changes that alter insulin/PI3K/mTORC1 signalling in SCs appear to have some effect on DCG biogenesis. Surprisingly, however, knockdown of *PTEN*, which has the strongest activation of signalling, does not produce an abnormal phenotype in DCG morphology.

Finally, I also scored the percentage of DCGs with a large (≥1 μm diameter) GFP-negative centre (Figure 9D). Previous studies have shown that some manipulations that reduce aggregate dissociation from the limiting membranes in SC DCG compartments lead to increased numbers of these abnormal DCGs, perhaps because the aggregates fail to assemble normally at the centre of the compartment (Singh et al., 2025). *Akt1*-RNAi #2 and *PTEN* overexpression produced an increased proportion of these defective DCGs, clearly seen for UAS-*PTEN* in Figure 6, while UAS-*InR* showed a more modest increase.

These findings indicate that genetic modulation of components within the insulin/PI3K/mTORC1 pathway contributes to various DCG compartment abnormalities. Increased activity appears to accelerate biogenesis, as expected, leading to increased production and accumulation of compartments within SCs. Increasing or decreasing signalling interferes with different stages of DCG biogenesis, though the absence of a phenotype with *PTEN*-RNAi suggests that the impact of increased signalling is complex.

## Insulin/PI3K/mTORC1 signalling regulated endolysosomal trafficking in SCs and the uptake of secreted proteins by MCs

To examine whether modulating the insulin/PI3K/mTORC1 signalling pathway affects endolysosomal trafficking in SCs, I assessed the % of acidified DCG compartments and the % SC area that was acidified for all genotypes (Figure 10). In genotypes where DCG biogenesis is disrupted, endolysosomal trafficking is increased, and when trafficking of acidified compartments to lysosomes is blocked, acidified DCG compartments accumulate, a phenotype observed in Aβ-expressing cells (Singh et al., 2025). As previously observed, expressing control RNAis in SCs produces a significant increase in acidified compartments within these cells.

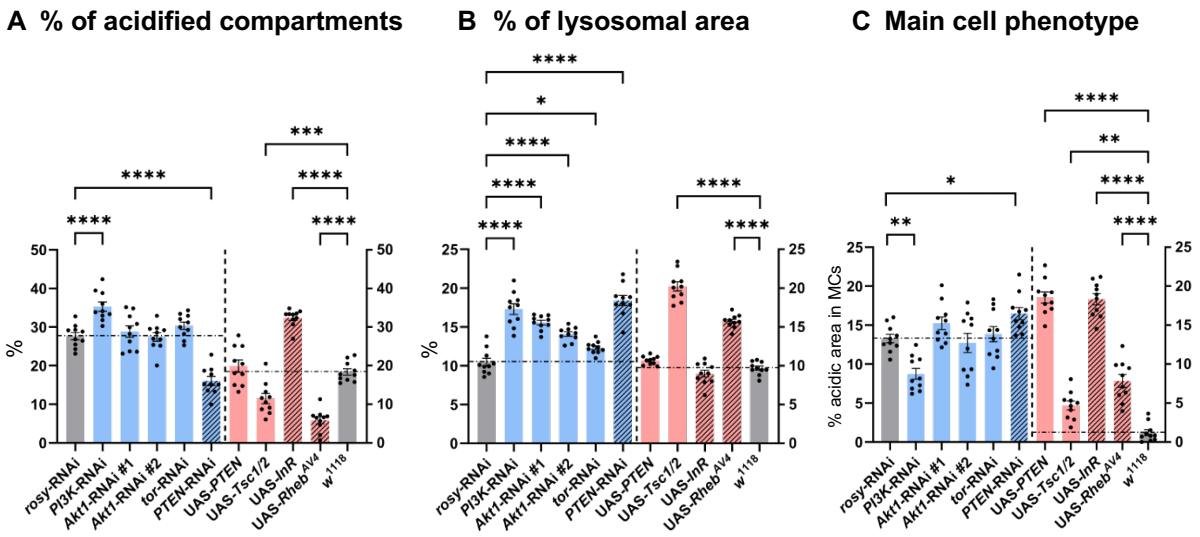


**Figure 10. Bar charts showing the effects of insulin/PI3K/mTORC1 signalling pathway manipulations on SC endolysosomal trafficking and MC uptake of secreted proteins.**

(A) % of acidified compartments in SCs (B) % of lysosomal area in SCs and (C) main cell uptake phenotype, expressed as % acidic area in MCs containing GFP-MFAS. The x-axis indicates the different genotypes. Blue bars represent UAS-RNAi transgenes, which were compared with the *rosy*-RNAi control (left y-axis), and red bars represent UAS-transgenes, which were compared with the $w^{1118}$ control (right y-axis). Non-shaded bars correspond to genotypes that downregulate the insulin/PI3K/mTORC1 signalling pathway, whereas shaded bars indicate genotypes that upregulate pathway activity. Data are shown as mean ± SEM, with each dot representing the average measurement from an individual fly (n = 10). Data were normally distributed and statistical analysis was therefore performed using the ordinary one-way ANOVA followed by post hoc multiple comparisons (the Dunnett's multiple comparison test with automatic correction of p-values). Significance levels are indicated as *p < 0.05, **p < 0.01, ***p < 0.001, ****p < 0.0001, bars without asterisks are not significantly different from controls.

Interestingly, all manipulations that reduced insulin/PI3K/mTORC1 signalling, except for *PTEN* overexpression, increased the percentage of lysosomal area in SCs (Figure 10B), consistent with the known role of this pathway in increasing lysosome biogenesis (Kaushal Asrani et al., 2019). However, *PI3K*-RNAi uniquely also increased the percentage of acidified compartments (Figure 10A), suggesting that it may have additional effects on endolysosomal trafficking, although surprisingly overexpressed *Tsc1/Tsc2* reduced the accumulation of these acidified DCG compartments.

Again, the effects of increasing insulin/PI3K/mTORC1 signalling were more variable. *PTEN*-RNAi and overexpressed *Rheb* produced a strong reduction in acidified compartments, but an increase in lysosomal area, suggesting that increased DCG compartment biogenesis may induce an increased flux through the endolysosomal trafficking pathway (Figure 10A and 10B). However, UAS-*InR* significantly increased the percentage of acidified compartments, while not affecting lysosomal area, suggesting that activating the downstream pathway which does not involve PI3K/mTORC1, might interfere with endolysosomal trafficking.

Finally, I analysed the effects of modulating insulin/PI3K/mTORC1 signalling on uptake of secreted SC proteins by MCs. Previous studies have already revealed that this phenotype is highly influenced by genetic background (Singh et al., 2025). Most notably, many RNAi knockdowns in SCs seem to enhance uptake, perhaps because the RNAi cellular response induces changes in DCG biogenesis (see controls in Figures 9C, 9D, 10A). Compared with *rosy*-RNAi, *PI3K*-RNAi significantly reduced the presence of enlarged main cell compartments containing GFP-MFAS, whereas

*PTEN*-RNAi markedly increased it (Figure 10C). When compared with $w^{1118}$, overexpression of several genes led to high levels of GFP-MFAS in main cells, *Rheb, InR, Tsc1/Tsc2 and PTEN*. These results suggest that disrupting DCG maturation events in SCs may alter the uptake of proteins by MCs that are secreted from SCs. However, this interpretation should be considered with caution, given that the effects of RNAis and gene overexpression can produce opposite results, even if they both reduce signalling, e.g. *PI3K*-RNAi versus *Tsc1/Tsc2* or *PTEN* overexpression.

In summary, these findings highlight that either decreasing or increasing insulin/PI3K/mTORC1 signalling pathway in SCs appears to disturb a delicate balance of control in the secretory and endolysosomal pathways. My data are consistent with a model where increased signalling drives elevated secretory flux and more lysosome accumulation, while reduced signalling probably does the opposite, but also increased lysosome biogenesis, so that lysosomal area increases. Changing signalling also disrupts DCG biogenesis itself, with reduced signalling having the strongest effects, particularly when *PI3K* mRNA levels are decreased.

Having demonstrated that insulin/PI3K/mTORC1 signalling plays an important role in balancing multiple aspects of DCG biogenesis, secretory and endolysosomal trafficking in SCs, I next examined whether manipulating this regulatory network also influences or even rescues secretory defects induced by pathological protein expression relevant to AD. Disrupted insulin signalling has been tightly correlated to Tau pathology in AD, where metabolic dysregulation and Tau toxicity can aggravate

each other, impairing vesicular trafficking and exacerbating the cognitive decline in AD (Deng et al., 2009; El et al., 2014; Gonçalves et al., 2019).

To address this, a fly line carrying UAS-human Tau (2N4R isoform, wild type) was applied to model tau overexpression in *Drosophila* SCs and generated endolysosomal phenotypes reminiscent of the pathology in AD (*$w^{1118}$; P{UAS-hTau.2N4R.wt}attP40; +,* BDSC #90949) (Gorsky et al., 2016). For experiments involving overexpressing hTau2N4R in this thesis, our lab recombined the UAS-hTau2N4R-WT element into the td-GFP-MFAS background, creating the genotype *$w^{1118}$; hTau-2N4R-WT, tub-GAL80$^{ts}$/CyO; dsx-GAL4, GFP-mfas/TM6B.* This model provides a suitable system to investigate how modulation of insulin/PI3K/mTORC1 signalling components influences the abnormal secretory and endolysosomal trafficking phenotypes induced by hTau2N4R overexpression, which might be relevant to tauopathy-associated defects observed in AD.

Controls included crosses to a UAS-*rosy*-RNAi line, since this gene is not thought to affect DCG biogenesis in SCs, and to a *$w^{1118}$* line containing no transgenes. RNAi-mediated knockdown was performed for the Class I PI3-kinase catalytic subunit Dp110 (UAS-*PI3K*-RNAi), Akt (UAS-*Akt1*-RNAi #1; UAS-*Akt1*-RNAi #2), mTOR (UAS-*tor*-RNAi) and PTEN (UAS-*PTEN*-RNAi). In addition, the overexpression of Insulin-like Receptor (UAS-*InR*) was used in this part of experiments.

The overexpression lines UAS-*PTEN*, UAS-*Tsc1/2*, and UAS-*Rheb$^{AV4}$* were excluded from this part of experiments. Crosses combining these strong activators or repressors of insulin/PI3K/mTORC1 signalling in the presence of hTau2N4R

overexpression produced very few viable progenies, and the resulting offsprings were often unhealthy and failed to survive beyond six days of incubation at 29°C. This outcome likely reflects the combined phenotypic severity arising from the co-overexpression of hTau2N4R with these potent overexpression constructs. As shown previously (Figure 6), each of these latter lines produced relatively strong effects on DCG biogenesis and endolysosomal trafficking, even in the absence of Tau.

The recombinant line td-GFP-MFAS-Tau2N4R was first screened to confirm its baseline phenotype in SCs. Overexpression of hTau2N4R alone affected DCG morphology, producing cylindrical cores, often with one end in contact with the compartmental limiting membrane, as shown in Figure 11. In addition to these structural changes, Tau overexpression dramatically increased both the number of DCG compartments and the overall lysosomal area. These served as the reference phenotype for upcoming genetic manipulations. Notably, these features resemble the phenotype observed from cofilin knockdown, a known actin cytoskeletal regulator (see introduction), suggesting that Tau may indirectly interfere with the actin cytoskeletal network involved in DCG-aggregate priming and dissociation, as well as endolysosomal trafficking.

*hTau-2N4R-WT, tub-GAL80$^{ts}$; dsx-GAL4, GFP-mfas*

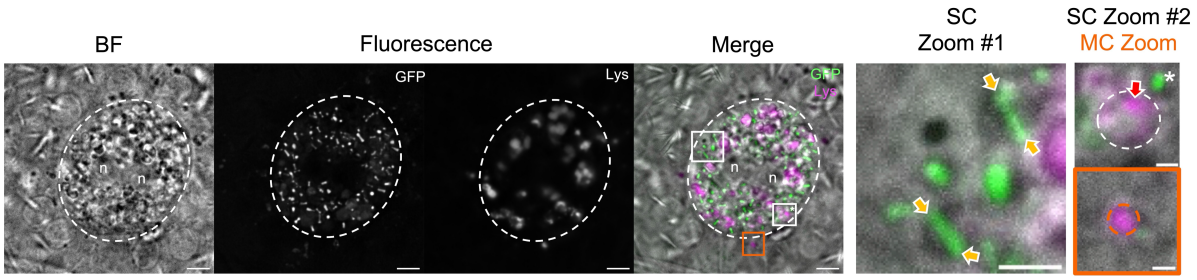


**Figure 11. Overexpression of human Tau2N4R in SCs affects DCG biogenesis and morphology.**

Representative images of SCs expressing the td-GFP-MFAS-Tau2N4R line, in which human Tau2N4R is overexpressed in SCs without additional UAS or RNAi transgenes. In the BF, Fluorescence, and Merge columns, the SC boundary is outlined by white dashed lines. In the Merge column, white boxes mark regions magnified in the SC zoom panels #1 and #2. The SC zoom #1 panel shows representative DCG phenotypes. Yellow arrowheads point to compartments with cylindrical cores that contact the DCG compartment limiting membrane at both ends. White Zoom box marked with the asterisk indicates DCG acidification phenotype (SC Zoom #2 panel), where red arrowhead highlights selected acidic microdomain. Orange box in the Merge column illustrates the region that is magnified in the MC Zoom panel, which displays the corresponding merged image (BF, GFP and Lys). This line is illustrated as showing minimal abnormal accumulation of GFP-MFAS but with some associated increased areas of acidification in main cell (MC) endolysosomes, which are normally small and marked by orange dashed outlines in the MC Zoom panel image. In all images, n marks nuclei and LysoTracker Red (magenta) labels the acidic endosomal domains/compartments and lysosomes. Scale bars: 5 μm (BF, fluorescence, Merge), 2 μm (SC Zoom #1) and 1 μm (SC Zoom #2 and MC Zoom).

Representative images of single SCs for each genotype are shown in Figures 12 and 13.

*hTau-2N4R-WT, tub-GAL80$^{ts}$; dsx-GAL4, GFP-mfas*

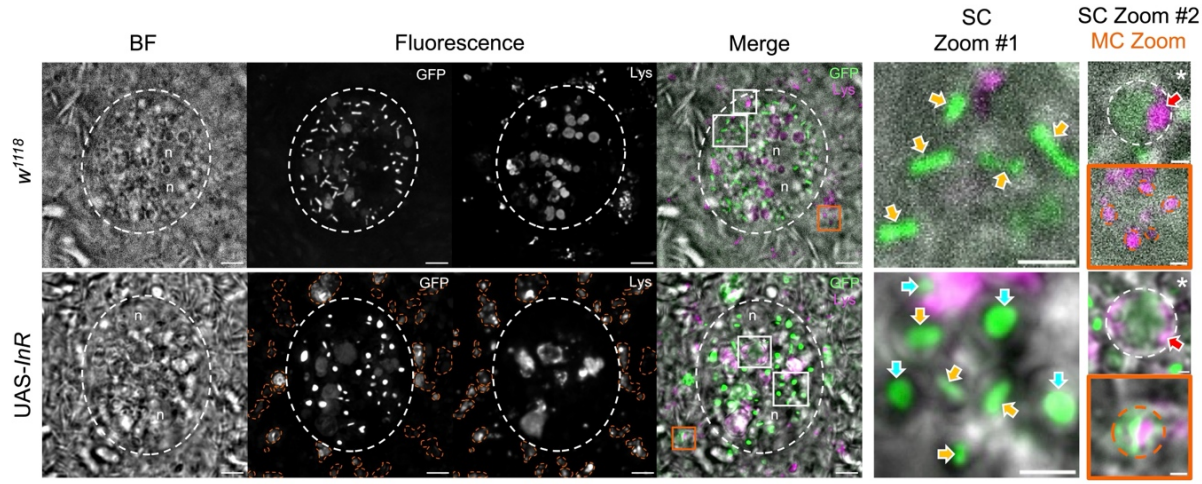


**Figure 12. Modulating the insulin/PI3K/mTORC1 signalling pathway suppresses defective DCG biogenesis in SCs with hTau2N4R overexpression.** Representative images of SCs expressing td-GFP-MFAS-Tau2N4R and no other transgene ($w^{1118}$) or overexpressing SC-specific UAS-*InR*. In the BF, Fluorescence and Merge columns, the SC boundary is outlined by white dashed lines. Abnormal accumulation of GFP-MFAS and associated increased areas of acidification in main cell (MC) endolysosomes are highlighted by orange dashed outlines in the fluorescence images. In the Merge column, white boxes mark regions magnified in the SC zoom panels #1 and #2. The SC zoom #1 panels show representative DCG phenotypes. Yellow arrowheads point out the DCG compartments with cylindrical cores and light blue arrowheads mark the circular DCGs, which show the rescued phenotype ratio. White Zoom boxes marked with asterisks indicate DCG acidification phenotype (SC Zoom #2 panels), where red arrowheads highlight selected acidic microdomains. Orange boxes in the Merge column illustrate regions magnified in the

MC Zoom panels, displaying the corresponding merged images (BF, GFP and Lys). In all images, n marks nuclei and LysoTracker Red (magenta) labels the acidic endosomal domains/compartments and lysosomes. Scale bars: 5 μm (BF, fluorescence, Merge), 2 μm (SC Zoom #1) and 1 μm (SC Zoom #2 and MC Zoom).

*hTau-2N4R-WT, tub-GAL80$^{ts}$; dsx-GAL4, GFP-mfas*

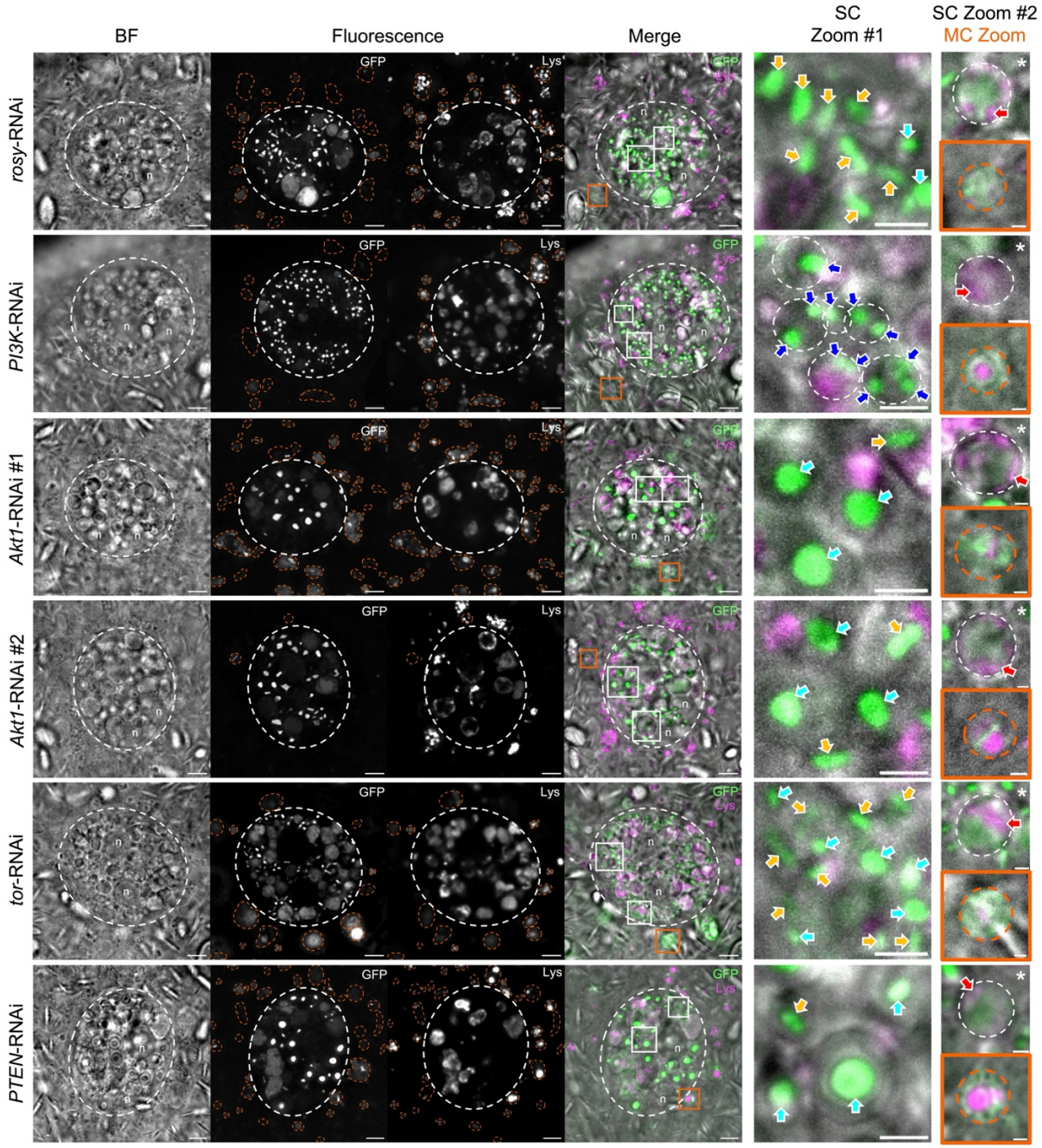


**Figure 13. Modulating the insulin/PI3K/mTORC1 signalling pathway suppresses defective DCG biogenesis in SCs with hTau2N4R overexpression.** Representative images of SCs expressing td-GFP-MFAS-Tau2N4R and in combination with SC-specific control RNAi (*rosy*-RNAi) or RNAi knockdown of *PI3K* (*PI3K*-RNAi), *Akt1* (*Akt1*-RNAi #1 and #2), *tor* (*tor*-RNAi) and *PTEN* (*PTEN*-RNAi). In

the BF, Fluorescence and Merge columns, the SC boundary is outlined by white dashed lines. Abnormal accumulation of GFP-MFAS and associated increased areas of acidification in main cell (MC) endolysosomes are highlighted by orange dashed outlines in the fluorescence images. In the Merge column, white boxes mark regions magnified in the SC zoom panels #1 and #2. The SC zoom #1 panels show representative DCG phenotypes. Yellow arrowheads point out the DCG compartments with cylindrical cores and light blue arrowheads mark the circular DCGs, which show the rescued phenotype ratio. In *PI3K*-RNAi genotype, dark blue arrowheads indicate multiple mini-cores contacting the compartmental limiting membrane. White Zoom boxes marked with asterisks indicate DCG acidification phenotype (SC Zoom #2 panels), where red arrowheads point out selected acidic microdomains. Orange boxes in the Merge column illustrate regions magnified in the MC Zoom panels, displaying the corresponding merged images (BF, GFP and Lys). In all images, n marks nuclei and LysoTracker Red (magenta) labels the acidic endosomal domains/compartments and lysosomes. Scale bars: 5 μm (BF, fluorescence, Merge), 2 μm (SC Zoom #1) and 1 μm (SC Zoom #2 and MC Zoom).

## Modulating insulin/PI3K/mTORC1 signalling partially normalized DCG biogenesis and morphology in SCs overexpressing hTau2N4R

I analysed the number and morphology of DCG compartments following different genetic manipulations affecting insulin/PI3K/mTORC1 signalling in SCs overexpressing hTau2N4R (Figure 14A–D). If either the abnormally elevated number of DCG compartments or the proportion of DCG compartments with cylindrical cores was reduced, this was considered a rescue, indicating that the cytoskeletal and DCG biogenesis defects induced by hTau2N4R overexpression had been partially corrected. The large number of DCG compartments in SCs overexpressing hTau2N4R made it difficult to count the total number of compartments. I therefore counted the compartments in a single plane that passed through the centre of the two SC nuclei to provide an approximate measure of total compartment count.

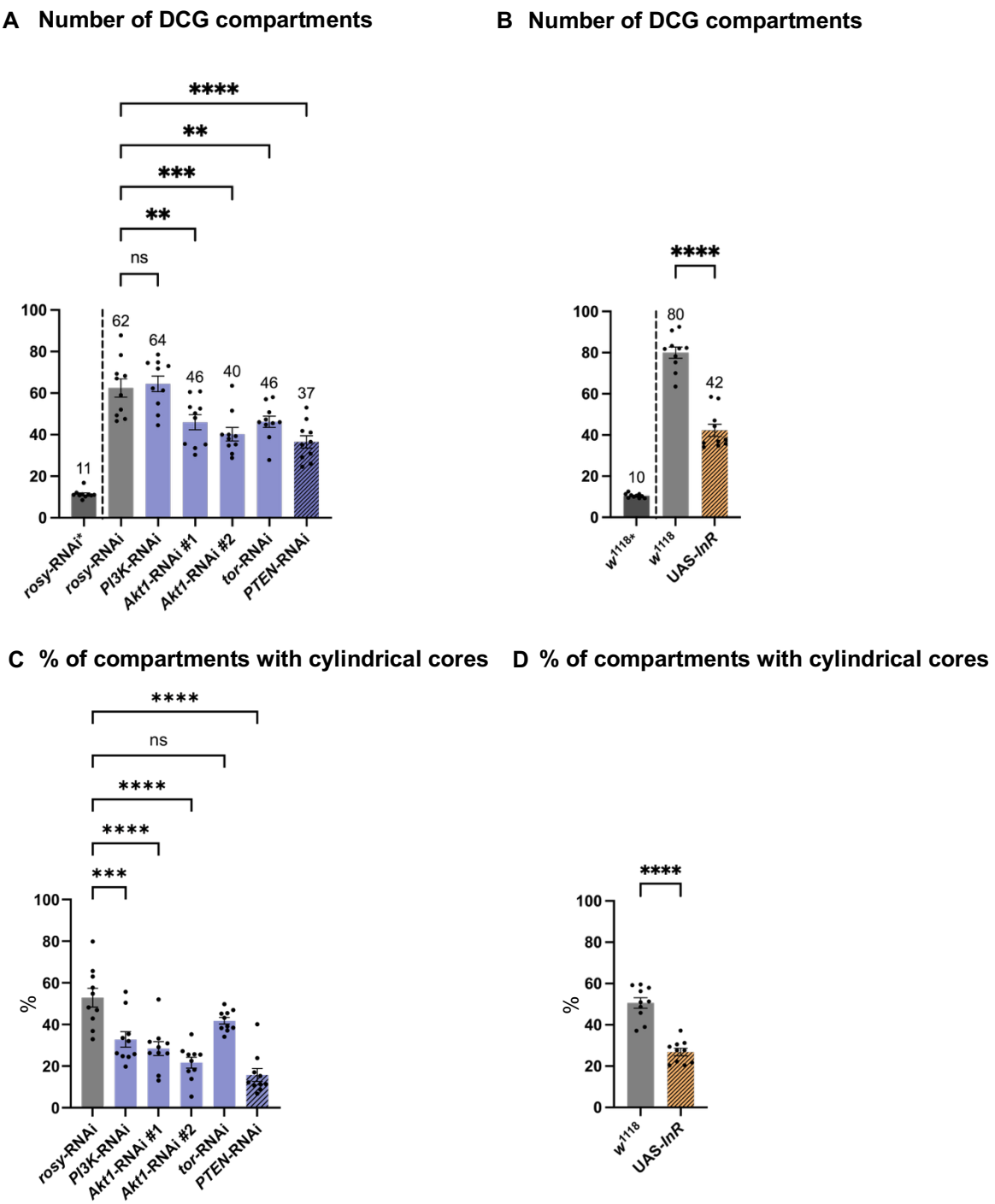


**Figure 14. Bar charts showing the effects of insulin/PI3K/mTORC1 signalling pathway manipulations on DCG number and morphology, in the td-GFP-MFAS-Tau2N4R model.**

Number of DCG compartments in SCs overexpressing hTau2N4R with either SC-specific RNAi knockdowns (A) or overexpression transgenes **(**B) of insulin/PI3K/mTORC1 pathway components. In both panels (A) and (B), *rosy*-RNA*

and $w^{1118}$* shown at the far left of each graph represent control genotypes without hTau2N4R overexpression from Figure 9A. These controls were included for visual reference only to illustrate baseline DCG compartment numbers. They were not included in the statistical analysis, which was restricted to genotypes overexpressing hTau2N4R, as the control samples with asterisks were quantified using a different measurement approach as described in the Methods and therefore were not directly comparable statistically. Numbers annotated above each bar indicate mean values rounded to the nearest integer to provide clear visual comparison of DCG compartment numbers across genotypes. Percentage of DCG compartments with cylindrical cores under the same genetic conditions: SC-specific RNAi knockdowns (C) and overexpression transgenes (D). The x-axis indicates the different genotypes. Purple bars represent UAS-RNAi transgenes, which were compared with the *rosy*-RNAi control. The yellow bar represents a UAS-transgene (UAS-*InR*), compared with the $w^{1118}$ control. Non-shaded bars correspond to genotypes that downregulate insulin/PI3K/mTORC1 signalling, whereas shaded bars (*PTEN*-RNAi and UAS-*InR*) indicate genotypes that upregulate pathway activity. Data are shown as mean ± SEM, with each dot representing the average measurement from an individual fly (n = 10). Data were normally distributed and statistical analysis was performed using the ordinary one-way ANOVA followed by post hoc multiple comparisons, specifically the Dunnett's multiple comparison test with automatic correction of p-values. Significance levels are indicated as *p < 0.05, **p < 0.01, ***p < 0.001, ****p < 0.0001, bars without asterisks are not significantly (ns) different from controls.

In Figure 14A and 14C, among genotypes that decreased insulin/PI3K/mTORC1 signalling activity, *Ak*t-RNAi #1 and *Akt*-RNAi #2 both showed a significant decrease in the number of DCG compartments, when compared with the *rosy*-RNAi control. At the same time, there was a drastic reduction in the percentage of DCG compartments with cylindrical cores, with nearly half of the compartments rescued to circular core morphology. *tor*-RNAi produced a mild but significant reduction in the number of DCG compartments, but DCG morphology was not significantly rescued. Notably, *PI3K*-RNAi resulted in a comparable number of DCG compartments to *rosy*-RNAi, but showed a strong and significant decrease in the percentage of compartments with cylindrical cores. This interpretation should be treated with caution. As shown in Figure 13, this genotype displayed unique “mini-cores” phenotype, similar to those observed when crossed with td-GFP-MFAS without Tau overexpression. Since the Fiji software counted each mini-core as an individual compartment, it likely overestimated the total number of DCG compartments.

Among genotypes that increased signalling activity, *PTEN*-RNAi and UAS-*InR* showed strong rescued phenotypes compared with the *rosy*-RNAi and $w^{1118}$ controls respectively, each reducing the number of DCG compartments by approximately half (Figure 14A and 14B). *PTEN*-RNAi produced the most pronounced effect, with less than 20% of DCG compartments with cylindrical cores (Figure 14C), but UAS-*InR* also had a major impact on morphology (Figure 14D).

These results suggest that manipulating the insulin/PI3K/mTORC1 signalling pathway, whether by increasing or decreasing its activity can partially restore normal DCG-aggregate priming and membrane dissociation disrupted by hTau2N4R

overexpression. The most notable effect was observed with *PTEN*-RNAi, which displayed the strongest rescuing phenotype on both the number and morphology of DCG compartments.

## Modulating insulin/PI3K/mTORC1 signalling further exacerbated endolysosomal trafficking defects in SCs overexpressing hTau2N4R

The recombinant line td-GFP-MFAS-Tau2N4R alone increased the acidified and lysosomal areas within SCs, suggesting altered endolysosomal trafficking dynamics. To further investigate whether modulating insulin/PI3K/mTORC1 signalling could rescue this phenotype, I assessed the % of acidified DCG compartments and the % of total lysosomal area in SCs for all genotypes (Figure 15).

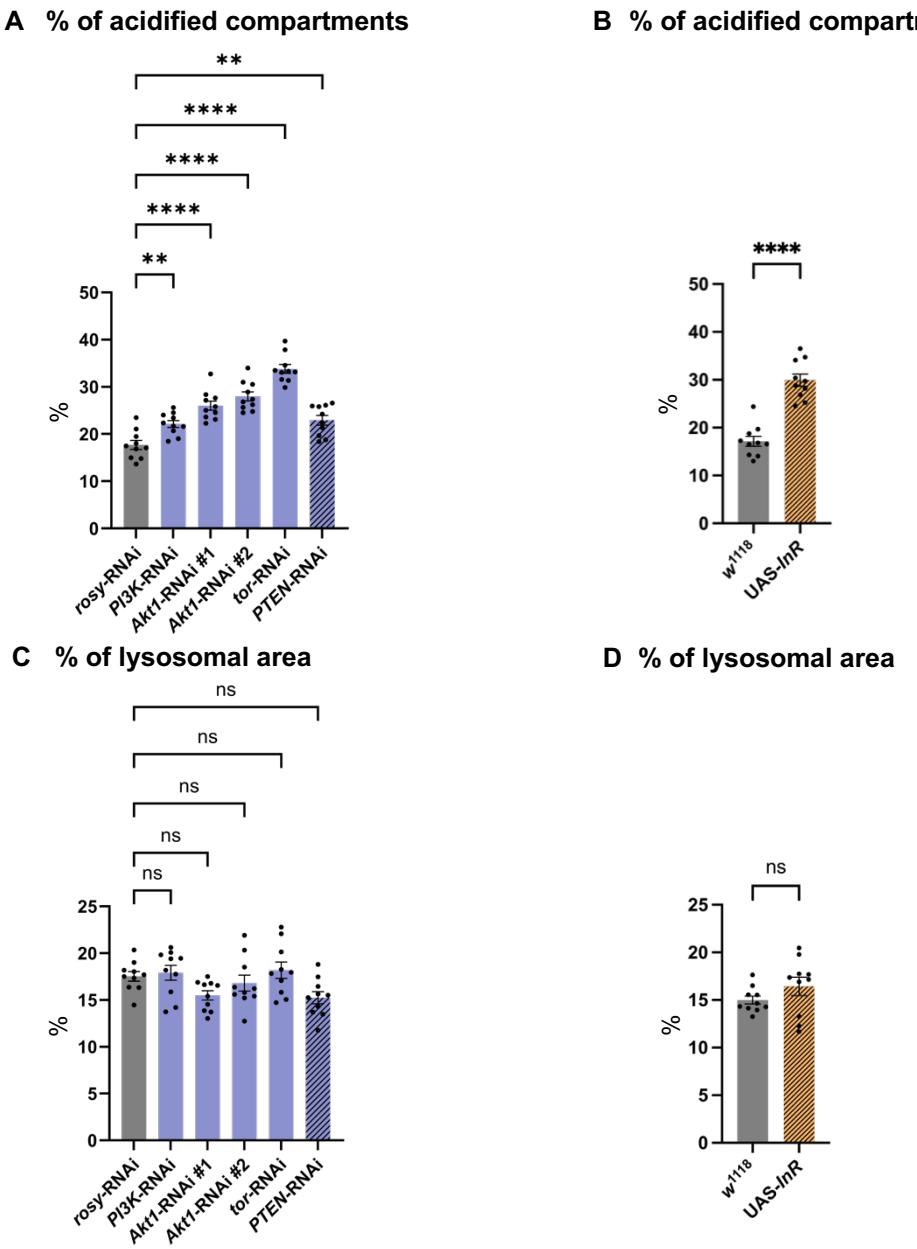


**Figure 15. Bar charts showing the effects of insulin/PI3K/mTORC1 signalling pathway manipulations on SC endolysosomal trafficking, in the td-GFP-MFAS-Tau2N4R model.**

(A,B) Percentage of acidified compartments in SCs overexpressing hTau2N4R with either SC-specific RNAi knockdowns (A) or overexpression transgenes (B) for insulin/PI3K/mTORC1 pathway components. (C,D) Percentage of lysosomal area in SCs under the same genetic conditions: RNAi knockdowns (C) and overexpression

(D). The x-axis indicates the different genotypes. Purple bars represent UAS-RNAi transgenes, which were compared with the *rosy*-RNAi control. The yellow bar represents a UAS-transgene (UAS-*InR*), compared with the $w^{1118}$ control. Non-shaded bars correspond to genotypes that downregulate insulin/PI3K/mTORC1 signalling, whereas shaded bars (*PTEN*-RNAi and UAS-*InR*) indicate genotypes that upregulate pathway activity. Data are shown as mean ± SEM, with each dot representing the average measurement from an individual fly (n = 10). Data were normally distributed and statistical analysis was performed using the ordinary one-way ANOVA followed by post hoc multiple comparisons (the Dunnett's multiple comparison test with automatic correction of p-values). Significance levels are indicated as *$p < 0.05$, **$p < 0.01$, ***$p < 0.001$, ****$p < 0.0001$, bars without asterisks are not significantly (ns) different from controls.

Among genotypes that decreased signalling activity in Figure 15A, all showed a significant increase in the percentage of acidified compartments compared with the *rosy*-RNAi control. A subtle trend was observed along the pathway, where manipulations targeting downstream components produced progressively stronger effects, with *tor*-RNAi exhibiting the most pronounced increase.

The effects of increasing insulin/PI3K/mTORC1 signalling were also consistent. Both *PTEN*-RNAi and UAS-*InR* led to a marked elevation in the percentage of acidified compartments, although the effect was greater for UAS-*InR* (Figures 15A and 15B). These results suggest that modulating pathway activity, whether up- or down-regulation enhances the formation or accumulation of acidified compartments in SCs overexpressing hTau2N4R.

In contrast, analysis of the percentage of lysosomal area showed no significant difference across any of the genotypes, regardless of whether signalling was increased or decreased, as shown in Figure 15C and 15D.

In summary, hTau2N4R overexpression disrupts DCG biogenesis, resulting in an increased number of abnormal DGC compartments with cylindrical cores, and elevated endolysosomal trafficking to lysosomes. Manipulations of the insulin/PI3K/mTORC1 signalling pathway appear to suppress the morphological defects in DCG compartments, but there may be a higher level of abnormal endolysosomal trafficking of these compartments, which then fail to fuse with lysosomes, even under conditions of low insulin/PI3K/mTORC1 signalling where lysosome biogenesis will be favoured.

Finally, I analysed the effects of modulating insulin/PI3K/mTORC1 signalling on the uptake of GFP-MFAS by main cells (MCs) in the td-GFP-MFAS-Tau2N4R model, as shown in Figure 16. As described in the first part of the results, several RNAi knockdowns in SCs appeared to enhance protein uptake by MCs, possibly because the RNAi-induced cellular stress influences DCG biogenesis and secretory pathway. In this context, comparing the *rosy*-RNAi control crossed with the td-GFP-MFAS-Tau2N4R line (Figure 13) to this recombinant line alone (Figure 11) showed that overexpression of hTau2N4R itself did not exacerbate MC uptake of GFP-MFAS, suggesting no obvious main cell phenotype.

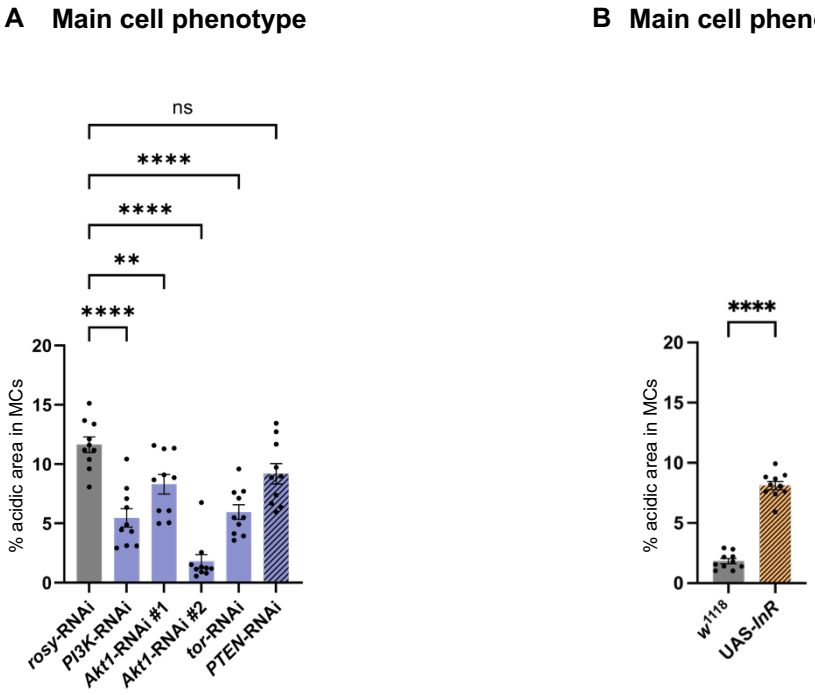


**Figure 16. Bar charts showing the effects of insulin/PI3K/mTORC1 signalling pathway manipulations on main cell (MC) uptake of SC secreted proteins, in the td-GFP-MFAS-Tau2N4R model.**

Main cell phenotype, expressed as the percentage of acidic area in MCs containing GFP-MFAS, in SCs overexpressing hTau2N4R with either SC-specific RNAi knockdowns (A) or overexpression transgenes (B) of insulin/PI3K/mTORC1 pathway components. The x-axis indicates the different genotypes. Purple bars represent UAS-RNAi transgenes, which were compared with the *rosy*-RNAi control. The yellow bar represents a UAS-transgene (UAS-*InR*), compared with the $w^{1118}$ control. Non-shaded bars correspond to genotypes that downregulate insulin/PI3K/mTORC1 signalling, whereas shaded bars (*PTEN*-RNAi and UAS-*InR*) indicate genotypes that upregulate pathway activity. Data are shown as mean ± SEM, with each dot representing the average measurement from an individual fly (n = 10). Data were normally distributed and statistical analysis was performed using the ordinary one-way ANOVA followed by post hoc multiple comparisons (the Dunnett's multiple comparison test with automatic correction of p-values). Significance levels are indicated as *p < 0.05, **p < 0.01, ***p < 0.001, ****p < 0.0001, bars without asterisks are not significantly (ns) different from controls.

For genotypes that downregulated the pathway in Figure 16A, both *PI3K*-RNAi and *tor*-RNAi produced a significant reduction in MC uptake of secreted GFP-MFAS when compared with the *rosy*-RNAi control,. Notably, *Akt1*-RNAi #2 caused the strongest effect, showing the most substantial decrease in MC uptake, whereas *Akt1*-RNAi #1 produced only a mild reduction.

For genotypes that increased pathway activity, *PTEN*-RNAi showed no significant change in MC uptake of secreted GFP-MFAS (Figure 16A). In contrast, *InR* overexpression resulted in more than a two-fold increase in MC uptake compared with the $w^{1118}$ control in Figure 16B. It was very difficult to interpret these results, because the two controls employed are so different from each other. However, one possible conclusion is that reduced insulin/PI3K/mTORC1 signalling suppresses macromolecular synthesis and secretory activity in SCs, and this therefore reduces the level of secreted GFP-MFAS accumulating in other cells through endocytosis.

Overall, these findings suggest that modulating the insulin/PI3K/mTORC1 signalling pathway, either through upregulation or downregulation, can partially rescue the abnormal DCG biogenesis in SCs induced by overexpressing hTau2N4R. As discussed previously, Tau functions as a cytoskeletal regulatory protein and its pathological overexpression disrupts the cytoskeleton network, leading to defects in DCG-aggregate priming and dissociation from the limiting membrane, as well as vesicular trafficking. Therefore, modulating insulin/PI3K/mTORC1 signalling may help to suppress the cytoskeletal defects that disturb DCG biogenesis, but these genetic manipulations may also affect endolysosomal trafficking and lead to the build-up of acidified compartments that do not fuse with lysosomes.

# Discussion

In my dissertation work, I first set out to examine how modulation of the insulin/PI3K/mTORC1 signalling pathway regulates DCG biogenesis, secretory and endolysosomal trafficking events in *Drosophila* male accessory gland SCs. Previous work by A. Wells (2024) demonstrated that this pathway plays a central role in intraluminal vesicles (ILVs) formation and E-cadherin microdomain organisation, which are considered precursor processes during early priming steps preceding DCG aggregation, dissociation from membrane microdomains and DCG maturation. Building on these findings, my study found that the insulin/PI3K/mTORC1 signalling must be tightly regulated to maintain normal DCG biogenesis, as both pathway downregulation and upregulation result in abnormalities in the number of DCG compartments or in their core morphology, thereby triggering abnormal endolysosomal trafficking. However, effects on overall cellular growth were observed only in limited number of genetic contexts. In addition, several RNAi manipulations appeared to promote main cell uptake of SCs secreted materials (propagation phenotype).

I next examined whether modulating insulin/PI3K/mTORC1 signalling pathway could influence or even rescue secretory and endolysosomal defects induced by overexpressing human Tau2N4R wild type (hTau2N4R) in SCs, a model relevant to AD. Overexpression of hTau2N4R resulted in abnormal cylindrical cores within DCG compartments, frequently contacting the limiting membrane, and was accompanied by an increased number of DCG compartments and an expansion of overall lysosomal area. My findings have demonstrated that modulation of insulin/PI3K/mTORC1 signalling, through either up- or down- regulation, can partially

rescue hTau2N4R-induced abnormalities in DCG biogenesis, however, without restoring the normal function of endolysosomal trafficking.

Together, these results support and extend conclusions from A. Wells (2024), reinforcing the conserved role of the insulin/PI3K/mTORC1 signalling pathway in secretory and endolysosomal trafficking in SCs, also its potential significance involved in tauopathy in AD.

## Regulation of cellular growth through insulin/PI3K/mTORC1 signalling

I observed some changes in SC size and nuclear size with only a few manipulations that altered insulin/PI3K/mTORC1 signalling. Co-overexpression of *Tsc1* and *Tsc2* led to a marked reduction in SC size, consistent with suppressed activity of the insulin/PI3K/mTORC1 pathway (Glaviano et al., 2023). This phenotype reflects the growth inhibitory role of the Tsc1/2 complex as a negative regulator of Rheb/mTORC1 signalling. Similar effects were observed by Potter et al. (2001), who demonstrated that while overexpression either *Tsc1* or *Tsc2* alone produced no effect, co-overexpression of both genes in the wing and eye drastically decreased cell size and number, as well as organ size.

Interestingly, the *PI3K*-RNAi #2 line, which had previously been excluded from the main experiments and analysis, produced an unexpected phenotype characterised by a slight enlargement of SC size together with a pronounced increase in nuclear size. This differs from the effects observed with other manipulations of the

insulin/PI3K/mTORC1 pathway. Since depletion of *PI3K* would normally be expected to suppress pathway activity and produce phenotypes similar to those observed with *Tsc1/2* overexpression, these observations suggest that the phenotype may not solely reflect reduced *PI3K* signalling.

One possible explanation for this discrepancy relates to line-specific characteristics of RNAi-based genetic manipulation. RNAi transgenes are often introduced into the genome through random insertion, meaning that independent RNAi lines may carry the construct at different and often unknown genomic locations (Pal-Bhadra et al., 2002). The chromatin environment surrounding the insertion site can strongly influence the level and spatial pattern of hairpin transcription under GAL4 control, resulting in variable knockdown efficiency between RNAi lines targeting the same gene (Ni et al., 2007). In some cases, the insertion itself may also disrupt nearby endogenous genes or regulatory regions, leading to unexpected phenotypes independent of the designed genetic manipulation. Furthermore, RNAi hairpins are processed into multiple small interfering RNAs, some of which may partially match other transcripts and produce off-target silencing (Scacheri et al., 2004). Such effects on genes involved in growth regulation or nuclear size control could therefore contribute to the enlargement phenotype observed with the *PI3K*-RNAi #2 line.

On the other hand, *PTEN* knockdown should elevate PIP3 levels and activate Akt/mTORC1 to upregulate this signalling cascade. Consistent with this, I observed increased SC size with *PTEN*-RNAi expression, in line with earlier findings that the loss of *Drosophila* PTEN boosts cell size and number by acting antagonistically to *Drosophila* PI3K (Goberdhan et al., 1999). However, other manipulations that

probably have more modest effects on this pathway did not affect growth significantly. Taken together, my results confirm that major changes in the insulin/PI3K/mTORC1 signalling pathway activity can modulate growth in SCs.

Interestingly, alterations in pathway activity also affected nuclear size in SCs. I found that conditions promoting cell growth (*Rheb* overexpression and *PTEN* knockdown) led to enlarged nuclei, whereas pathway downregulation showed a subtle trend to produce smaller nuclei. This may suggest that insulin/PI3K/mTORC1 signalling affects both endoreplication cycles and non-endoreplication driven growth in these polyploid secretory cells.

Previous work has demonstrated that *Drosophila* SCs nuclei normally enlarge during aging or following mating through a combination of endoreplication, a process that increases genomic content to support the increased secretory demands of the gland, and non-endoreplication-dependent mechanisms (Leiblich et al., 2019). In virgin male flies, SC nuclear growth is largely hormone-dependent, requiring ecdysone receptor (EcR) activation and BMP signalling to maintain normal growth, where no new DNA replication occurs in the two polyploid nuclei of mature SCs. However, after mating, a subset of SCs re-enter the endocycle, leading to additional genome duplication and a marked increase in nuclear size. In this project, all flies were virgin males, but *PTEN*-RNAi and *Rheb* overexpression both resulted in enlarged nuclei, implying that insulin/PI3K/mTORC1 signalling may act as an additional modulator of nuclear growth. Possible explanations would be that upregulated its signalling activity may induce endoreplication or enhance biosynthetic output in nuclei to meet cell growth demands via non-endoreplication-dependent mechanisms. In this

context, the observation that reduced insulin/PI3K/mTORC1 signalling was associated with only a weak tendency toward decreased nuclear size suggests that at least some aspects of nuclear size changes must be independent of endoreplication.

Regarding the effect of overexpressing *Rheb*, a small GTPase, it functions downstream of the Tsc1/2 complex to activate mTORC1 (Inoki et al., 2003). *In vivo* studies have showed that *Rheb* loss-of-function mutants display reduced cell size, while *Rheb* overexpression causes cellular and tissue overgrowth (Stocker et al., 2003). Moreover, *Rheb* overactivation has been shown to restore both cell and nuclear size under nutrient-restricted conditions in *Drosophila* salivary gland and fat body cells, where increased *Rheb* expression alleviates the endoreplication deficits typically associated with starvation.

In summary, the insulin/PI3K/mTORC1 signalling pathway regulates cellular and nuclear growth in SCs, although further experiments are required to show whether this involves any effects on endoreplication.

## Insulin/PI3K/mTORC1 signalling control of DCG biogenesis and morphology

Upregulating the insulin/PI3K/mTORC1 pathway in *Drosophila* SCs did not produce consistent effects on DCG biogenesis and morphology. *PTEN*-RNAi induced a drastic hypertrophy of SCs with enlarged nuclei, and a significant increase in the number of DCG compartments, yet only subtle granule abnormalities. This outcome

suggests that the expanded cytoplasmic volume and biosynthetic capacity in SCs with *PTEN* knockdown may accommodate additional compartment formation and secretion without major structural defects. Similar phenotypes have been observed in other *Drosophila* tissues, where loss of *PTEN* or hyperactivation of insulin/PI3K/mTORC1 signalling leads to cell hypertrophy and increased anabolic activity, enabling overgrowth without disrupting cellular architecture or differentiation (Yang & Xu, 2011).

By contrast, *Rheb* overexpression increased the number of DCG compartments without changing the SC size, and there were morphological defects in the resulting dense cores. This observation suggests that boosting DCG biogenesis without parallel expansion of cell volume may compromise normal secretory events. Indeed, the imbalance between secretory load and cellular capacity also triggers abnormal reactions in mammalian systems. For example, in pancreatic β-cells, when secretory processing is disrupted, cells experience hyper-anabolism and accumulate excessive non-functional and immature secretory granules (Brouwers et al., 2020). These findings indicate that a coordinated increase in cell size and secretory activity is essential for maintaining normal DCG biogenesis and morphology, and that although reducing PTEN activity appears to promote both processes in parallel, increased mTORC1 activity through *Rheb* overexpression does not.

Finally, overexpression of the insulin receptor (UAS-*InR*) produced increased numbers of DCGs with a GFP-MFAS-negative centre. This phenotype has previously been observed in genetic manipulations where the detachment of DCG aggregates from the compartmental limiting membranes may be delayed, e.g. β-secretase

knockdown (Singh et al., 2025). Related phenotypes were also observed in several other manipulations affecting the insulin/PI3K/mTORC1 signalling, suggesting that balanced signalling activity may be required to ensure proper DCG assembly, though the underlying mechanisms remain unclear.

When the pathway was downregulated, the most extreme phenotype observed was that *PI3K*-RNAi induced a mini-core phenotype, in which small granules were tightly contacted with the limiting membrane. In contrast, overexpression of *PTEN*, which counteracts PI3K activity and would be expected to act similarly to *PI3K*-RNAi, produced only a small number of DCG compartments with deformed cores but a relatively large proportion of DCGs with GFP-negative centres. The most likely explanation for these phenotypic differences is that the *PI3K*-RNAi has a stronger suppressive effect on insulin/PI3K/mTORC1 signalling activity, thereby disrupting early steps of DCG-aggregate priming and membrane dissociation.

As described previously, DCG biogenesis takes place within Rab11-positive secretory compartments, which act as platforms for both granule condensation and intraluminal vesicles (ILVs) formation. Within these compartments, E-cadherin enriched lipid microdomains (ELMs) appear to recruit the ESCRT machinery to form ILVs. Wells (2024) previously found that *PI3K*-RNAi caused a drastic reduction in Rab-11 compartments containing ILVs, representing the strongest phenotype among all inhibitory manipulations affecting the insulin/PI3K/mTORC1 signalling. UAS-*PTEN* produced only a modest decline. *PI3K* depletion also induced defective DCG biogenesis, as scored by phase contrast microscopy, and reduced E-cadherin microdomain formation, consistent with my data.

One possible explanation for the effects of PI3K is that PIP3 signalling is involved in events controlling DCG compartment maturation. For instance, small GTPases Rac1/Cdc42 are known downstream targets of PI3K/PIP3 signalling that regulate the actin cytoskeleton (Hong-Geller & Cerione, 2000). There is evidence from mammalian secretory cells that active Rac1/Cdc42 stimulate the maturation of secretory granules and their exocytosis by promoting actin-driven vesicle transport and release. The role of ELMs in ILVs and DCG aggregate formation might be modulated by *PI3K* knockdown. Although further work will be required to explore these mechanisms in detail, the current data clearly indicate that the insulin/PI3K/mTORC1 signalling pathway is intricately linked to DCG biogenesis.

## Bidirectional insulin/PI3K/mTORC1 signalling modulation partially rescues Tau-induced DCG defects

Overexpression of human Tau 2N4R wild type in SCs induced several pathological phenotypes, including aberrant DCG morphology in cylindrical cores with at least one end touching the compartment limiting membrane, potentially reduced exocytosis, leading to large numbers of DCG compartments and accumulation of lysosomes, as shown in Figure 17B and noted previously (Verma, unpublished results). These defects mirror how tau pathology disrupts the secretory and endolysosomal systems, perhaps by excessive binding of tau to microtubules, which hinders the cytoskeletal transport and alters the microtubule and microfilament network organization (Prezel et al., 2018). Tau acts as a cytoskeletal toxin in this context, leading to the accumulation of defective secretory granules and potentially blockage of the degradation pathways.

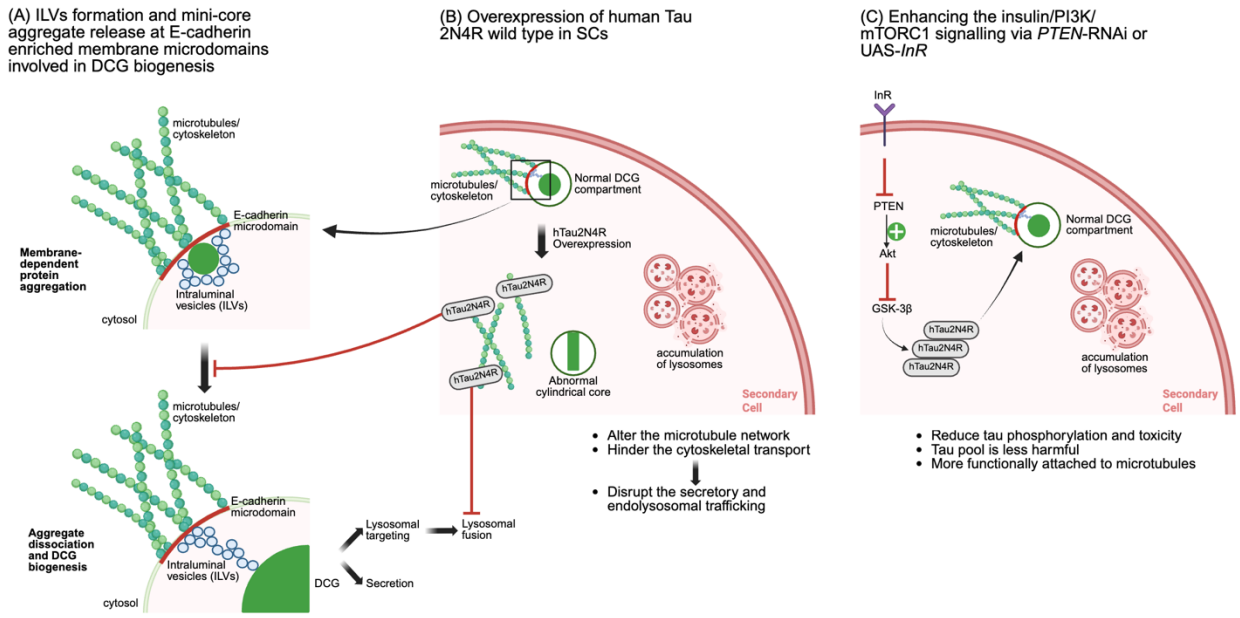


**Figure 17.** Schematic model linking DCG biogenesis, tau overexpression-induced defects on secretory and endolysosomal trafficking, with the insulin/PI3K/mTORC1 signalling acting as a modulatory pathway in SCs.

In this project, enhancing insulin/PI3K/mTORC1 signalling via *PTEN* knockdown and overexpressing *InR* provided a partial rescue of DCG compartment number and morphology. Chatterjee et al. (2019), using *Drosophila* models overexpressing the full-length human tau isoform 2N4R, found that overexpression of hTau in the retina caused a classic “rough eye” phenotype, reflecting tau-induced neurotoxicity. This abnormal phenotype was suppressed by overexpressing *Chico*, the *Drosophila* homologue of mammalian insulin receptor substrate, which positively regulates signalling. It reduced total and phosphorylated tau levels, thus decreasing tau aggregation. Meanwhile, in human neuronal cell models, okadaic acid, a toxin that inhibits tau phosphatases, induces tau hyperphosphorylation and neurodegeneration in AD, which can be significantly alleviated by PTEN inhibition (Chen et al., 2012).

The potential mechanisms underlying the rescued phenotype may involve another downstream component in insulin signalling pathway (IIS). PTEN inhibition heightens Akt activity, which suppresses GSK-3β, a key tau-associated kinase that accelerates tau aggregation (Chakraborty et al., 2024), thereby reducing tau phosphorylation and toxicity in cytosol, as illustrated in Figure 17C. In SCs, upregulating insulin/PI3K/mTORC1 signalling via *PTEN*-RNAi or UAS-*InR* may lead to a tau pool that is less harmful and more functionally attached to microtubules, thus preserving a series of events involved in DCG biogenesis, including DCG-aggregate priming from ELMs, ILVs formation, and fusion of aggregates into a central DCG, consistent with the model summarised in Figure 17A.

Furthermore, Liraglutide, a GLP-1 receptor agonist known to enhance insulin signalling (IIS), was shown to significantly reduce pathology-specific tau phosphorylation and improve motor function in the hTauP301L transgenic mouse model, which mimics frontotemporal dementia-like tauopathy (Hansen et al., 2016). The therapeutic values of Liraglutide suggest that enhanced insulin signalling can mitigate tau toxicity across different neurodegenerative diseases with tauopathy, not just in AD.

Equally interesting, reducing insulin/PI3K/mTORC1 signalling also led to improvements in tau-induced defects in this study. SCs in this case showed more circular DCGs and more normal compartment organisation than Tau control alone. This might seem contradictory alongside the *PTEN*-RNAi and UAS-*InR* results, but it suggests that modulating the pathway in both directions can interfere with tau pathology, presumably through different routes.

Co-expression of *PI3K*-RNAi and hTau2N4R showed a unique phenotype. The total number of DCG compartments appeared unchanged, though this was difficult to measure. As shown in Figure 13, most compartments displayed the mini-core phenotype, consistent with what was previously observed in SCs without hTau2N4R overexpression. Interestingly, when comparing with abnormal cylindrical cores induced by hTau2N4R overexpression, *PI3K*-RNAi seemed to override the tau-dependent morphology, suggesting that PI3K may act downstream of Tau in a specific aspect of DCG biogenesis. As discussed above, inhibition of PI3K causes a drastic reduction in PIP3 at the limiting membrane, reduces the formation of ELMs and the recruitment of ESCRT machinery (Wells, 2024), as well as impairing Rac1/Cdc42-mediated actin remodeling essential for secretory granule maturation (Bader et al., 2004; Schulz et al., 2015). DCG aggregates fail to condense centrally and remain as mini-cores. Since tau primarily modulates the cytoskeletal microtubules, its effect on DCG morphology may be secondary to the loss of actin-dependent membrane scaffolding due to *PI3K* knockdown, correcting the tau-induced phenotype, but inducing a mini-core phenotype instead. These data suggest that Tau-dependent effects on DCG morphology require intact PI3K/PIP3 signalling, placing PI3K functionally downstream or epistatic to Tau in this context.

Reduced insulin/PI3K/mTORC1 signalling activity decreased the number of DCG compartments, as well as restoring DCG circular morphology. A study using multiple transgenic *Drosophila* lines expressing human tau found that whether expressing human tau wild type or mutant forms can lead to overactivation of the IIS pathway (None Pragati & Sarkar, 2023). Downregulating the insulin signalling tone suppressed the human tau-mediated neurodegeneration and neurotoxicity,

potentially by reducing overall cellular stress, improving autophagic response and re-establishing balance between different kinases (e.g. GSK3β). Rescue was also observed for other tau isoforms in this study (Kim & Lee, 2013; Tolkovsky & Spillantini, 2021). In parallel with neurodegeneration and nutrition-related research, reduced IIS or dietary restriction can extend lifespan from yeast to mammals and reduce aberrant protein aggregation, partly via enhanced autophagy and stress resistance, improving behavioural impairment and alleviating neuroinflammation as positive results (Steinkraus et al., 2008; Cohen et al., 2009).

In summary, previous studies have reported a conflicting role for the insulin/PI3K/mTORC1 signalling pathway within AD. Findings presented in this thesis highlight that both upward and downward changes in this signalling cascade can be protective for SCs, presumably by using different routes to target tau pathology, suggesting that the critical determinant is to restore the balanced physiological state, though via different mechanisms.

## Insulin/PI3K/mTORC1 signalling regulates lysosomal dynamics and endolysosomal trafficking

Live cell imaging and lysotracker staining revealed that modulation of insulin/PI3K/mTORC1 pathway activity markedly influences the abundance of acidified compartments and endolysosomal trafficking in SCs. In general, downregulating insulin/PI3K/mTORC1 signalling led to significant increases in lysosomal area per SC, but only *PI3K*-RNAi increased the number of acidified DCG compartments compared with control, possibly due to the accumulation of abnormal

mini-core-containing compartments, whose targeting to lysosomes is frequently disrupted (Singh et al., 2025).

As shown in Figure 18A, when the insulin/PI3K/mTORC1 signalling is low, mTORC1 activity is suppressed and cells often compensate by maximising the rate of autophagy and lysosome biogenesis (Di Malta & Ballabio, 2017). Mechanistically, the master regulator TFEB and other related transcription factors are activated by mTOR inhibition, thus translocating to the nucleus to induce expression of lysosomal and autophagy genes (Medina et al., 2015). Treatments with rapamycin which inhibit mTOR or overexpressing TFEB can contribute to neuronal protection by enhancing the autophagy-lysosome pathway and alleviating cellular apoptosis (Panwar et al., 2023). Therefore, SCs with reduced insulin/PI3K/mTORC1 signalling would be expected to have increased lysosomal area, consistent with lysotracker results presented in this thesis.

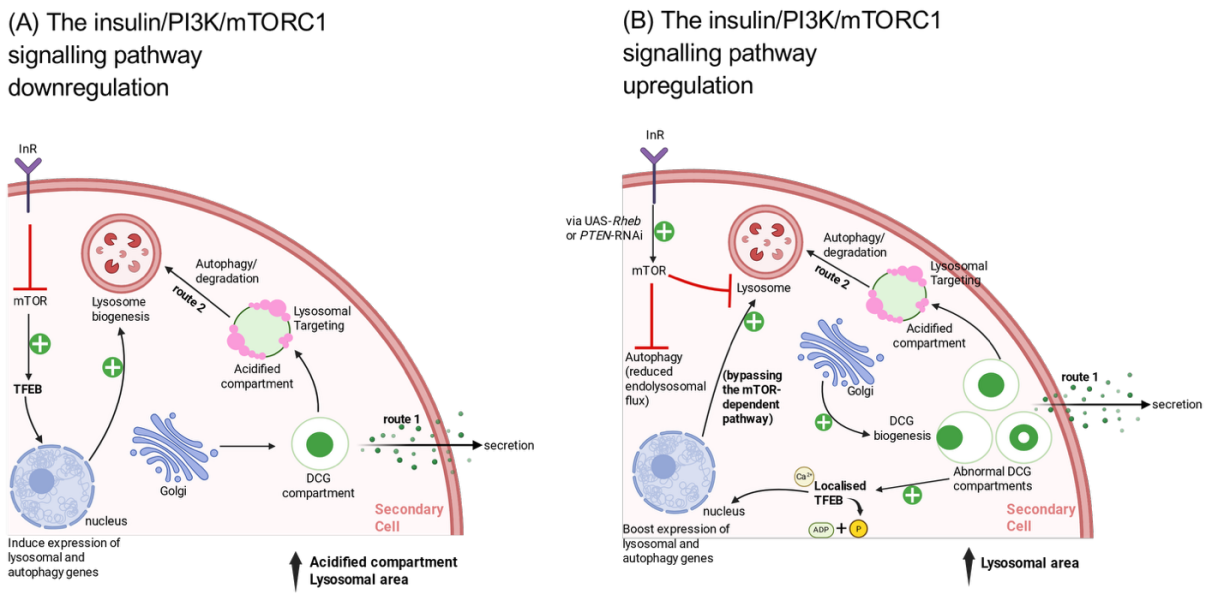


**Figure 18. Schematic models illustrating the insulin/PI3K/mTORC1 signalling dependent regulation of secretory and endolysosomal trafficking in SCs.**

Green crosses represent activation of the indicated processes. DCG compartments generated at the Golgi body can follow two principal routes. Route one supports maturation and secretion of DCG cargo, while route two directs DCG compartments toward lysosomal targeting and autophagy.

In contrast, upregulating insulin/PI3K/mTORC1 signalling via *Rheb* overexpression or *PTEN*-RNAi tended to reduce the prevalence of acidic endolysosomal compartments, but greatly increased lysosomal area. With high mTORC1 signalling, autophagy and lysosomal activity are suppressed, resulting in reduced endolysosomal flux (Menon et al., 2014), as shown in Figure 17B. Nevertheless, SCs overexpressing *Rheb* or *PTEN*-RNAi displayed an obvious increase in total lysosomal area. As described previously, upregulated insulin/PI3K/mTORC1 signalling promotes DCG biogenesis, but simultaneously produces a higher proportion of defective compartments during maturation. These abnormalities may activate compensatory routes that increase lysosomal activity, while bypassing the mTOR-dependent pathway (Puertollano et al., 2018). Given that TFEB localization is regulated by multi-site phosphorylation, local calcium/calcineurin signalling can directly dephosphorylate a fraction of TFEB, allowing its nuclear translocation and boosting lysosomal gene expression even if mTOR is still active (Medina et al., 2015; Tong & Song, 2015). In this context, it should be noted that increasing *InR* expression in SCs elevated the number of acidified DCG compartments, but not lysosomal area, potentially indicating that the InR may regulate an additional PI3K-independent pathway that prevents suppression of lysosomal trafficking.

## Tau overexpression induces trafficking impairments

Overexpression of human tau proteins is known to disrupt vesicle trafficking and lysosomal degradation in both cell and animal models (Ebneth et al., 1998; Yu et al., 2019). In the *Drosophila* SC model used in this study, overexpressing human Tau2N4R wild type induces remarkable phenotypes that reflect DCG biogenesis,

secretory and endolysosomal trafficking defects. Such defects mirror what has been found in neurons during AD and related tauopathies. Endolysosomal network dysfunction is an early pathology in AD (Chen et al., 2025).

## Insulin/PI3K/mTORC1 signalling modulation of endolysosomal trafficking under Tau overexpression

In the *Drosophila* SCs model overexpressing hTau2N4R, it was observed that both downregulating and upregulating insulin/PI3K/mTORC1 signalling increased the number of acidified DCG compartments without significantly changing the total lysosomal area.

This was surprising for insulin/PI3K/mTORC1 signalling downregulation, since reduced mTORC1 activity triggers robust autophagy, which can ameliorate tau pathology (Caccamo et al., 2013; Morawe et al., 2022), and by itself, reduced signalling increased lysosomal area in SCs. In Tau-overexpressing SCs, it seems that although decreasing insulin/PI3K/mTORC1 signalling can partially suppress cylindrical DCGs formation, there must still be defects in endolysosomal trafficking of those abnormal DCG compartments produced that leads to accumulation of partially degraded compartments.

When the insulin/PI3K/mTORC1 signalling is upregulated by *PTEN*-RNAi or *InR* overexpression in SCs, autophagy or lysosomal degradation would expect to be suppressed by high mTORC1 activity, and this might lead to accumulation of acidified compartments, but not lysosomal area, despite the partial suppression of

the DCG morphological defects induced by Tau. This was not observed in SCs with elevated IIS that were not overexpressing tau, at least for *PTEN*-RNAi, but the increased levels of abnormal DCG compartments produced in the presence of hTau2N4R might be sufficient to saturate the system and lead to blockade in lysosomal trafficking.

In conclusion, our *Drosophila* SC model illustrates that DCG biogenesis and endolysosomal trafficking are affected when tau is overexpressed. The insulin/PI3K/mTORC1 signalling pathway is an essential regulator of DCG formation, endolysosomal trafficking and lysosome biogenesis, and modulating its signalling can suppress some tau-induced effects, but the overall outcome is complex, because some phenotypes may be enhanced.

## Secretory propagation effects (main cell phenotype)

One interesting aspect of results is the propagation phenotype related to SC secretory output and its effect on surrounding cells, namely the accessory gland main cells. This propagates the endolysosomal phenotype. In this project, modulation of the insulin/PI3K/mTORC1 signalling displayed some inconsistent effects on this phenotype.

Both the *rosy*-RNAi control and other UAS-RNAi lines showed a relatively strong main cell phenotype, suggesting that these genetic manipulations might influence the secretory or endolysosomal trafficking balance of SCs. it is possible that siRNA machinery itself applies mild off-target effects on the SCs-related secretory events

and affects the intercellular communication. Together, these hypotheses could underlie the strong enhancement of main cell phenotype seen across RNAi backgrounds, although further investigations are required to provide solid evidence. In contrast to other RNAi conditions, *PI3K*-RNAi represented a significant exception, showing a reduction in the main cell phenotype, thereby appearing to suppress the intercellular transfer process. As previously discussed, downregulating insulin/PI3K/mTORC1 signalling pathway by *PI3K* knockdown affects the formation of intraluminal vesicles (ILVs) within DCG compartments, which are secreted as exosome-like vesicles, potentially by reducing overall secretory flux (A. Arous & A. Cording, unpublished data).

Further investigation will be required to dissect these overlapping mechanisms and define how each contributes to the control of intercellular communication in the accessory gland. According to these scenarios described above, the main cell phenotype observed in those experiments remain difficult to interpret with confidence.

## Limitations

While the SC model provides valuable insights into the regulation of secretory processes, certain limitations should be mentioned. The *Drosophila* SC is a specialised type of secretory cell with polyploid nuclei with functions that are primarily reproductive, which may not have a direct counterpart in the mammalian system. Therefore, translating observations from this model to mammalian cells and/or human neurons with AD requires careful interpretation. The tauopathy model

here involves overexpressing human Tau2N4R in non-neuronal cells. Although this is advantageous for quantifying and analysing cellular secretory and trafficking events, it will not fully capture all perspectives of neuronal reactions in AD, such as trans-synaptic dysfunction in tauopathy and perhaps tau seeding between neurons.

Beyond this, variation in the extent of phenotypic rescue was observed in Tau-overexpressing SCs following modulation of insulin/PI3K/mTORC1 signalling. This variability could originate from differences in expression of each transgene or even cell-to-cell differences in the ability to cope with tau accumulation. This outcome further complicates the interpretation, therefore suggesting that the interactions between tau overexpression and insulin pathway activity is complex and may involve additional cell-intrinsic confounding factors.

Moreover, viability issues in SCs limited the ability to examine all downstream components of the insulin/PI3K/mTORC1 signalling pathway, when relatively strong pathway modulators were crossed with the td-GFP-MFAS-Tau2N4R line. For example, co-overexpressing hTau2N4R with *PTEN*, *Tsc1/2* or *Rheb* resulted in SC lethality and poor adult fly survival, making it difficult to quantify phenotypes and further suggesting the presence of confounding factors that may bias analyses toward cells better able to tolerate cellular stress.

In addition to these experimental constraints, some limitations arise from the genetic regulatory system used to control transgene expression. In this study, transgene expression was regulated using the UAS/GAL4 system combined with temperature-sensitive GAL80. However, GAL80 repression is temperature-dependent and may

not be fully effective at commonly used culture temperatures such as 25°C. Under these conditions, low levels of GAL4 activity can occur, leading to partial transcription of UAS-RNAi constructs prior to the intended post-developmental induction period. Such leaky expression may introduce baseline perturbations of insulin signalling or other pathways, potentially contributing to variability in phenotypic outcomes. Maintaining flies at lower temperatures, such as 19°C, before experimental induction could provide tighter repression and improve temporal control of transgene expression in future experiments.

Another limitation concerns the genetic background of the fly stocks used in this study and the choice of control genotypes. Many RNAi and UAS transgenic lines are generated in different parental strains and maintained using markers such as *rosy*. Since the chromosomal location of these markers and associated transgene insertions can vary between stocks, combining lines through crosses may introduce variation beyond the intended manipulation. In this study, *rosy*-RNAi was used as a control to match the RNAi structure of those experimental lines, but as *rosy* is an endogenous gene, its knockdown could potentially affect cellular physiology. Future experiments could therefore benefit from using neutral RNAi controls targeting non-*Drosophila* sequences, such as luciferase or mCherry RNAi, which minimise effects on endogenous pathways. Additionally, $w^{1118}$ lacks a UAS insertion and therefore does not fully match the genetic background of overexpression lines, so controls carrying comparable UAS constructs without affecting the pathway of interest would provide more appropriate comparisons.

In this study, the primary focus was placed on the Insulin/PI3K/mTORC1 signalling pathway. However, it should be acknowledged that the insulin signalling (IIS) network is highly complex and interconnected, involving multiple downstream branches that regulate a wide range of cellular processes. Results from this project can only represent one of the major signalling cascades downstream of insulin receptor activation. Parallel cascades such as the Ras/MAPK pathway, as well as Akt-mediated regulation of effectors including FOXO, NFkB, and GSK3β, were not directly assessed in this project. Therefore, it is not possible to conclude that the secretory changes and partial rescue observed with human Tau overexpression are controlled only through Insulin/PI3K/mTORC1 pathway, as interactions with other branches may also trigger broader systemic effects that extend beyond local modulation within this cascade. To understand the whole insulin signalling pathway more comprehensively, future investigations should focus on how different branches and components cooperate or counteract each other, thus constructing a more integrated network for understanding how the insulin signalling pathway collectively regulates AD-relevant secretory and endolysosomal trafficking events in the *Drosophila* SC model.

## Future directions

More work is needed to fully understand how the integrated insulin/PI3K/mTORC1 signalling network interacts and functions during the early stages of AD, and how its gradual impairments lead to the worsening of pathology over time, highlighting potential directions for early intervention and therapeutic development. While several specific experiments have already been suggested in previous sections to further investigate the role of this pathway, the following paragraphs will focus on outlining broader strategies.

Regarding the other AD hallmark pathology, Aβ oligomerization and plaque formation, similar experiments could be carried out under the same conditions of insulin/PI3K/mTORC1 signalling modulation, but using genetic backgrounds that overexpress Aβ42 wild type as well as the Iowa or Dutch mutants. This would allow direct comparison with the current results from Singh et al. (2025) and help to determine whether modulation of insulin/PI3K/mTORC1 signalling can rescue abnormal cellular changes driven by Aβ overexpression. Both the Iowa and Dutch mutants showed the strong mini-core phenotypes and endolysosomal trafficking defects when overexpressed in SCs. Based on my previous results, *PI3K* knockdown in healthy SCs also caused similar mini-core phenotypes. However, it remains unclear whether these mini cores remain tightly associated with the limiting membrane of secretory compartments, as observed in Aβ-overexpressing cells. Further analysis is therefore required, as this membrane attachment may be important for generating the trafficking and propagation phenotypes observed in the Aβ mutants. Moreover, Aβ overexpression produces more pronounced main cell

propagation phenotypes than the Tau overexpression model, providing a stronger system in which to test the role of insulin/PI3K/mTORC1 signalling in this process.

Meanwhile, to further clarify the mini-core phenotypes caused by *PI3K* knockdown, future experiments can directly test the role of Rac1/Cdc42 or other actin regulators. For example, manipulation of Rac1/Cdc42 activity in SCs could be used to determine whether this mimics or rescues the effects of *PI3K*-RNAi on DCG biogenesis and morphology. If reduced *PI3K* activity impairs DCG maturation via actin cytoskeletal changes driven by low Rac1 activity, then Rac1 overexpression might rescue secretory granule formation even when *PI3K* activity is low, whereas Rac1 suppression might phenocopy the *PI3K*-RNAi condition. Identifying a link between PI3K-PIP3-Rac1 mediated cytoskeletal regulation and secretory compartment biogenesis would provide a strong foundation for future experiments aimed at understanding how this pathway is regulated.

Direct cytoskeletal imaging using the confocal microscope could be applied to visualise structural changes in the SCs cytoskeleton during the secretory process, possibly using fluorescently labelled actin, kinesin or tubulin, or other cytoskeletal interactors (Sampathkumar et al., 2011; Villanueva et al., 2022). This could be carried out under the same insulin/PI3K/mTORC1 signalling modulations and in flies overexpressing Tau or Aβ peptides. These experiments would help to link the morphological phenotypes we observed to specific cytoskeletal changes that occur during DCG biogenesis and maturation, and provide new assays for future experiments.

Regarding the medical and therapeutic relevance, our SC model provides an effective system for evaluating clinically used diabetic drugs under AD-related genetic backgrounds. For instance, compounds such as metformin and semaglutide have attracted increasing attention for their potential neuroprotective effects. Growing evidence indicates that the use of these diabetic treatments is associated with a reduced risk of cognitive decline and may help prevent or slow the progression of AD (Wang et al., 2024; Daly & Imbimbo, 2024;2025). These observations are also consistent with a model in which dysregulated glucose metabolism represents a primary mechanism contributing to AD-related pathology, closely linked to insulin/PI3K/mTORC1 signalling (Butterfield & Halliwell, 2019). Such experiments would not only help to validate my findings from this project, but also hint at what existing diabetic treatments might be beneficial to AD.

Lastly, to test whether the mechanisms drawn from SCs are conserved in other systems, it will be necessary to conduct parallel experiments in either *Drosophila* neuronal models or mammalian cell lines used for neurodegeneration and AD study. Cross-system validation would reinforce the translational relevance of my findings.

# Conclusion

Regarding the summary of key findings from this project, modulation of the insulin/PI3K/mTORC1 pathway in healthy SCs indicated that both upregulating and downregulating this signalling cascade disrupt normal DCG biogenesis as well as secretory and endolysosomal trafficking. A fine balance of signalling appears to be crucial for regulating DCG biogenesis, maturation and secretion/degradation, and any disruptions in either direction may impair this equilibrium. As discussed, one possible explanation involves the effects of this pathway on ELMs and actin-dependent trafficking, thereby linking metabolic signaling with cytoskeletal regulation.

When overexpressing human Tau2N4R in SCs, an increased number of DCG compartments with abnormal cylindrical cores and excessive lysosomal area were observed, consistent with Tau-induced cytoskeletal disruption and impaired interactions between the cytoskeleton and DCG aggregates, as well as defective lysosomal degradation. Both activation of the insulin/PI3K/mTORC1 signalling pathway (*PTEN*-RNAi and *InR* overexpression) and its suppression partially rescued DCG number and morphology, but led to elevated numbers of acidified compartments that were presumably not degraded efficiently. These results suggest that the insulin/PI3K/mTORC1 pathway may not function in a simple linear manner to modulate the defects induced by tau overexpression. Instead, multiple routes are likely to be engaged by insulin/PI3K/mTORC1 signalling to restore the cytoskeletal network and endolysosomal system, some of which may act antagonistically.

Through my research in SCs, I have advanced the understanding of how modulation of the insulin/PI3K/mTORC1 signalling pathway affects AD-related secretory and endolysosomal trafficking. By manipulating signalling activity to mimic the metabolic dysregulation observed in T2DM, my findings support the theory that impaired signalling may predispose neurons to early pathological changes characteristic of AD (Stanley et al., 2016; Hölscher, 2019). In particular, disruptions in endolysosomal trafficking and the accumulation of abnormally formed and partially degraded secretory compartments appear to be closely linked to defects in this pathway, and maintaining an appropriate signalling balance may help to alleviate these abnormalities. Together, these results contribute to a deeper understanding of the molecular mechanisms underlying early neurodegenerative processes and strengthen the potential mechanistic connection between T2DM and the early onset of AD.

# Bibliography

A. Ebneth, R. Godemann, Stamer, K., S. Illenberger, B. Trinczek, Mandelkow, E.-M., & Mandelkow, E. (1998). Overexpression of Tau Protein Inhibits Kinesin-dependent Trafficking of Vesicles, Mitochondria, and Endoplasmic Reticulum: Implications for Alzheimer's Disease. *The Journal of Cell Biology*, *143*(3), 777–794. https://doi.org/10.1083/jcb.143.3.777

Acker, V., Bretou, M., & Wim Annaert. (2019). Endo-lysosomal dysregulations and late-onset Alzheimer's disease: impact of genetic risk factors. *Molecular Neurodegeneration*, *14*(1), 20–20. https://doi.org/10.1186/s13024-019-0323-7

Aleksandra Sędzikowska, & Szablewski, L. (2021). Insulin and Insulin Resistance in Alzheimer's Disease. *International Journal of Molecular Sciences*, *22*(18), 9987–9987. https://doi.org/10.3390/ijms22189987

Alquezar, C., Arya, S., & Kao, A. W. (2021). Tau Post-translational Modifications: Dynamic Transformers of Tau Function, Degradation, and Aggregation. *Frontiers in Neurology*, *11*, 595532–595532. https://doi.org/10.3389/fneur.2020.595532

Anke Fossgreen, Bodo Brückner, Czech, C., Masters, C. L., Konrad Beyreuther, & Paro, R. (1998). Transgenic *Drosophila* expressing human amyloid precursor protein show γ-secretase activity and a blistered-wing phenotype. *Proceedings of the National Academy of Sciences*, *95*(23), 13703–13708. https://doi.org/10.1073/pnas.95.23.13703

Antonino, M., Marmo, P., Freites, C. L., Quassollo, G. E., Sánchez, M. F., Lorenzo, A., & Bignante, E. A. (2022). Aβ Assemblies Promote Amyloidogenic Processing of APP and Intracellular Accumulation of Aβ42 Through Go/Gβγ Signaling. *Frontiers in Cell and Developmental Biology*, *10*. https://doi.org/10.3389/fcell.2022.852738

Aviva M. Tolkovsky, & Maria Grazia Spillantini. (2021). Tau aggregation and its relation to selected forms of neuronal cell death. *Essays in Biochemistry*, *65*(7), 847–857. https://doi.org/10.1042/ebc20210030

Bachmann, S., Bell, M., Klimek, J., & Zempel, H. (2021). Differential Effects of the Six Human TAU Isoforms: Somatic Retention of 2N-TAU and Increased Microtubule Number Induced by 4R-TAU. *Frontiers in Neuroscience*, *15*. https://doi.org/10.3389/fnins.2021.643115

Bader, M.-F., Frédéric Doussau, Sylvette Chasserot-Golaz, Vitale, N., & Gasman, S. (2004). Coupling actin and membrane dynamics during calcium-regulated exocytosis: a role for Rho and ARF GTPases. *Biochimica et Biophysica Acta (BBA) - Molecular Cell Research*, *1742*(1-3), 37–49. https://doi.org/10.1016/j.bbamcr.2004.09.028

Balzac, F., Avolio, M., Degani, S., Kaverina, I., Torti, M., Silengo, L., Small, J. V., & Retta, S. F. (2005). E-cadherin endocytosis regulates the activity of Rap1: a traffic light GTPase at the crossroads between cadherin and integrin function. *Journal of Cell Science*, *118*(20), 4765–4783. https://doi.org/10.1242/jcs.02584

Berlanga-Acosta, J., Guillén-Nieto, G., Rodríguez-Rodríguez, N., Bringas-Vega, M. L., García-del-Barco-Herrera, D., Berlanga-Saez, J. O., García-Ojalvo, A., Valdés-Sosa, M. J., & Valdés-Sosa, P. A. (2020). Insulin Resistance at the Crossroad of Alzheimer Disease Pathology: A Review. *Frontiers in Endocrinology*, *11*. https://doi.org/10.3389/fendo.2020.560375

Boccalini, C., Federica Ribaldi, Hristovska, I., Arnone, A., Peretti, D. E., Mu, L., Scheffler, M., Perani, D., Frisoni, G. B., & Garibotto, V. (2024). The impact of tau deposition and hypometabolism on cognitive impairment and longitudinal cognitive decline. *Alzheimer S & Dementia*, *20*(1), 221–233. https://doi.org/10.1002/alz.13355

Boland, B., Kumar, A., Lee, S., Platt, F. M., Wegiel, J., Yu, W. H., & Nixon, R. A. (2008). Autophagy Induction and Autophagosome Clearance in Neurons: Relationship to Autophagic Pathology in Alzheimer's Disease. *Journal of Neuroscience*, *28*(27), 6926–6937. https://doi.org/10.1523/jneurosci.0800-08.2008

Boucher, J., A. Kleinridders, & Kahn, C. R. (2014). Insulin Receptor Signaling in Normal and Insulin-Resistant States. *Cold Spring Harbor Perspectives in Biology*, *6*(1), a009191–a009191. https://doi.org/10.1101/cshperspect.a009191

Brogiolo, W., Stocker, H., Tomoatsu Ikeya, Rintelen, F., Fernandez, R., & Hafen, E. (2001). An evolutionarily conserved function of the Drosophila insulin receptor and insulin-like peptides in growth control. *Current Biology*, *11*(4), 213–221. https://doi.org/10.1016/s0960-9822(01)00068-9

Brouwers, B., Coppola, I., Vints, K., Dislich, B., Jouvet, N., Lommel, L. V., Gounko, N. V., Thorrez, L., Schuit, F., Lichtenthaler, S. F., Estall, J. L., Declercq, J., Ramos-Molina, B., & Creemers, J. W. M. (2020). Furin controls β cell function via mTORC1 signaling. *bioRxiv*. https://doi.org/10.1101/2020.04.09.027839

Buchholz, S., & Zempel, H. (2024). The six brain-specific TAU isoforms and their role in Alzheimer's disease and related neurodegenerative dementia syndromes. *Alzheimer's & Dementia*, *20*(5), 3606–3628. https://doi.org/10.1002/alz.13784

C. Mazzucchelli, & Brambilla, R. (2000). Ras-related and MAPK signalling in neuronal plasticity and memory formation. *Cellular and Molecular Life Sciences*, *57*(4), 604–611. https://doi.org/10.1007/pl00000722

Caccamo, A., Magrì, A., Medina, D. X., Wisely, E. V., López-Aranda, M. F., Silva, A. J., & Oddo, S. (2013). mTOR regulates tau phosphorylation and degradation: implications for Alzheimer's disease and other tauopathies. *Aging Cell*, *12*(3), 370–380. https://doi.org/10.1111/acel.12057

Calafate, S., Flavin, W., Patrik Verstreken, & Diederik Moechars. (2016). Loss of Bin1 Promotes the Propagation of Tau Pathology. *Cell Reports*, *17*(4), 931–940. https://doi.org/10.1016/j.celrep.2016.09.063

Cao, F., Yang, F., Li, J., Guo, W., Zhang, C., Gao, F., Sun, X., Zhou, Y., & Zhang, W. (2024). The relationship between diabetes and the dementia risk: a meta-analysis. *Diabetology & Metabolic Syndrome*, *16*(1). https://doi.org/10.1186/s13098-024-01346-4

Cario, A., & Berger, C. L. (2023). Tau, microtubule dynamics, and axonal transport: New paradigms for neurodegenerative disease. *BioEssays*, *45*(8). https://doi.org/10.1002/bies.202200138

Chakraborty, P., Ibáñez de Opakua, A., Purslow, J. A., Fromm, S. A., Chatterjee, D., Zachrdla, M., Zhuang, S., Puri, S., Wolozin, B., & Zweckstetter, M. (2024). GSK3β phosphorylation catalyzes the aggregation of tau into Alzheimer's disease-like filaments. *Proceedings of the National Academy of Sciences*, *121*(52). https://doi.org/10.1073/pnas.2414176121

Chatterjee, S., Ambegaokar, Suren. S., Jackson, G. R., & Mudher, A. (2019). Insulin-Mediated Changes in Tau Hyperphosphorylation and Autophagy in a Drosophila Model of Tauopathy and Neuroblastoma Cells. *Frontiers in Neuroscience*, *13*. https://doi.org/10.3389/fnins.2019.00801

Chen, S.-D., Zhang, B., Wang, Y., Li, H., Xiong, R., Zhao, Z., Chu, X., Li, Q., & Sun, S. (2016). Neuroprotective effects of salidroside through PI3K/Akt pathway activation in Alzheimer's disease models. *Drug Design, Development and Therapy*, 1335. https://doi.org/10.2147/dddt.s99958

Chen, X., Zuo, X., Becker, A., & Mobley, W. C. (2025). Hyperactivation of RAB5 disrupts the endosomal Rab cascade leading to endolysosomal dysregulation in Down syndrome: A necessary role for increased *APP* gene dose. *Alzheimer S & Dementia*, *21*(5), e70046–e70046. https://doi.org/10.1002/alz.70046

Chen, Z., Chen, B., Xu, W., Liu, R., Yang, J., & Yu, C. (2012). Effects of PTEN inhibition on regulation of tau phosphorylation in an okadaic acid-induced neurodegeneration model. *International Journal of Developmental Neuroscience*, *30*(6), 411–419. https://doi.org/10.1016/j.ijdevneu.2012.08.003

Cheng, L., Chen, Y., Guo, D., Zhong, Y., Li, W., Lin, Y., & Miao, Y. (2023). mTOR-dependent TFEB activation and TFEB overexpression enhance autophagy-lysosome pathway and ameliorate Alzheimer's disease-like pathology in diabetic encephalopathy. *Cell Communication and Signaling*, *21*(1), 91–91. https://doi.org/10.1186/s12964-023-01097-1

Choy, R. W.-Y., Cheng, Z., & Schekman, R. (2012). Amyloid precursor protein (APP) traffics from the cell surface via endosomes for amyloid β (Aβ) production in the *trans* -Golgi network. *Proceedings of the National Academy of Sciences*, *109*(30). https://doi.org/10.1073/pnas.1208635109

Cichon, J., Sun, C., Chen, B., Jiang, M., Chen, X. A., Sun, Y., Wang, Y., & Chen, G. (2012). Cofilin Aggregation Blocks Intracellular Trafficking and Induces Synaptic Loss in Hippocampal Neurons. *Journal of Biological Chemistry*, *287*(6), 3919–3929. https://doi.org/10.1074/jbc.m111.301911

Cohen, E., Paulsson, J. F., Blinder, P., Tal Burstyn-Cohen, Du, D., Estepa, G., Adame, A., Pham, H. M., Holzenberger, M., Kelly, J. W., Eliezer Masliah, & Dillin, A. (2009). Reduced IGF-1 Signaling Delays Age-Associated Proteotoxicity in Mice. *Cell*, *139*(6), 1157–1169. https://doi.org/10.1016/j.cell.2009.11.014

Congdon, E. E., Ji, C., Tetlow, A. M., Jiang, Y., & Sigurdsson, E. M. (2023). Tau-targeting therapies for Alzheimer disease: current status and future directions. *Nature Reviews Neurology*, *19*(12), 715–736. https://doi.org/10.1038/s41582-023-00883-2

Corrigan, L., Siamak Redhai, Leiblich, A., Fan, S.-J., Perera, S. M. W., Patel, R., Gandy, C., Wainwright, S. M., Morris, J. F., Hamdy, F., Goberdhan, D. C. I., & Wilson, C. (2014). BMP-regulated exosomes from *Drosophila* male reproductive glands reprogram female behavior. *The Journal of Cell Biology*, *206*(5), 671–688. https://doi.org/10.1083/jcb.201401072

Curwin, A. J., von Blume, J., & Malhotra, V. (2012). Cofilin-mediated sorting and export of specific cargo from the Golgi apparatus in yeast. *Molecular Biology of the Cell*, *23*(12), 2327–2338. https://doi.org/10.1091/mbc.e11-09-0826

Dalinda Liazoghli, Perreault, S., Micheva, K. D., Desjardins, M., & Leclerc, N. (2005). Fragmentation of the Golgi Apparatus Induced by the Overexpression of Wild-Type and Mutant Human Tau Forms in Neurons. *American Journal of Pathology*, *166*(5), 1499–1514. https://doi.org/10.1016/s0002-9440(10)62366-8

Daly, J. L., Danson, C. M., Lewis, P. A., Zhao, L., Riccardo, S., Filippo, L. D., Davide Cacchiarelli, Lee, D., Cross, S. J., Heesom, K. J., Xiong, W.-C., Ballabio, A., Edgar, J. R., & Cullen, P. J. (2023). Multi-omic approach characterises the neuroprotective role of retromer in regulating lysosomal health. *Nature Communications*, *14*(1), 3086–3086. https://doi.org/10.1038/s41467-023-38719-8

Das, U., Wang, L., Ganguly, A., Saikia, J. M., Wagner, S. L., Koo, E. H., & Roy, S. (2015). Visualizing APP and BACE-1 approximation in neurons yields insight into the amyloidogenic pathway. *Nature Neuroscience*, *19*(1), 55–64. https://doi.org/10.1038/nn.4188

De la Monte, S. M., & Wands, J. R. (2008). Alzheimer's Disease is Type 3 Diabetes—Evidence Reviewed. *Journal of Diabetes Science and Technology*, *2*(6), 1101–1113. https://doi.org/10.1177/193229680800200619

Deng, Y., Li, B., Liu, Y., Iqbal, K., Grundke-Iqbal, I., & Gong, C.-X. (2009). Dysregulation of Insulin Signaling, Glucose Transporters, O-GlcNAcylation, and Phosphorylation of Tau and Neurofilaments in the Brain. *American Journal of Pathology*, *175*(5), 2089–2098. https://doi.org/10.2353/ajpath.2009.090157

DeTure, M. A., & Dickson, D. W. (2019). The neuropathological diagnosis of Alzheimer's disease. *Molecular Neurodegeneration*, *14*(1). https://doi.org/10.1186/s13024-019-0333-5

Di Malta, C., & Ballabio, A. (2017). TFEB-mTORC1 feedback loop in metabolism and cancer. *Cell Stress*, *1*(1), 7–10. https://doi.org/10.15698/cst2017.10.103

Dongliang Lv, Feng, P., Guan, X., Liu, Z., Li, D., Xue, C., Bai, B., & Hölscher, C. (2024). Neuroprotective effects of GLP-1 class drugs in Parkinson's disease. *Frontiers in Neurology*, *15*, 1462240–1462240. https://doi.org/10.3389/fneur.2024.1462240

Eckman, E. A., Clausen, D. M., Solé-Domėnech, S., Lee, C. W., Sinobas-Pereira, C., Domalewski, R. J., Nichols, M. R., & Pacheco-Quinto, J. (2023). Nascent Aβ42 Fibrillization in Synaptic Endosomes Precedes Plaque Formation in a Mouse Model of Alzheimer's-like β-Amyloidosis. *Journal of Neuroscience*, *43*(50). https://doi.org/10.1523/JNEUROSCI.1318-23.2023

El, B., Gratuze, M., Marie-Amélie Papon, Bretteville, A., & Planel, E. (2014). Insulin dysfunction and Tau pathology. *Frontiers in Cellular Neuroscience*, *8*, 22–22. https://doi.org/10.3389/fncel.2014.00022

Elea Prezel, Elie, A., Delaroche, J., Virginie Stoppin-Mellet, Christophe Bosc, Serre, L., Fourest-Lieuvin, A., Andrieux, A., Vantard, M., & Arnal, I. (2018). Tau can switch microtubule network organizations: from random networks to dynamic and stable bundles. *Molecular Biology of the Cell*, *29*(2), 154–165. https://doi.org/10.1091/mbc.e17-06-0429

Elham Razani, Atieh Pourbagheri-Sigaroodi, Safaroghli-Azar, A., Anahita Zoghi, Mahsa Shanaki-Bavarsad, & Davood Bashash. (2021). The PI3K/Akt signaling axis in Alzheimer's disease: a valuable target to stimulate or suppress? *Cell Stress and Chaperones*, *26*(6), 871–887. https://doi.org/10.1007/s12192-021-01231-3

Fan, S., Kroeger, B., Marie, P. P., Bridges, E. M., Mason, J. D., McCormick, K., Zois, C. E., Sheldon, H., Khalid Alham, N., Johnson, E., Ellis, M., Stefana, M. I., Mendes, C. C., Wainwright, S. M., Cunningham, C., Hamdy, F. C., Morris, J. F., Harris, A. L., Wilson, C., & Goberdhan, D. C. (2020). Glutamine deprivation alters the origin and function of cancer cell exosomes. *The EMBO Journal*, *39*(16). https://doi.org/10.15252/embj.2019103009

Ferreira, A., & Milán, M. (2015). Dally Proteoglycan Mediates the Autonomous and Nonautonomous Effects on Tissue Growth Caused by Activation of the PI3K and TOR Pathways. *PLOS Biology*, *13*(8), e1002239. https://doi.org/10.1371/journal.pbio.1002239

Florent Ubelmann, Burrinha, T., Salavessa, L., Gomes, R., Ferreira, C., Moreno, N., & Almeida, C. G. (2016). Bin1 and CD 2 AP polarise the endocytic generation of beta-amyloid. *EMBO Reports*, *18*(1), 102–122. https://doi.org/10.15252/embr.201642738

Franco-Juárez, B., Coronel-Cruz, C., Hernández-Ochoa, B., Saúl Gómez-Manzo, Cárdenas-Rodríguez, N., Arreguin-Espinosa, R., Bandala, C., Canseco-Ávila, L. M., & Ortega-Cuellar, D. (2022). TFEB; Beyond Its Role as an Autophagy and Lysosomes Regulator. *Cells*, *11*(19), 3153–3153. https://doi.org/10.3390/cells11193153

Frappaolo, A., & Giansanti, M. G. (2023). Using Drosophila melanogaster to Dissect the Roles of the mTOR Signaling Pathway in Cell Growth. *Cells*, *12*(22), 2622–2622. https://doi.org/10.3390/cells12222622

Gao, Y., Wang, L., Tosca Doeswijk, Winblad, B., Schedin-Weiss, S., & Tjernberg, L. O. (2025). Intraneuronal Aβ accumulation causes tau hyperphosphorylation via endolysosomal leakage. *Alzheimer S & Dementia*, *21*(3), e70091–e70091. https://doi.org/10.1002/alz.70091

Georg Dietzl, Chen, D., Schnorrer, F., Su, K.-C., Yulia Barinova, Fellner, M., Gasser, B., Kinsey, K., Oppel, S., Scheiblauer, S., Couto, A., Marra, V., Keleman, K., & Dickson, B. J. (2007). A genome-wide transgenic RNAi library for conditional gene inactivation in Drosophila. *Nature*, *448*(7150), 151–156. https://doi.org/10.1038/nature05954

Georgescu, M.-M. (2010). PTEN Tumor Suppressor Network in PI3K-Akt Pathway Control. *Genes & Cancer*, *1*(12), 1170–1177. https://doi.org/10.1177/1947601911407325

Giannakou, M. E., & Partridge, L. (2007). Role of insulin-like signalling in Drosophila lifespan. *Trends in Biochemical Sciences*, *32*(4). https://doi.org/10.1016/j.tibs.2007.02.007

Glaviano, A., Aaron, Lam, H. Y., Kenneth, Jacot, W., Jones, R. H., Eng, H., Nair, M. G., Pooyan Makvandi, Geoerger, B., Kulke, M. H., Baird, R. D., Prabhu, J. S., Carbone, D., Pecoraro, C., Daniel, Sethi, G., Cavalieri, V., Lin, K. H., & Javidi-Sharifi, N. R. (2023). PI3K/AKT/mTOR signaling transduction pathway and targeted therapies in cancer. *Molecular Cancer*, *22*(1), 138–138. https://doi.org/10.1186/s12943-023-01827-6

Goberdhan, D. C. I., Nuria Paricio, Goodman, E. C., Mlodzik, M., & Wilson, C. (1999). Drosophila tumor suppressor PTEN controls cell size and number by antagonizing the Chico/PI3-kinase signaling pathway. *Genes & Development*, *13*(24), 3244–3258. https://genesdev.cshlp.org/content/13/24/3244

Gonçalves, R. A., Wijesekara, N., Fraser, P. E., & De Felice, F. G. (2019). The Link Between Tau and Insulin Signaling: Implications for Alzheimer's Disease and Other Tauopathies. *Frontiers in Cellular Neuroscience*, *13*. https://doi.org/10.3389/fncel.2019.00017

Gorsky, M. K., Burnouf, S., Dols, J., Mandelkow, E., & Partridge, L. (2016). Acetylation mimic of lysine 280 exacerbates human Tau neurotoxicity in vivo. *Scientific Reports*, *6*(1), 22685–22685. https://doi.org/10.1038/srep22685

Gouras, G. K., Olsson, T. T., & Hansson, O. (2014). β-amyloid Peptides and Amyloid Plaques in Alzheimer's Disease. *Neurotherapeutics*, *12*(1), 3–11. https://doi.org/10.1007/s13311-014-0313-y

Gravandi, M. M., Sadaf Abdian, Maedeh Tahvilian, Amin Iranpanah, Moradi, S. Z., Fakhri, S., & Echeverría, J. (2023). Therapeutic targeting of Ras/Raf/MAPK pathway by natural products: A systematic and mechanistic approach for neurodegeneration. *Phytomedicine*, *115*, 154821–154821. https://doi.org/10.1016/j.phymed.2023.154821

Grönke, S., Clarke, D.-F., Broughton, S., Andrews, T. D., & Partridge, L. (2010). Molecular Evolution and Functional Characterization of Drosophila Insulin-Like Peptides. *PLoS Genetics*, *6*(2), e1000857–e1000857. https://doi.org/10.1371/journal.pgen.1000857

Hansen, H. H., Barkholt, P., Fabricius, K., Jelsing, J., Terwel, D., Pyke, C., Knudsen, L. B., & Vrang, N. (2016). The GLP-1 receptor agonist liraglutide reduces pathology-specific tau phosphorylation and improves motor function in a transgenic hTauP301L mouse model of tauopathy. *Brain Research*, *1634*, 158–170. https://doi.org/10.1016/j.brainres.2015.12.052

Hayashi, H., Kimura, N., Yamaguchi, H., Hasegawa, K., Yokoseki, T., Shibata, M., Yamamoto, N., Michikawa, M., Yoshikawa, Y., Terao, K., Matsuzaki, K., Lemere, C. A., Selkoe, D. J., Naiki, H., & Yanagisawa, K. (2004). A Seed for Alzheimer Amyloid in the Brain. *Journal of Neuroscience*, *24*(20). https://doi.org/10.1523/JNEUROSCI.0861-04.2004

Héctor Albert-Gascó, Ros-Bernal, F., Castillo-Gómez, E., & Olucha-Bordonau, F. E. (2020). MAP/ERK Signaling in Developing Cognitive and Emotional Function and Its Effect on Pathological and Neurodegenerative Processes. *International Journal of Molecular Sciences*, *21*(12), 4471–4471. https://doi.org/10.3390/ijms21124471

Heidary, G., & Fortini, M. E. (2001). Identification and characterization of the Drosophila tau homolog. *Mechanisms of Development*, *108*(1-2), 171–178. https://doi.org/10.1016/s0925-4773(01)00487-7

Hervy, J., & Bicout, D. J. (2019). Dynamical decoration of stabilized-microtubules by Tau-proteins. *Scientific Reports*, *9*(1), 12473–12473. https://doi.org/10.1038/s41598-019-48790-1

Holmes, C., Boche, D., Wilkinson, D., Yadegarfar, G., Hopkins, V., Bayer, A., Jones, R. W., Bullock, R., Love, S., Neal, J. W., Zotova, E., & Nicoll, J. A. (2008). Long-term effects of Aβ42 immunisation in Alzheimer's disease: follow-up of a randomised, placebo-controlled phase I trial. *The Lancet*, *372*(9634), 216–223. https://doi.org/10.1016/s0140-6736(08)61075-2

Hong-Geller, E., & Cerione, R. A. (2000). Cdc42 and Rac Stimulate Exocytosis of Secretory Granules by Activating the Ip3/Calcium Pathway in Rbl-2h3 Mast Cells. *The Journal of Cell Biology*, *148*(3), 481–494. https://doi.org/10.1083/jcb.148.3.481

Hong, M., Chen, D. C. R., Klein, P. S., & Lee, V. M.-Y. . (1997). Lithium Reduces Tau Phosphorylation by Inhibition of Glycogen Synthase Kinase-3. *Journal of Biological Chemistry*, *272*(40), 25326–25332. https://doi.org/10.1074/jbc.272.40.25326

Hu, S., Sonnenfeld, M., Stahl, S., & Crews, S. T. (1998). Midline fasciclin: A Drosophila fasciclin-I-related membrane protein localized to the CNS midline cells and trachea. *Journal of Neurobiology*, *35*(1). https://doi.org/10.1002/(SICI)1097-4695(199804)35:1<77::AID-NEU7>3.0.CO;2-8

Hur, J.-Y. (2022). γ-Secretase in Alzheimer's disease. *Experimental & Molecular Medicine*, *54*(4), 433–446. https://doi.org/10.1038/s12276-022-00754-8

Inoki, K., Li, Y., Xu, T., & Guan, K.-L. (2003). Rheb GTPase is a direct target of TSC2 GAP activity and regulates mTOR signaling. *Genes & Development*, *17*(15), 1829–1834. https://doi.org/10.1101/gad.1110003

Iqbal, K., Liu, F., Gong, C.-X. ., & Grundke-Iqbal, I. (2010). Tau in Alzheimer Disease and Related Tauopathies. *Current Alzheimer Research*, *7*(8), 656–664. https://doi.org/10.2174/156720510793611592

Januário, Y. C., Eden, J., de Oliveira, L. S., De Pace, R., Tavares, L. A., da Silva-Januário, M. E., Apolloni, V. B., Wilby, E. L., Altmeyer, R., Burgos, P. V., Corrêa, S. A. L., Gershlick, D. C., & daSilva, L. L. P. (2022). Clathrin adaptor AP-1–mediated Golgi export of amyloid precursor protein is crucial for the production of neurotoxic amyloid fragments. *Journal of Biological Chemistry*, *298*(8), 102172. https://doi.org/10.1016/j.jbc.2022.102172

Jeon, Y., Lee, J. H., Choi, B., Won, S.-Y., & Cho, K. S. (2020). Genetic Dissection of Alzheimer's Disease Using Drosophila Models. *International Journal of Molecular Sciences*, *21*(3), 884. https://doi.org/10.3390/ijms21030884

Jiang, Q., Wang, L., Guan, Y., Xu, H., Niu, Y., Han, L., Wei, Y.-P., Lin, L., Chu, J., Wang, Q., Yang, Y., Pei, L., Wang, J.-Z., & Tian, Q. (2014). Golgin-84-associated Golgi fragmentation triggers tau hyperphosphorylation by activation of cyclin-dependent kinase-5 and extracellular signal-regulated kinase. *Neurobiology of Aging*, *35*(6), 1352–1363. https://doi.org/10.1016/j.neurobiolaging.2013.11.022

Joshi, G., Bekier, M. E., & Wang, Y. (2015). Golgi fragmentation in Alzheimer's disease. *Frontiers in Neuroscience*, *9*. https://doi.org/10.3389/fnins.2015.00340

Katryna Pampuscenko, Ramune Morkuniene, Lukas Krasauskas, Vytautas Smirnovas, Tomita, T., & Vilmante Borutaite. (2021). Distinct Neurotoxic Effects of Extracellular Tau Species in Primary Neuronal-Glial Cultures. *Molecular Neurobiology*, *58*(2), 658–667. https://doi.org/10.1007/s12035-020-02150-7

Kaushal Asrani, Murali, S., Lam, B., Chan-Hyun Na, Phatak, P., Sood, A., Kaur, H., Khan, Z., Michaël Noë, Anchoori, R. K., Talbot, C. C., Smith, B., Skaro, M., & Lotan, T. L. (2019). mTORC1 feedback to AKT modulates lysosomal biogenesis through MiT/TFE regulation. *Journal of Clinical Investigation*, *129*(12), 5584–5599. https://doi.org/10.1172/jci128287

Kciuk, M., Kruczkowska, W., Gałęziewska, J., Wanke, K., Kałuzińska-Kołat, Ż., Aleksandrowicz, M., Kontek, R., Kciuk, M., Kruczkowska, W., Gałęziewska, J., Wanke, K., Kałuzińska-Kołat, Ż., Aleksandrowicz, M., & Kontek, R. (2024). Alzheimer's Disease as Type 3 Diabetes: Understanding the Link and Implications. *International Journal of Molecular Sciences 2024, Vol. 25, Page 11955*, *25*(22). https://doi.org/10.3390/ijms252211955

Kim, K. H., & Lee, M.-S. (2013). Autophagy as a crosstalk mediator of metabolic organs in regulation of energy metabolism. *Reviews in Endocrine and Metabolic Disorders*, *15*(1), 11–20. https://doi.org/10.1007/s11154-013-9272-6

Kim, S.-H., Cho, Y.-S., Kim, Y., Park, J., Yoo, S.-M., Gwak, J., Kim, Y., Gwon, Y., Kam, T.-i., & Jung, Y.-K. (2023). Endolysosomal impairment by binding of amyloid beta or MAPT/Tau to V-ATPase and rescue via the HYAL-CD44 axis in Alzheimer disease. *Autophagy*, *19*(8). https://doi.org/10.1080/15548627.2023.2181614

Kitagishi, Y., Nakanishi, A., Ogura, Y., & Matsuda, S. (2014). Dietary regulation of PI3K/AKT/GSK-3β pathway in Alzheimer's disease. *Alzheimer S Research & Therapy*, *6*(3), 35–35. https://doi.org/10.1186/alzrt265

Krishnan, H., Ahmed, S., Hubbard, S. R., & Miller, W. T. (2024). Biochemical characterization of the *Drosophila* insulin receptor kinase and longevity-associated mutants. *The FASEB Journal*, *38*(1), e23355–e23355. https://doi.org/10.1096/fj.202301948r

Kumar, M., & Bansal, N. (2021). Implications of Phosphoinositide 3-Kinase-Akt (PI3K-Akt) Pathway in the Pathogenesis of Alzheimer's Disease. *Molecular Neurobiology*, *59*(1), 354–385. https://doi.org/10.1007/s12035-021-02611-7

Lee, J.-H., Yang, D.-S., Goulbourne, C. N., Im, E., Stavrides, P., Pensalfini, A., Chan, H., Bouchet-Marquis, C., Bleiwas, C., Berg, M. J., Huo, C., Peddy, J., Pawlik, M., Levy, E., Rao, M., Mathias Staufenbiel, & Nixon, R. A. (2022). Faulty autolysosome acidification in Alzheimer's disease mouse models induces autophagic build-up of Aβ in neurons, yielding senile plaques. *Nature Neuroscience*, *25*(6), 688–701. https://doi.org/10.1038/s41593-022-01084-8

Leiblich, A., Josephine, Sekar, A., Gandy, C., Mendes, C. C., Siamak Redhai, Mason, J., Wainwright, M., Marie, P., Deborah, Hamdy, F. C., & Wilson, C. (2019). Mating induces switch from hormone-dependent to hormone-independent steroid receptor–mediated growth in Drosophila secondary cells. *PLoS Biology*, *17*(10), e3000145–e3000145. https://doi.org/10.1371/journal.pbio.3000145

Leiblich, A., Marsden, L., Gandy, C., Corrigan, L., Jenkins, R., Hamdy, F., & Wilson, C. (2012). Bone morphogenetic protein- and mating-dependent secretory cell growth and migration in the *Drosophila* accessory gland. *Proceedings of the National Academy of Sciences*, *109*(47), 19292–19297. https://doi.org/10.1073/pnas.1214517109

Liang, T., Wu, Z., Li, J., Wu, S., Shi, W., & Wang, L. (2023). The emerging double-edged sword role of exosomes in Alzheimer's disease. *Frontiers in Aging Neuroscience*, *15*, 1209115–1209115. https://doi.org/10.3389/fnagi.2023.1209115

Luo, L., Tully, T., & White, K. (1992). Human amyloid precursor protein ameliorates behavioral deficit of flies deleted for appl gene. *Neuron*, *9*(4), 595–605. https://doi.org/10.1016/0896-6273(92)90024-8

Marie, P. P., Fan, S., Mason, J., Wells, A., Mendes, C. C., Wainwright, S. M., Scott, S., Fischer, R., Harris, A. L., Wilson, C., & Goberdhan, D. C. I. (2023). Accessory ESCRT-III proteins are conserved and selective regulators of Rab11a-exosome formation. *Journal of Extracellular Vesicles*, *12*(3). https://doi.org/10.1002/jev2.12311

Mateusz Kciuk, Weronika Kruczkowska, Gałęziewska, J., Wanke, K., Żaneta Kałuzińska-Kołat, Aleksandrowicz, M., & Kontek, R. (2025). Alzheimer's Disease as Type 3 Diabetes: Understanding the Link and Implications. *International Journal of Molecular Sciences*, *25*(22), 11955–11955. https://doi.org/10.3390/ijms252211955

McClure, C. D., Hassan, A., Aughey, G. N., Butt, K., Estacio-Gómez, A., Duggal, A., Ying Sia, C., Barber, A. F., & Southall, T. D. (2022). An auxin-inducible, GAL4-compatible, gene expression system for Drosophila. *ELife*, *11*. https://doi.org/10.7554/elife.67598

McGuire, S. (2004). Gene expression systems in Drosophila: a synthesis of time and space. *Trends in Genetics*, *20*(8), 384–391. https://doi.org/10.1016/j.tig.2004.06.012

Medina, D. L., Di Paola, S., Peluso, I., Armani, A., De Stefani, D., Venditti, R., Montefusco, S., Scotto-Rosato, A., Prezioso, C., Forrester, A., Settembre, C., Wang, W., Gao, Q., Xu, H., Sandri, M., Rizzuto, R., De Matteis, M. A., & Ballabio, A. (2015). Lysosomal calcium signalling regulates autophagy through calcineurin and TFEB. *Nature Cell Biology*, *17*(3), 288–299. https://doi.org/10.1038/ncb3114

Menon, S., Dibble, C., Talbott, G., Gerta Hoxhaj, Alexander J. Valvezan, Takahashi, H., Cantley, L., & Manning, B. (2014). Spatial Control of the TSC Complex Integrates Insulin and Nutrient Regulation of mTORC1 at the Lysosome. *Cell*, *156*(4), 771–785. https://doi.org/10.1016/j.cell.2013.11.049

Miao, J., Zhang, Y., Su, C., Zheng, Q., & Guo, J. (2024). Insulin-Like Growth Factor Signaling in Alzheimer's Disease: Pathophysiology and Therapeutic Strategies. *Molecular Neurobiology*, *62*(3), 3195–3225. https://doi.org/10.1007/s12035-024-04457-1

Morawe, M. P., Liao, F., Amberg, W., van Bergeijk, J., Chang, R., Gulino, M., Hamilton, C., Hoft, C., Lumpkin, C., Mastis, B., McGlame, E., Nuber, J., Plaas, C., Ravikumar, B., Roy, K., Schanzenbächer, M., Tierno, J., Lakics, V., Dellovade, T., & Townsend, M. (2022). Pharmacological mTOR-inhibition facilitates clearance of AD-related tau aggregates in the mouse brain. *European Journal of Pharmacology*, *934*, 175301. https://doi.org/10.1016/j.ejphar.2022.175301

Morfini, G., Györgyi Szebenyi, Ravindhra Elluru, Ratner, N., & Brady, S. T. (2002). Glycogen synthase kinase 3 phosphorylates kinesin light chains and negatively regulates kinesin-based motility. *The EMBO Journal*, *21*(3), 281–293. https://doi.org/10.1093/emboj/21.3.281

Ni, J.-Q., Liu, L.-P., Binari, R., Hardy, R., Shim, H.-S., Cavallaro, A., Booker, M., Pfeiffer, B. D., Markstein, M., Wang, H., Villalta, C., Laverty, T. R., Perkins, L. A., & Perrimon, N. (2009). A Drosophila Resource of Transgenic RNAi Lines for Neurogenetics. *Genetics*, *182*(4), 1089–1100. https://doi.org/10.1534/genetics.109.103630

Ni, J.-Q., Markstein, M., Binari, R., Pfeiffer, B., Liu, L.-P., Villalta, C., Booker, M., Perkins, L., & Perrimon, N. (2007). Vector and parameters for targeted transgenic RNA interference in Drosophila melanogaster. Nature Methods, 5(1), 49–51. https://doi.org/10.1038/nmeth1146

Niels Henning Skotte, Pouladi, M. A., Ehrnhoefer, D. E., Huynh, K., Qiu, X., Marie, S., Nielsen, T. T., Nørremølle, A., & Hayden, M. R. (2020). Compromised IGF signaling causes caspase-6 activation in Huntington disease. *Experimental Neurology*, *332*, 113396–113396. https://doi.org/10.1016/j.expneurol.2020.113396

Nixon, R. A. (2017). Amyloid precursor protein and endosomal-lysosomal dysfunction in Alzheimer's disease: inseparable partners in a multifactorial disease. *The FASEB Journal*, *31*(7), 2729–2743. https://doi.org/10.1096/fj.201700359

None Pragati, & Sarkar, S. (2023). Reinstated Activity of Human Tau-induced Enhanced Insulin Signaling Restricts Disease Pathogenesis by Regulating the Functioning of Kinases/Phosphatases and Tau Hyperphosphorylation in Drosophila. *Molecular Neurobiology*, *61*(2), 982–1001. https://doi.org/10.1007/s12035-023-03599-y

Ohashi, K., Toshihiko Hosoya, Takahashi, K., Hing, H., & Mizuno, K. (2000). A Drosophila Homolog of LIM-Kinase Phosphorylates Cofilin and Induces Actin Cytoskeletal Reorganization. *Biochemical and Biophysical Research Communications*, *276*(3), 1178–1185. https://doi.org/10.1006/bbrc.2000.3599

Pal-Bhadra, M., Bhadra, U., & Birchler, J. A. (2002). RNAi Related Mechanisms Affect Both Transcriptional and Posttranscriptional Transgene Silencing in Drosophila. Molecular Cell, 9(2), 315–327. https://doi.org/10.1016/s1097-2765(02)00440-9

Pasternak, S. H., Bagshaw, R. D., Guiral, M., Zhang, S., Ackerley, C. A., Pak, B. J., Callahan, J. W., & Mahuran, D. J. (2003). Presenilin-1, Nicastrin, Amyloid Precursor Protein, and γ-Secretase Activity Are Co-localized in the Lysosomal Membrane. *Journal of Biological Chemistry*, *278*(29), 26687–26694. https://doi.org/10.1074/jbc.m304009200

Patel, P. H., Thapar, N., Guo, L., Martinez, M., Maris, J., Gau, C.-L., Lengyel, J. A., & Tamanoi, F. (2003). *Drosophila*Rheb GTPase is required for cell cycle progression and cell growth. *Journal of Cell Science*, *116*(17), 3601–3610. https://doi.org/10.1242/jcs.00661

Perez-Gonzalez, R., Gauthier, S. A., Kumar, A., & Levy, E. (2012). The Exosome Secretory Pathway Transports Amyloid Precursor Protein Carboxyl-terminal Fragments from the Cell into the Brain Extracellular Space. *Journal of Biological Chemistry*, *287*(51), 43108–43115. https://doi.org/10.1074/jbc.m112.404467

Potter, C. J., Huang, H., & Xu, T. (2001). Drosophila Tsc1 Functions with Tsc2 to Antagonize Insulin Signaling in Regulating Cell Growth, Cell Proliferation, and Organ Size. *Cell*, *105*(3), 357–368. https://doi.org/10.1016/s0092-8674(01)00333-6

Puertollano, R., Ferguson, S. M., Brugarolas, J., & Ballabio, A. (2018). The complex relationship between TFEB transcription factor phosphorylation and subcellular localization. *The EMBO Journal*, *37*(11). https://doi.org/10.15252/embj.201798804

Rambur, A., Lours-Calet, C., Beaudoin, C., Buñay, J., Vialat, M., Mirouse, V., Trousson, A., Renaud, Y., Lobaccaro, J.-M. A., Baron, S., Morel, L., & Cyrille de Joussineau. (2020). Sequential Ras/MAPK and PI3K/AKT/mTOR pathways recruitment drives basal extrusion in the prostate-like gland of Drosophila. *Nature Communications*, *11*(1), 2300–2300. https://doi.org/10.1038/s41467-020-16123-w

Reddy, P. H. (2011). Abnormal tau, mitochondrial dysfunction, impaired axonal transport of mitochondria, and synaptic deprivation in Alzheimer's disease. *Brain Research*, *1415*, 136–148. https://doi.org/10.1016/j.brainres.2011.07.052

Redhai, S., Hellberg, J. E. E. U., Wainwright, M., Perera, S. W., Castellanos, F., Kroeger, B., Gandy, C., Leiblich, A., Corrigan, L., Hilton, T., Patel, B., Fan, S.-J., Hamdy, F., Goberdhan, D. C. I., & Wilson, C. (2016). Regulation of Dense-Core Granule Replenishment by Autocrine BMP Signalling in Drosophila Secondary Cells. *PLOS Genetics*, *12*(10), e1006366. https://doi.org/10.1371/journal.pgen.1006366

Rideout, E. J., Dornan, A. J., Neville, M. C., Eadie, S., & Goodwin, S. F. (2010). Control of sexual differentiation and behavior by the doublesex gene in Drosophila melanogaster. *Nature Neuroscience*, *13*(4), 458–466. https://doi.org/10.1038/nn.2515

Rivera, E. J., Goldin, A., Fulmer, N., Tavares, R., Wands, J. R., & de la Monte, S. M. (2005). Insulin and insulin-like growth factor expression and function deteriorate with progression of Alzheimer's disease: Link to brain reductions in acetylcholine. *Journal of Alzheimer's Disease*, *8*(3), 247–268. https://doi.org/10.3233/jad-2005-8304

Rolland, M., Powell, R., Jacquier-Sarlin, M., Boisseau, S., Reynaud-Dulaurier, R., Martinez-Hernandez, J., André, L., Borel, E., Buisson, A., & Lanté, F. (2020). Effect of Aβ Oligomers on Neuronal APP Triggers a Vicious Cycle Leading to the Propagation of Synaptic Plasticity Alterations to Healthy Neurons. *Journal of Neuroscience*, *40*(27). https://doi.org/10.1523/JNEUROSCI.2501-19.2020

Rush, T., Martinez-Hernandez, J., Dollmeyer, M., Frandemiche, M. L., Borel, E., Boisseau, S., Jacquier-Sarlin, M., & Buisson, A. (2018). Synaptotoxicity in Alzheimer's Disease Involved a Dysregulation of Actin Cytoskeleton Dynamics through Cofilin 1 Phosphorylation. *Journal of Neuroscience*, *38*(48), 10349–10361. https://doi.org/10.1523/JNEUROSCI.1409-18.2018

Sadagurski, M., & White, M. F. (2012). Integrating Metabolism and Longevity Through Insulin and IGF1 Signaling. *Endocrinology and Metabolism Clinics of North America*, *42*(1), 127–148. https://doi.org/10.1016/j.ecl.2012.11.008

Sanchis, A., María Adelaida García-Gimeno, Cañada-Martínez, A. J., María Dolores Sequedo, José María Millán, Sanz, P., & Vázquez-Manrique, R. P. (2019). Metformin treatment reduces motor and neuropsychiatric phenotypes in the zQ175 mouse model of Huntington disease. *Experimental & Molecular Medicine*, *51*(6), 1–16. https://doi.org/10.1038/s12276-019-0264-9

Santiago, J. A., Karthikeyan, M., Lackey, M., Villavicencio, D., & Potashkin, J. A. (2023). Diabetes: a tipping point in neurodegenerative diseases. *Trends in Molecular Medicine*, *29*(12), 1029–1044. https://doi.org/10.1016/j.molmed.2023.09.005

Scacheri, P. C., Rozenblatt-Rosen, O., Caplen, N. J., Wolfsberg, T. G., Umayam, L., Lee, J. C., Hughes, C. M., Shanmugam, K. S., Bhattacharjee, A., Meyerson, M., & Collins, F. S. (2004). Short interfering RNAs can induce unexpected and divergent changes in the levels of untargeted proteins in mammalian cells. Proceedings of the National Academy of Sciences, 101(7), 1892–1897. https://doi.org/10.1073/pnas.0308698100

Scherer, T., Sakamoto, K., & Buettner, C. (2021). Brain insulin signalling in metabolic homeostasis and disease. *Nature Reviews Endocrinology*, *17*(8), 468–483. https://doi.org/10.1038/s41574-021-00498-x

Schulz, A. M., Stutte, S., Hogl, S., Luckashenak, N., Dudziak, D., Leroy, C., Forné, I., Imhof, A., Müller, S. A., Brakebusch, C. H., Lichtenthaler, S. F., & Brocker, T. (2015). Cdc42-dependent actin dynamics controls maturation and secretory activity of dendritic cells. *Journal of Cell Biology*, *211*(3), 553–567. https://doi.org/10.1083/jcb.201503128

Sekar, A., Leiblich, A., Wainwright, S. M., Mendes, C. C., Sarma, D., Hellberg, J. E. E. U., Gandy, C., Goberdhan, D. C. I., Hamdy, F. C., & Wilson, C. (2023). Rbf/E2F1 control growth and endoreplication via steroid-independent Ecdysone Receptor signalling in Drosophila prostate-like secondary cells. *PLOS Genetics*, *19*(6), e1010815. https://doi.org/10.1371/journal.pgen.1010815

Shahpasand-Kroner, H., Portillo, J., Lantz, C., Seidler, P. M., Sarafian, N., Loo, J. A., & Bitan, G. (2022). Three-repeat and four-repeat tau isoforms form different oligomers. *Protein Science*, *31*(3), 613–627. https://doi.org/10.1002/pro.4257

Singh, P. J., Verma, B., Wells, A., Mendes, C. C., Dunn, D., Chen, Y.-N., Oh, J., Blincowe, L., Wainwright, S. M., Fischer, R., Fan, S.-J., Harris, A. L., Goberdhan, D. C. I., & Wilson, C. (2025). Amyloid-β disrupts APP-regulated protein aggregation and dissociation from recycling endosomal membranes. *The EMBO Journal*, *44*(16), 4443–4472. https://doi.org/10.1038/s44318-025-00497-y

Small, S. A., Simoes-Spassov, S., Mayeux, R., & Petsko, G. A. (2017). Endosomal Traffic Jams Represent a Pathogenic Hub and Therapeutic Target in Alzheimer's Disease. *Trends in Neurosciences*, *40*(10), 592–602. https://doi.org/10.1016/j.tins.2017.08.003

Son, S. M., Song, H., Byun, J., Park, K. S., Jang, H. C., Park, Y. J., & Inhee Mook-Jung. (2012). Altered APP Processing in Insulin-Resistant Conditions Is Mediated by Autophagosome Accumulation via the Inhibition of Mammalian Target of Rapamycin Pathway. *Diabetes*, *61*(12), 3126–3138. https://doi.org/10.2337/db11-1735

Sonal Nagarkar-Jaiswal, Lee, P.-T., Campbell, M. E., Chen, K., Anguiano-Zarate, S., Gutierrez, M. C., Busby, T., Lin, W.-W., He, Y., Schulze, K. L., Booth, B. W., Evans-Holm, M., Koen JT Venken, Levis, R. W., Spradling, A. C., Hoskins, R. A., & Bellen, H. J. (2015). A library of MiMICs allows tagging of genes and reversible, spatial and temporal knockdown of proteins in Drosophila. *ELife*, *4*. https://doi.org/10.7554/elife.05338

Song, J., Wang, T., Hong, J.-S., Wang, Y., & Feng, J. (2025). TFEB-dependent autophagy-lysosomal pathway is required for NRF2-driven antioxidative action in obstructive sleep apnea-induced neuronal injury. *Cellular Signalling*, *128*, 111630–111630. https://doi.org/10.1016/j.cellsig.2025.111630

Sowade, R. F., & Jahn, T. R. (2017). Seed-induced acceleration of amyloid-β mediated neurotoxicity in vivo. *Nature Communications*, *8*(1), 512–512. https://doi.org/10.1038/s41467-017-00579-4

Spilman, P., Podlutskaya, N., Hart, M. J., Debnath, J., Gorostiza, O., Bredesen, D., Richardson, A., Strong, R., & Galvan, V. (2010). Inhibition of mTOR by Rapamycin Abolishes Cognitive Deficits and Reduces Amyloid-β Levels in a Mouse Model of Alzheimer's Disease. *PLoS ONE*, *5*(4), e9979–e9979. https://doi.org/10.1371/journal.pone.0009979

Steen, E., Terry, B. M., J. Rivera, E., Cannon, J. L., Neely, T. R., Tavares, R., Xu, X. J., Wands, J. R., & de la Monte, S. M. (2005). Impaired insulin and insulin-like growth factor expression and signaling mechanisms in Alzheimer's disease – is this type 3 diabetes? *Journal of Alzheimer's Disease*, *7*(1), 63–80. https://doi.org/10.3233/jad-2005-7107

Steinkraus, K. A., Smith, E. D., Davis, C., Carr, D., Pendergrass, W. R., Sutphin, G. L., Kennedy, B. K., & Kaeberlein, M. (2008). Dietary restriction suppresses proteotoxicity and enhances longevity by an *hsf-1* -dependent mechanism in *Caenorhabditis elegans*. *Aging Cell*, *7*(3), 394–404. https://doi.org/10.1111/j.1474-9726.2008.00385.x

Stocker, H., Radimerski, T., Benno Schindelholz, Wittwer, F., Priyanka Belawat, Daram, P., Breuer, S., Thomas, G., & Hafen, E. (2003). Rheb is an essential regulator of S6K in controlling cell growth in Drosophila. *Nature Cell Biology*, *5*(6), 559–566. https://doi.org/10.1038/ncb995

Stockhammer, A., Adarska, P., Natalia, V., Heuhsen, A., Klemt, A., Bregu, G., Harel, S., Rodilla-Ramirez, C., Spalt, C., Özsoy, E., Leupold, P., Grindel, A., Fox, E., Mejedo, J. O., Zehtabian, A., Ewers, H., Puchkov, D., Haucke, V., & Bottanelli, F. (2024). ARF1 compartments direct cargo flow via maturation into recycling endosomes. *Nature Cell Biology*, *26*(11), 1845–1859. https://doi.org/10.1038/s41556-024-01518-4

Templeman, N. M., & Murphy, C. T. (2018). Regulation of reproduction and longevity by nutrient-sensing pathways. *Journal of Cell Biology*, *217*(1), 93–106. https://doi.org/10.1083/jcb.201707168

Thal, D. R., Udo Rüb, Orantes, M., & Braak, H. (2002). Phases of Aβ-deposition in the human brain and its relevance for the development of AD. *Neurology*, *58*(12), 1791–1800. https://doi.org/10.1212/wnl.58.12.1791

Tong, Y., & Song, F. (2015). Intracellular calcium signaling regulates autophagy via calcineurin-mediated TFEB dephosphorylation. *Autophagy*, *11*(7). https://doi.org/10.1080/15548627.2015.1054594

Toshio Ariga, Kobayashi, K., Hasegawa, A., Kiso, M., Ishida, H., & Miyatake, T. (2001). Characterization of High-Affinity Binding between Gangliosides and Amyloid β-Protein. *Archives of Biochemistry and Biophysics*, *388*(2), 225–230. https://doi.org/10.1006/abbi.2001.2304

Uliana Semaniuk, Piskovatska, V., Olha Strilbytska, Tetiana Strutynska, Burdyliuk, N., Vaiserman, A., Bubalo, V., Storey, K. B., & Oleh Lushchak. (2021). *Drosophila* insulin-like peptides: from expression to functions – a review. *Entomologia Experimentalis et Applicata*, *169*(2), 195–208. https://doi.org/10.1111/eea.12981

Verheyen, E. M. (2022). The power of *Drosophila* in modeling human disease mechanisms. *Disease Models & Mechanisms*, *15*(3). https://doi.org/10.1242/dmm.049549

Villegas, S., Roda, A., Serra-Mir, G., Montoliu-Gaya, L., & Tiessler, L. (2022). Amyloid-beta peptide and tau protein crosstalk in Alzheimer's disease. *Neural Regeneration Research*, *17*(8), 1666. https://doi.org/10.4103/1673-5374.332127

Vivek Panwar, Singh, A., Bhatt, M., Tonk, R. K., Shavkatjon Azizov, Raza, A. S., Sengupta, S., Kumar, D., & Garg, M. (2023). Multifaceted role of mTOR (mammalian target of rapamycin) signaling pathway in human health and disease. *Signal Transduction and Targeted Therapy*, *8*(1), 375–375. https://doi.org/10.1038/s41392-023-01608-z

Walsh, R. B., Dresselhaus, E. C., Becalska, A. N., Zunitch, M. J., Blanchette, C. R., Scalera, A. L., Lemos, T., Lee, S. M., Apiki, J., Wang, S., Isaac, B., Yeh, A., Koles, K., & Rodal, A. A. (2021). Opposing functions for retromer and Rab11 in extracellular vesicle traffic at presynaptic terminals. *Journal of Cell Biology*, *220*(8). https://doi.org/10.1083/jcb.202012034

Wei, C., Ji, T., Xu, J., Zheng, Y., Zheng, F., Wang, S., Gao, C., Wan, Y., Li, Z., Deng, J., & Xiong, H. (2025). Rapamycin alleviates neurodegeneration in a Drosophila model of spinocerebellar ataxia type 51. *Journal of Genetics and Genomics/Journal of Genetics and Genomics*, *52*(10), 1259–1267. https://doi.org/10.1016/j.jgg.2025.08.010

Wells, A., Mendes, C. C., Castellanos, F., Mountain, P., Wright, T., Wainwright, S. M., Stefana, M. I., Harris, A. L., Goberdhan, D. C. I., & Wilson, C. (2023). A Rab6 to Rab11 transition is required for dense-core granule and exosome biogenesis in Drosophila secondary cells. *PLOS Genetics*, *19*(10), e1010979. https://doi.org/10.1371/journal.pgen.1010979

Wittmann, C. W., Wszolek, M. F., Shulman, J. M., Salvaterra, P. M., Lewis, J., Hutton, M., & Feany, M. B. (2001). Tauopathy in *Drosophila* : Neurodegeneration Without Neurofibrillary Tangles. *Science*, *293*(5530), 711–714. https://doi.org/10.1126/science.1062382

Xue, M., Xu, W., Ou, Y.-N., Cao, X.-P., Tan, M.-S., Tan, L., & Yu, J.-T. (2019). Diabetes mellitus and risks of cognitive impairment and dementia: A systematic review and meta-analysis of 144 prospective studies. *Ageing Research Reviews*, *55*, 100944–100944. https://doi.org/10.1016/j.arr.2019.100944

Yadav, A. K., Saripella Srikrishna, & Gupta, S. C. (2016). Cancer Drug Development Using Drosophila as an in vivo Tool: From Bedside to Bench and Back. *Trends in Pharmacological Sciences*, *37*(9), 789–806. https://doi.org/10.1016/j.tips.2016.05.010

Yang, W., Liu, Y., Xu, Q.-Q., Xian, Y.-F., & Lin, Z.-X. (2020). Sulforaphene Ameliorates Neuroinflammation and Hyperphosphorylated Tau Protein via Regulating the PI3K/Akt/GSK-3*β*Pathway in Experimental Models of Alzheimer's Disease. *Oxidative Medicine and Cellular Longevity*, *2020*, 1–17. https://doi.org/10.1155/2020/4754195

Yang, X., & Xu, T. (2011). Molecular mechanism of size control in development and human diseases. *Cell Research*, *21*(5), 715–729. https://doi.org/10.1038/cr.2011.63

Ye, Y., & Fortini, M. E. (1999). Apoptotic Activities of Wild-Type and Alzheimer's Disease-Related Mutant Presenilins in *Drosophila melanogaster*. *The Journal of Cell Biology*, *146*(6), 1351–1364. https://doi.org/10.1083/jcb.146.6.1351

Yu, A., Fox, S. G., Cavallini, A., Kerridge, C., O'Neill, M. J., Wolak, J., Bose, S., & Morimoto, R. I. (2019). Tau protein aggregates inhibit the protein-folding and vesicular trafficking arms of the cellular proteostasis network. *Journal of Biological Chemistry*, *294*(19), 7917–7930. https://doi.org/10.1074/jbc.ra119.007527

Zeba Mueed, Tandon, P., Sanjeev Kumar Maurya, Deval, R., Kamal, M. A., & Poddar, N. K. (2019). Tau and mTOR: The Hotspots for Multifarious Diseases in Alzheimer's Development. *Frontiers in Neuroscience*, *12*, 1017–1017. https://doi.org/10.3389/fnins.2018.01017

Zhang, Y., Huang, N., Yan, F., Jin, H., Zhou, S., Shi, J., & Jin, F. (2018). Diabetes mellitus and Alzheimer's disease: GSK-3β as a potential link. *Behavioural Brain Research*, *339*, 57–65. https://doi.org/10.1016/j.bbr.2017.11.015

Zheng, Q., & Wang, X. (2025). Alzheimer's disease: insights into pathology, molecular mechanisms, and therapy. *Protein & Cell*, *16*(2), 83–120. https://doi.org/10.1093/procel/pwae026